

Developing and testing a novel busbar protection scheme for impedance-earthed distribution networks

Milan Jankovski

Developing and testing a novel busbar protection scheme for impedance-earthed distribution networks

by

Milan Jankovski

to obtain the degree of Master of Science
at the Delft University of Technology,
to be defended publicly on Friday August 26, 2022 at 10:00 AM.

Student number:	5262011	
Project duration:	December 1, 2021 – August 26, 2022	
Thesis committee:	Dr. ir. Marjan Popov, Dr. Aleksandra Lekic, Dr. ir. Mohamad Ghaffarian Niasar, Ir. Evita Parabirsing, Ir. Ernst Wierenga,	TU Delft, supervisor TU Delft, daily supervisor TU Delft Stedin Stedin

An electronic version of this thesis is available at <http://repository.tudelft.nl/>.

Preface

First of all, I would like to thank my supervisor from the Delft University of Technology, dr. ir. Marjan Popov for introducing me to Stedin, constantly helping me throughout the project, and believing in me. A special thanks also go to my daily supervisor, dr. Aleksandra Lekic, for helping me throughout the research whenever I had the need of that. Also, I would like to thank Stedin for providing me with the opportunity to work on this project and carry out research, from which I learned a lot. I would especially like to express my gratitude to my supervisors, Evita Parabirsing, for constantly providing me guidance and support throughout the project and Ernst Wierenga, for being supportive and enthusiastic during the whole project. I am grateful to Joey Godefrooi for always helping me with specific questions and always being there for me. A big thanks go to Remko Koorneef, too, for helping me connect the IEDs to the RTDS, which with all the problems that arose, was a time-consuming, but fun process. Furthermore, I would like to thank dr. ir. Mohamad Ghaffarian Niasar for agreeing to be part of the thesis committee and evaluating my work and report. At last I would like to thank all Stedin colleagues from the department Netautomatisering. They were always eager to help me and accepted me as their colleague in the previous months. I was able to learn a lot from the people here and from the project itself and work on my (personal) learning goals, which has made me grow as a person.

*Milan Jankovski
Delft, August 2022*

Abstract

Busbars are one of the most crucial components in the electricity grid and, as such, must always be protected against all types of faults. The busbar differential protection is a protection scheme typically utilized to protect the busbar system in high-voltage substations. Nevertheless, due to the vast number of substations in the distribution level and the high cost of differential busbar protection, DSOs try to implement more cost-effective protection schemes for the busbars. This includes using various communication-based protection schemes, such as the reverse-blocking scheme that Stedin implements. However, due to impedance grounding, the single-phase-to-ground short circuit current can reach small values in magnitude in medium voltage distribution grids, making detecting it more challenging for these protection schemes. That is the problem that Stedin experiences in its network. In this thesis, a novel communication-based protection scheme is proposed as a solution to this problem. The protection scheme utilizes the IEC 61850 standard and the currently available infrastructure Stedin owns. The scheme can be considered a distributed protection scheme. The grid is modeled in RTDS, and a HiL simulation is carried out to test the protection scheme. The extensive simulations show that this scheme can detect single-phase-to-ground busbar faults in impedance earthed networks. Some limitations of the proposed scheme are also seen in the simulation results. Furthermore, a centralized approach for busbar protection is discussed. Two algorithms are developed based on GOOSE and SV messages, respectively. HiL simulations are carried out for these centralized algorithms too. The advantages and the considerations for implementing centralized protection are discussed. These findings can serve as a basis for further research for Stedin in the domain of centralized protection.

Keywords: busbar protection, IEC 61850, distributed protection scheme, centralized protection, RTDS testing

Contents

Preface	i
Abstract	ii
Nomenclature	viii
1 Introduction	1
1.1 Introduction to power system protection	1
1.2 Symmetrical components	2
1.3 IEC 61850 standard	3
1.4 Problem definition	4
1.5 Research questions	5
1.6 Thesis outline	6
2 Overcurrent protection	8
2.1 Introduction of overcurrent protection	9
2.2 Definite-time overcurrent relays	9
2.3 Inverse-time overcurrent relays	10
2.4 Earth-fault protection and negative-sequence overcurrent protection	11
3 Zero-sequence tripping scheme	12
3.1 Current busbar protection in Stedin	13
3.2 Single-phase-to-ground busbar fault current distribution	14
3.3 Zero-sequence tripping algorithm	18
3.4 Testing the protection scheme by Omicron RelaySimTest	23
4 Testing the algorithm in RTDS	26
4.1 Modeling the grid in RSCAD	27
4.2 Communication between the Sprecher IED and the RTDS	28
4.3 HiL simulation	30
4.4 Simulation results	32
4.5 Conclusion	43
5 Centralized protection	46
5.1 Background	47
5.2 Design of a centralized protection	50
5.3 GOOSE based algorithm	52
5.3.1 Principle of operation	52
5.3.2 Conclusion for the GOOSE-based centralized algorithm	62
5.4 SV based central protection	63
5.4.1 Conclusion for the SV-based centralized algorithm	66
6 Conclusions and Recommendations	69
6.1 Conclusions	69
6.2 Recommendations	70
A Transformer groups in zero-sequence representation	73
B NX PLUS C datasheet	74
C Network parameters	75
D Sprecher IED setting	77
E CMS - 156 Datasheet	81

F	Siemens IEDs setting	82
G	MATLAB centralized platform based on GOOSE messages	84
H	MATLAB centralized platform based on SV messages	89

List of Figures

1.1	Possible division of a grid in protection zones [1]	2
1.2	Decomposition of an unbalanced system in symmetrical components	2
1.3	One-line diagram of a typical 10kV substation in Stedin's network	4
1.4	Schematic of the connection of a ZZ transformer	5
2.1	Definite time operating characteristic of an overcurrent relay	9
2.2	Overcurrent protection selectivity by time-grading	10
2.3	Example of two stages of definite-time overcurrent protection	10
2.4	Inverse time characteristics according to IEC 60255 [14]	11
2.5	Connection of CTs for extracting residual component	11
3.1	Reverse blocking scheme - fault on the busbar	13
3.2	Reverse blocking scheme - fault on the outgoing feeder	14
3.3	Simplified grid topology to explain the current distribution during a single-phase-to-ground busbar fault	15
3.4	Positive-sequence circuit for a single-phase-to-ground busbar fault	16
3.5	Negative-sequence circuit for a single-phase-to-ground busbar fault	16
3.6	Zero-sequence circuit for a single-phase-to-ground busbar fault	16
3.7	Complete circuit for the calculation of a single-phase-to-ground busbar fault	17
3.8	Zero-sequence current distribution for a fault on an outgoing feeder	18
3.9	Zero-sequence current distribution for a fault on the busbar	18
3.10	Principle of operation of the zero-sequence current tripping scheme	19
3.11	Test grid for testing the zero-sequence tripping algorithm	20
3.12	Operation of the scheme when the bus section coupler is closed	21
3.13	Operation of the scheme when the bus section coupler is open	21
3.14	Current distribution for a single-phase-to-ground fault on the ZZ feeder	22
3.15	Zero-sequence current distribution for a fault between the secondary side of the transformer and the current transformer	23
3.16	Simulated grid in Omicron RelaySimTest	24
3.17	Test setup for the offline testing with Omicron in the MOTA environment	24
4.1	Model of the substation in RSCAD	27
4.2	Model of the outgoing feeder IED in RSCAD	28
4.3	Illustration of the HiL test setup for testing the zero-sequence tripping scheme	29
4.4	Adjustment of the IEC 61850 communication test setup	30
4.5	One-line diagram of the simulated grid in RSCAD	31
4.6	Topology 1 - sections disconnected	32
4.7	Topology 2 - One incoming feeder and one ZZ transformer	32
4.8	Topology 3 - Two incoming feeders and one ZZ transformer	32
4.9	Topology 4 - Two incoming feeders and two ZZ transformers	32
4.10	Case 1: Fault on an outgoing feeder in Topology 3	33
4.11	Simulation results for a fault on an outgoing feeder in Topology 3	34
4.12	Case 2: Fault on Section 1 in Topology 1	35
4.13	Simulation results for a fault on Section 1 in Topology 1	36
4.14	Case 3: Fault on Section 1 in Topology 3	37
4.15	Simulation results for a fault on Section 1 in Topology 3	38
4.16	Case 4: Fault on ZZ transformer 1 feeder in Topology 3	39
4.17	Simulation results for a fault on the ZZ transformer 1 feeder in Topology 3	39
4.18	Case 5: Fault on ZZ transformer 1 feeder in Topology 4	40

4.19	Simulation results for a fault on the ZZ feeder in Topology 4	41
4.20	Current distribution for a fault on the ZZ feeder in Topology 4	42
4.21	Simulation results for a fault on the ZZ feeder in Topology 4, after the improvement of the protection scheme	43
5.1	CPC connected with MUs directly through point-to-point process bus architecture [21]	47
5.2	CPC connected to MUs through Ethernet LAN architecture [21]	48
5.3	IEDs take values through copper wires and are interfaced with the CPC [21]	49
5.4	IEDs and CPC connected to MUs over point-to-point process bus architecture [21]	49
5.5	IEDs and CPC connected to MUs over Ethernet LAN connection [21]	50
5.6	Proposed hybrid centralized protection scheme	51
5.7	Communication setup for testing the centralized protection algorithms	51
5.8	Test case network for the centralized protection	53
5.9	Distribution of the zero-sequence current for a fault on the bus coupler in Topology 3 . .	53
5.10	Tripping times from the centralized GOOSE algorithm for a fault on the bus coupler in Topology 3	55
5.11	Distribution of the zero-sequence current for a fault on Section 1, with only ZZ transformer 1 connected	56
5.12	Distribution of the zero-sequence current for a fault on Section 2, with only ZZ transformer 1 connected	56
5.13	Tripping times from the centralized GOOSE algorithm for a fault on Section 1 in Topology 3	58
5.14	Tripping times from the centralized GOOSE algorithm for a fault on Section 2 in Topology 3	59
5.15	Distribution of the zero-sequence current for a fault on Section 1, with both ZZ transformers connected	60
5.16	Tripping times from the centralized GOOSE algorithm for a fault on the bus coupler in Topology 4	61
5.17	Tripping times from the centralized GOOSE algorithm for a fault on ZZ transformer 1 feeder in Topology 4	62
5.18	Pre-processing of the data for the SV-based centralized algorithm	64
5.19	Zone 1 of the SV-based centralized algorithm	65
5.20	Zone 2 of the SV-based centralized algorithm	65
5.21	Zone 3 of the SV-based centralized algorithm	65
5.22	Tripping times from the SV-based algorithm for a fault on the bus coupler in Topology 4	66

List of Tables

3.1	Protection settings for a medium-voltage substation	22
3.2	Simulation results from Omicron for a fault on the outgoing feeder	25
3.3	Simulation results from Omicron for a fault on section 1, when the bus coupler is open	25
3.4	Simulation results from Omicron for a fault in the transformer protection zone	25
4.1	Settings of the outgoing feeder IED in RSCAD	28
4.2	Operation of the zero-sequence tripping algorithm for different fault locations in different grid topologies	44
5.1	Logic table for the GOOSE algorithm when a fault occurs on the bus coupler, with only one ZZ transformer switched in	54
5.2	Logic table for the GOOSE algorithm when the ZZ transformer is connected on Section 1	57
5.3	Logic table for the algorithm when the ZZ transformer is connected on Section 2	60
5.4	Operation of the GOOSE based centralized algorithm for different fault locations in different grid topologies	63
5.5	Operation of the SV based centralized algorithm for different fault locations in different grid topologies	67

Nomenclature

Abbreviation	Definition
BC	Bus Coupler
CB	Circuit Breaker
CT	Current Transformer
DSO	Distribution System Operator
DSP	Digital Signal Processor
GOOSE	Generic Object Oriented Substation Event
HiL	Hardware-in-the-Loop
IED	Intelligent Electronic Device
$I_{>}$	current setting for the first stage of the over-current protection
$I_{>}.Op$	operating signal from the first stage of the over-current protection
$I_{>}.Str$	pickup signal from the first stage of the over-current protection
$I_{>>}$	current setting for the second stage of the over-current protection
$I_{>>}.Op$	operating signal from the second stage of the over-current protection
$I_{>>}.Str$	pickup signal from the second stage of the over-current protection
$I_{e>}$	current setting for the first stage of the earth-fault protection
$I_{e>}.Op$	operating signal from the first stage of the earth-fault protection
$I_{e>}.Str$	pickup signal from the first stage of the earth-fault protection
$I_{e>>}$	current setting for the second stage of the earth-fault protection
$I_{e>>}.Op$	operating signal from the second stage of the earth-fault protection
$I_{e>>}.Str$	pickup signal from the second stage of the earth-fault protection
$I_{neg>}$	current setting for the negative over-current protection
$I_{neg>}.Op$	operating signal from the negative over-current protection
$I_{neg>}.Str$	pickup signal from the negative over-current protection
MU	Merging Unit
NCIT	Non-Conventional Instrument Transformers
SiL	Software-in-the-Loop
SV	Sampled Values
$t_{>}$	time delay for the first stage of the over-current protection
$t_{>>}$	time delay for the second stage of the over-current protection
$t_{e>}$	time delay for the first stage of the earth-fault protection
$t_{e>>}$	time delay for the second stage of the earth-fault protection
$t_{neg>}$	time delay for the negative over-current protection
$V0_{>}$	voltage setting for the zero-sequence over-voltage protection

Abbreviation	Definition
$V_{0>}.Op$	operating signals from the zero-sequence over-voltage protection
$V_{0>}.Str$	pickup signal from the zero-sequence over-voltage protection
VT	Voltage Transformer

1

Introduction

1.1. Introduction to power system protection

The electrical power system serves to generate and supply electrical energy to consumers in a reliable way. As such, it needs to operate in a safe and reliable manner at all times. Even though electrical power systems operate with a high level of reliability, they are still vulnerable to severe disturbances resulting from a variety of faults and other contingencies like sudden disconnection of heavily loaded lines, lightning or sudden outage of components.

The protection system aims not to prevent the occurrence of faults completely but to detect the faults and take corrective actions to ensure personnel safety and limit the possible system and equipment damage.

The four most important requirements for the protection (also known as the **4S**) are:

- **Speed** : the protection device must detect the fault and take corrective actions in a fast manner in order to decrease the damage that is caused. Usually, the times are in the order of milliseconds.
- **Selectivity** : the protection device must interrupt only the faulted components, thus disconnecting only the minimal part of the network. Coordination of the protection devices (with operating or timing characteristics) is essential in achieving selectivity.
- **Sensitivity** : the protection device needs to be sensitive enough in order to detect abnormal conditions and initiate corrective actions for every fault in their zone of protection.
- **Security** : the protection device must not operate improperly for any fault type outside their respective protection zones or for normal grid conditions.

Prompt and reliable operation of the protection is necessary in order to achieve the required reliability of the power system. To accomplish this, the system is normally divided into protection zones (which can overlap), each one of which has its own protection scheme that monitors the voltage and current in it for any abnormalities. One possible way of dividing the system in protection zones is presented in Figure 1.1, where the different colours represent different protection zones. In this figure (from left to right), one can see: a feeder protection zone, busbar zone, another feeder and one more busbar zone, a transformer protection zone, and finally a generator protection zone.

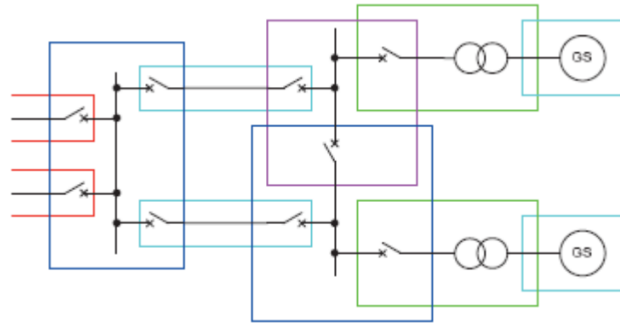


Figure 1.1: Possible division of a grid in protection zones [1]

In case of a fault, the protection system that is nearest to the fault will operate and disconnect its zone, thus providing selectivity of the protection. Zones are intentionally made to overlap, in which way it is guaranteed that no part of the network is left unprotected.

1.2. Symmetrical components

Any set of three unbalanced phasors of a three-phase system can be decomposed into a set of three balanced systems of phasors [2].

The new set of the three balanced systems will consist of three positive-sequence quantities, three negative-sequence quantities and three zero-sequence quantities. The first of which is equal in magnitude and symmetrically displaced by 120° (electrical degrees) in the same direction as the phase displacement of the original set of unbalanced phasors. The second ones are also equal in magnitude and symmetrically displaced by 120° , however the phase displacement is in the opposite direction than the phase displacement of the original set of phasors. Finally, the zero-sequence quantities are equal in magnitude and phase [3]. Graphically this is presented in Figure 1.2.

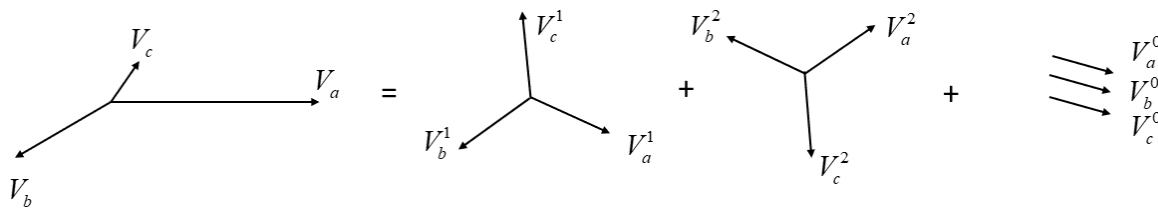


Figure 1.2: Decomposition of an unbalanced system in symmetrical components

If we assume that the phasors shown in the above figure are voltage phasors ¹, then for the initial set of phasors we can write:

$$V_a = \frac{1}{\sqrt{3}}(V_a^1 + V_a^2 + V_a^0), \quad (1.1)$$

$$V_b = \frac{1}{\sqrt{3}}(V_b^1 + V_b^2 + V_b^0), \quad (1.2)$$

$$V_c = \frac{1}{\sqrt{3}}(V_c^1 + V_c^2 + V_c^0). \quad (1.3)$$

¹the same principle is used for the current phasors as well

If one follows the above-mentioned correlation between the positive-sequence, negative-sequence, and zero-sequence components, and the operator a is introduced as $a = e^{j2\pi/3}$, the following conversion matrix between the unsymmetrical phasors and the set of symmetrical components is derived:

$$\begin{bmatrix} V_a \\ V_b \\ V_c \end{bmatrix} = \frac{1}{\sqrt{3}} \begin{bmatrix} 1 & 1 & 1 \\ 1 & a^2 & a \\ 1 & a & a^2 \end{bmatrix} \begin{bmatrix} V_a^0 \\ V_a^1 \\ V_a^2 \end{bmatrix}. \quad (1.4)$$

For calculating the other way around, from unsymmetrical to symmetrical components, the following equation can be used ²:

$$\begin{bmatrix} V_a^0 \\ V_a^1 \\ V_a^2 \end{bmatrix} = \frac{1}{\sqrt{3}} \begin{bmatrix} 1 & 1 & 1 \\ 1 & a & a^2 \\ 1 & a^2 & a \end{bmatrix} \begin{bmatrix} V_a \\ V_b \\ V_c \end{bmatrix}. \quad (1.5)$$

By decomposing the three-phase unbalanced system by the method of symmetrical components, the unsymmetrical components can be treated in the same manner as the symmetrical ones, which means that solving them becomes an easier task. This makes the method of symmetrical components an attractive tool for protection engineers. Since some of the symmetrical components can be treated as signature values for specific types of faults (i.e., the zero-sequence component is mainly related to single phase-to-ground faults), an increasing number of protection functions are operating solely based on the symmetrical values [3].

1.3. IEC 61850 standard

Nowadays, Intelligent Electronic Devices (IEDs) are the backbone of the protection schemes [4]. They receive a set of signals from the Current Transformer (CT) and the Voltage Transformer (VT) or non-conventional instrument transformers (NCIT) and act based on the implemented protection logic. These devices use digital signal processors (DSP) optimised for real-time signal processing, which are running the mathematical algorithms for the different protection functions [1]. The digitisation of these devices also implies that communication among IEDs is easier to be achieved. In order to facilitate communication in substations, the IEC 61850 communication standard was developed [5]. This provides a standardized communication protocol within substations, which provides a powerful user-defined programming and a state-of-the-art communication platform [6]. As a result, this standard allows for interoperability and communication between IEDs independent of their vendor since they all support the IEC 61850 protocol. As such, it is a prerequisite for intelligent applications and empowers the use of new, more custom-designed communication-based protection schemes, making them more feasible and easy to implement [7].

Some of the specific communication service mappings [8], are:

- Generic Object Oriented Substation Event (GOOSE), which serves for transmitting circuit breaker statuses, blocking and tripping commands, interlocking, and other commands which are binary in nature. It can be seen as a Publish-Subscribe model, where there is at least one GOOSE sending IED and one or more GOOSE receiving IEDs. The message is sent to all of the IEDs that are connected to that network, however only the subscribing IEDs are actually retrieving this information and getting the required data.
- Sampled values (SV), which serve for transmitting measured values (voltages, currents, frequency) from the network to the IEDs. These measured values on the primary side are analog signals, which then are converted to digital before being processed and communicated.

²this is the power-invariant transformation, while also a power-variant transformation is possible as presented in [2]

1.4. Problem definition

Stedin is a Distribution System Operator (DSO) in the provinces of South Holland, Utrecht, and Zeeland. It is responsible for the operation of the sub-transmission and distribution network. A standardized operational grid topology according to the policy of Stedin is shown in Figure 1.3.

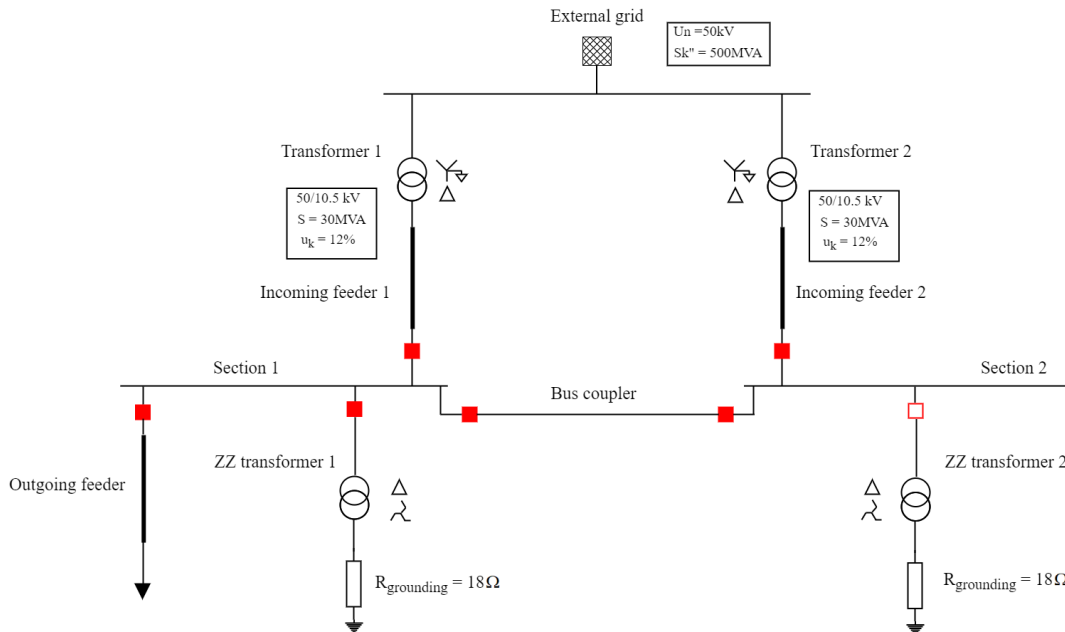


Figure 1.3: One-line diagram of a typical 10kV substation in Stedin's network

This part of the network is a 10 kV substation fed from the 50 kV sub-transmission grid through two power transformers in YNd connection. In some operating scenarios, one of the power transformers can be switched off and serve as a hot backup, which means that the substation will be powered by only one power transformer.

The grid is grounded through a high resistance in order to limit the magnitude of the short-circuit faults compared to a directly grounded grid. On the other hand, it also decreases the magnitude of the transient over-voltages during faults compared to an isolated network, helps to minimize the effect of ferroresonance, and makes it possible for the short-circuit to be located [9] when compared to an isolated network. As the substation is connected to the delta side of the transformer, it means that there is no star-point available for the grounding, therefore a solution by making use of a zig-zag (ZZ^3) transformer is used. The ZZ transformer is a special type of transformer used to provide a star-point in delta networks through which the network can be grounded [10]. The one-line schematic of the connection of the ZZ transformer, along the zero-sequence current distribution in it, can be seen in Figure 1.4.

³in the rest of the thesis, the abbreviation ZZ will always be used for the zig-zag transformer

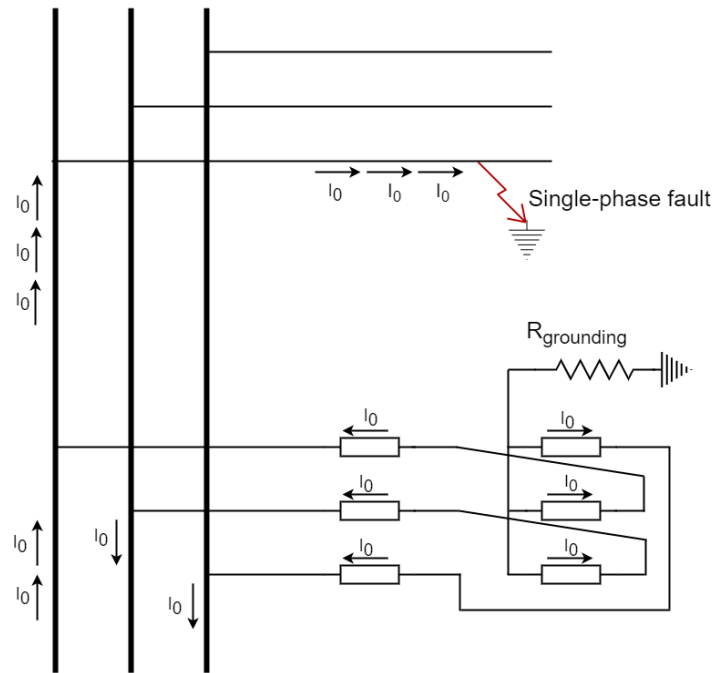


Figure 1.4: Schematic of the connection of a ZZ transformer

The resistance through which the ZZ transformer star point is earthed is chosen in such a way that it limits the zero-sequence current that passes through the ZZ transformer itself, in a case of a single-phase-to-ground fault, to 1000 A. According to this criterion, for 10kV substations, a resistance of 18Ω is used. Additionally, Stedin's policy requires that only one ZZ transformer can be connected at all times, meaning that one of them is only serving as a reserve. That can be seen from Figure 1.3, where the feeder that connects the ZZ transformer 2 to the busbar is switched off.

The outgoing feeders represent all the outgoing connections to other substations or to the customers, and in this scheme, for simplicity, they are presented as only one outgoing feeder. In reality, there are multiple outgoing feeders on both Section 1 and Section 2 of the busbar system.

The protection scheme of the substation is as follows:

- The transformers 1 and 2 are protected by using the transformer differential protection function.
- The incoming feeders, the outgoing feeders, the bus coupler, and both of the feeders through which the ZZ transformers are connected are protected by using non-directional and earth-fault over-current IEDs.
- The busbar system is protected with a combination of all of the over-current IEDs by utilizing the so-called reverse-blocking scheme (explained in Section 3.1).

In case of a short-circuit occurring on any of the outgoing feeders, only the IED on that outgoing feeder needs to take corrective actions (i.e., to trip the circuit breaker (CB) of that feeder), meaning that the rest of the network can continue its operation undisturbed. On the other hand, in the case of a short-circuit on the busbars, the IEDs on the incoming transformer feeders need to operate according to the logic of the reverse-blocking scheme and disconnect the busbar from the incoming source of power. However, according to Stedin experience, single-phase-to-ground faults on the busbar are not detected.

This prolonged duration of the short-circuit current can pose a danger to the system or the components of the system, as experienced by Stedin in two such independent failures in the recent past - in 2021 and 2022.

1.5. Research questions

As mentioned in Section 1.4, a single-phase-to-ground fault occurring on the busbar is not detected in this grid topology, which affects network operation in a safe and reliable manner. In the initial stage of this

project [11], the reasons for this protection malfunction were examined, and a new protection scheme⁴ was proposed to solve the existing protection blinding. It should be pointed out at this point that placing a differential busbar protection would solve the problem of detecting the single-phase-to-ground fault as well. The differential protection scheme operates on Kirchoff's current law, which states that the sum of all of the currents entering a node is equal to the sum of all the currents leaving a node [12]. Since a busbar can be treated as a node in the network, this protection scheme is applicable as busbar protection. However, it requires that measurements from all of the outgoing feeders have to be passed to the busbar differential IED. That requires another set of IEDs to be installed on every feeder, which will communicate their values to the differential busbar IED. This, in return, makes the busbar differential protection an expensive and complex solution. That is why one of Stedin's preferences for solving this problem was to use the currently available infrastructure, and the process of designing the new algorithm was in line with that constraint. This new protection scheme is considered a distributed protection scheme since the protection of one element and the decision-making is distributed among several IEDs.

The primary goal of this thesis is to expand further on busbar protection in medium voltage distribution grids. This includes more extensive testing of the earlier proposed algorithm in dynamic grid conditions (various operational topologies) and various fault conditions (various inception angles and fault resistances). The results from the tests will also show the limitations and shortcomings of the proposed protection scheme. Furthermore, the second objective of the thesis is to investigate the possibility of introducing centralized protection as busbar protection in distribution networks.

These objectives are then divided into several research questions in order to make it easier to be comprehended and achieve it:

1. Is the newly proposed scheme successfully clearing single-phase-to-ground busbar faults without endangering the system's integrity?
2. Do different fault characteristics (point of inception, fault resistance) influence the operation of the scheme?
3. What are the limitations of the proposed scheme in different operational scenarios?
4. Is centralized protection viable for overcoming the shortcomings of the proposed scheme?
5. What are the changes that DSOs need to carry on in order to facilitate centralized protection concept?

1.6. Thesis outline

Chapter 1 : Introduction

This introductory chapter introduces the basic principles of power system protection and the new developments in the protection devices and the communication that allow for more custom-based protection algorithms. The principle of symmetrical components, later used in the thesis, is also elaborated. Furthermore, the motivation for investigating the busbar protection is given, and the research objective is defined. Finally, the outline of the thesis is presented.

Chapter 2 : Overcurrent protection

The second chapter introduces the basics of overcurrent protection in power systems. The basic principle of operation is explained, and the differences between directional and non-directional overcurrent protection are briefly elaborated. Different time-current characteristics of the overcurrent protection devices are described. Finally, earth-fault and negative-sequence overcurrent protection are introduced as particular types of overcurrent protection.

Chapter 3 : Zero-sequence tripping scheme

In this chapter, the existing protection scheme that Stedin uses for its busbar systems is explained, and further explanation is given on why this scheme fails to detect single-phase-to-ground busbar faults. The behaviour of the short-circuit current is investigated, and the signature values of the single-phase-to-ground fault are extracted. A novel protection scheme for detecting single-phase-to-ground busbar

⁴in the rest of the thesis denoted as zero-sequence tripping scheme

faults in medium voltage impedance-earthed networks is presented, and its scheme of operation and some critical observations are also presented.

Chapter 4 : Real-time testing in RTDS and results

In Chapter 4, the entire process of the real-time testing of the proposed scheme in RTDS is explained. Firstly, the modeling of the grid in the RSCAD software is presented, and the setup of the Hardware-in-the-Loop testing is clarified. The procedure for enabling the proper communication between the IED and the RTDS is also elaborated. Finally, the different case scenarios for the simulations are explained, and the results of those simulations are presented. Meaningful conclusions from the obtained simulations are drawn.

Chapter 5 : Centralized protection

Chapter 5 gives an overview of the centralized protection and control concept, and the motivation behind its implementation. Different approaches and topologies for achieving redundancy are examined and different characteristics are explained. Furthermore, a step is taken into suggesting a centralized approach toward protecting the busbar system against single-phase-to-ground faults in impedance grounded networks. Two different algorithms are explained and tested with RTDS. Finally, conclusions and remarks are drawn with regard to the implementation of a centralized protection concept, and its robustness in terms of expanding DSO's infrastructure.

Chapter 6 : Conclusions and recommendations

Chapter 6 serves to summarize the work accomplished by the thesis. The main conclusions and results are discussed. Furthermore, some recommendations for continuing and improving this work are given.

2

Overcurrent protection

The protection of the power system components is of essential importance for the overall functioning of the power system. This protection can be achieved through a variety of different methods which are implemented in the IEDs. The measurements from the grid, which the IEDs usually require as inputs, are the system's currents, voltages, and frequency. Based on the protection scheme implemented, the IEDs can require more than one of these measurements. One of the most straightforward protection schemes is overcurrent protection, which generally requires only the system's currents as inputs. This chapter serves to give a basic introduction to overcurrent protection. Different types of time-current characteristics are presented, along with their benefits and drawbacks. Finally, it is explained how the input currents can be processed to achieve an overcurrent protection for specific symmetrical components.

2.1. Introduction of overcurrent protection

Protection against very high currents was naturally the first one to be developed [1]. Overcurrent relays are the most common protection devices to deal with these very high currents. They are primarily intended to protect only against excessive fault currents and not to serve as an overload protection [13]. The overcurrent relays measure only one of the system variables, namely the current. Because the current measurement does not indicate the current direction, these relays are considered non-directional. A directional overcurrent relay is achieved if the system voltage is added as an additional measurement input. Based on the difference between the angles of the appropriate currents and voltages, it can be concluded whether the fault is in the forward or the reverse direction. However, directional overcurrent relays are out of the scope of this research; thus, no further investigation will be carried out about them. Further information about achieving directionality in different network topologies can be found in [1].

Different operating characteristics can be created with the variable time and current. Based on their operating characteristics, the relays can be classified into definite-time, and inverse-time relays.

2.2. Definite-time overcurrent relays

The definite-time characteristic of an overcurrent relay can be seen in Figure 2.1. The relays with this characteristic operate when the fault current exceeds the current threshold ($I_{>}$) after the expiration of the appropriate time delay ($t_{>}$). The time delays can also be set to zero, which means that the relay will operate instantaneously in this situation.

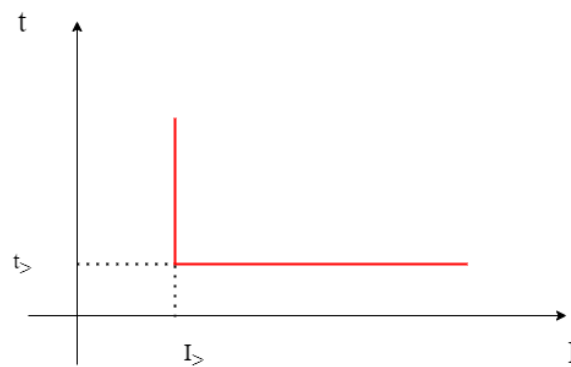


Figure 2.1: Definite time operating characteristic of an overcurrent relay

The time delays can be adjusted so that the IED closest to the fault will react in the fastest time, and the remaining IEDs are reacting in succession, with increasing time delays, moving back to the source. The difference between the time delays of two consecutive IEDs for the same current magnitude is called time discrimination. The time-discrimination of the IEDs allows for a greater selectivity of this protection, which is shown in Figure 2.2. One big drawback of this operating characteristic is that faults near the source will be cleared in a relatively long period of time, and those faults usually result in higher currents.

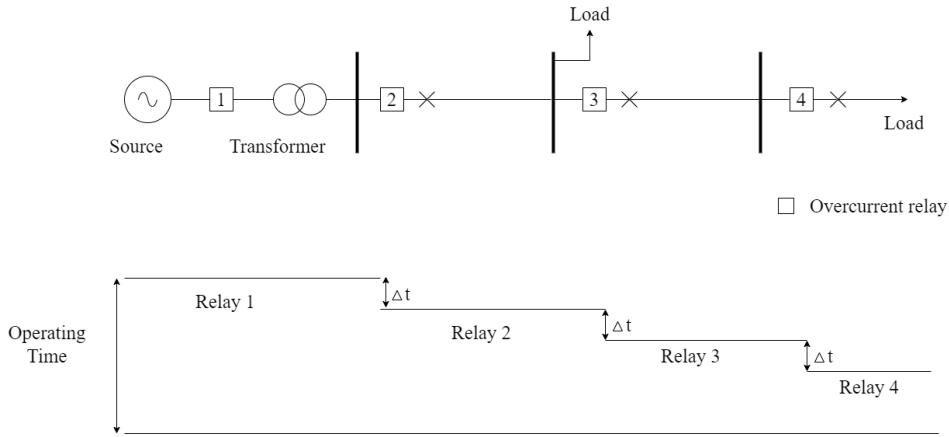


Figure 2.2: Overcurrent protection selectivity by time-grading

Furthermore, the IEDs allow for more than one time-definite characteristic to be implemented in their logic. In that way, multiple stages of operation of the overcurrent relay can be achieved, as shown in Figure 2.3.

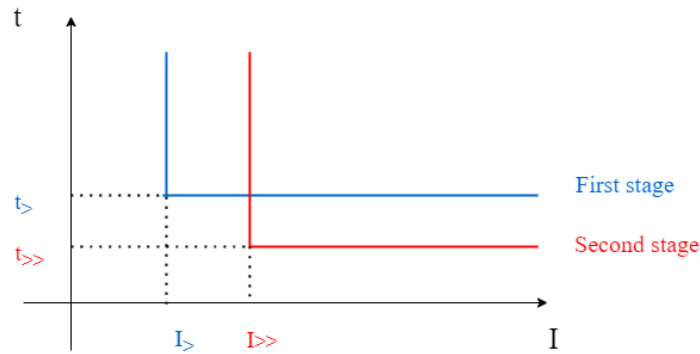


Figure 2.3: Example of two stages of definite-time overcurrent protection

As one can see, two stages of the definite-time characteristic are present in this relay. The first stage has the settings $I_{>}$ and $t_{>}$, while $I_{>>}$ and $t_{>>}$ are the settings of the second stage. The first stage usually operates for lower currents but with a greater time delay. It usually serves as backup protection for the following elements of the grid. In contrast, the second stage has a higher current threshold, but it operates with a shorter time delay. This stage is usually the primary protection of the protected element.

2.3. Inverse-time overcurrent relays

An inverse-time overcurrent relay denotes a relay that operates within a time inversely proportional to the fault current. This allows for much shorter tripping times in case of very high currents, without risk for the protection selectivity. Based on the characteristic curve, which indicates the operation speed, inverse time IEDs can be inverse (SI), very inverse (VI), or extremely inverse (EI). This division is according to the IEC60255 standard, and the different characteristic curves can be seen in Figure 2.4. Information about obtaining these curves can be found in [1]. The inverse-time relays are out of the scope of the thesis research, so they will not be further considered.

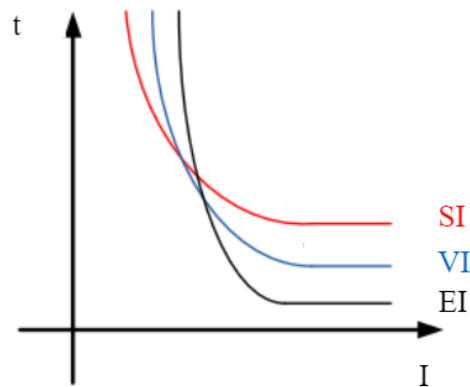


Figure 2.4: Inverse time characteristics according to IEC 60255 [14]

2.4. Earth-fault protection and negative-sequence overcurrent protection

A relay that responds only to the residual current of the system can provide a greater sensitivity against earth faults. This is because a residual component only appears in the system when fault current flows to earth. As such, the earth fault relay is entirely unaffected by the load currents. This implies that the threshold is limited only by the grid topology and the leakage/capacitance currents to the ground. This is crucial since the earth faults can be of very low magnitude, so the current threshold will usually have to be set to a small value. Overall, this allowed low settings for earth fault relays are very useful, as the earth faults are often greatly limited by the neutral earthing impedance. The residual component of the current can be extracted by connecting the CTs in parallel, as presented in Figure 2.5. Another possibility is by directly computing the residual current in the IED itself, based on the theory of symmetrical components.

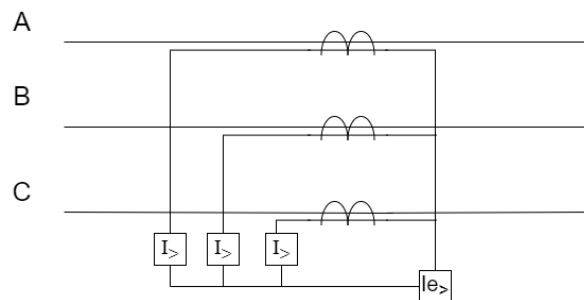


Figure 2.5: Connection of CTs for extracting residual component

Detection of earth fault currents in insulated networks can pose a challenge. This is because a single-phase-to-ground fault in a system like this would cause an earth fault current with a magnitude very close to zero. This problem can be solved by using a sensitive earth fault protection. This protection type is out of the scope of this research, and more information about it can be found in [1].

The digital and numerical relays offer the possibility for digitally extracting the symmetrical components of the currents. This allows for extraction of the negative-sequence component of the current, which can be used for detection of single-phase and two-phase faults. The same principles that were explained for the definite-time overcurrent protection are valid for the negative-sequence overcurrent protection too.

3

Zero-sequence tripping scheme

The busbar system is one of the most crucial components in the electrical network since it is a junction point for incoming and outgoing feeders of the grid. Any fault on the busbar with a long duration (of several hundreds of milliseconds) causes a lot of stress on the other components of the grid and/or may leave a part of the grid without energy supply. That is why the busbar protection has to act promptly and clear the faults as soon as possible, thus achieving greater reliability in the network operation. With the vast number of substations, distribution system operators (DSO), such as Stedin, implement alternatives to the busbar differential protection, which are cheaper, and at the same time, as reliable as the classical busbar differential protection. For a large part of their grid, Stedin makes use of the reverse-blocking scheme as busbar protection. However, research showed that this protection scheme fails to detect single-phase-to-ground faults. That is the reason why a new protection scheme had to be devised in order to help with the detection of these faults [11]. This novel algorithm fully utilizes the possibilities that the IEC 61850 offers in terms of fast communication (GOOSE messages) between multiple IEDs. This chapter gives an overview of this algorithm and the logic behind its implementation.

3.1. Current busbar protection in Stedin

Currently, in the medium-voltage grid of Stedin, the reverse-blocking scheme is applied to provide protection against busbar faults. The principle of operation of this protection scheme can be explained by Figure 3.1 and 3.2, where a simplified representation with only one incoming feeder and one outgoing feeder is presented.

Figure 3.1 shows the case of a fault that occurs in the busbar protection zone.

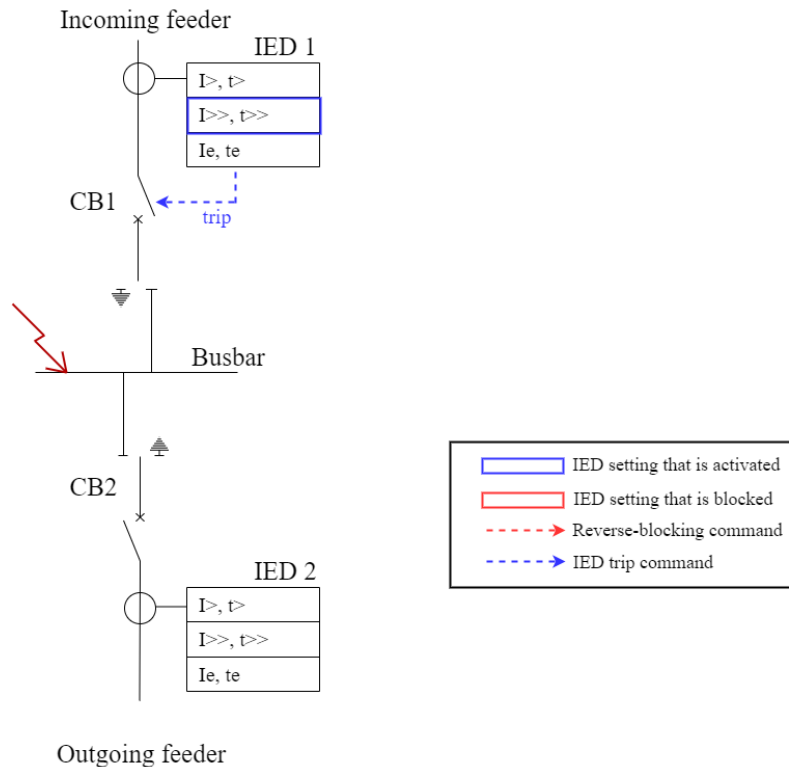


Figure 3.1: Reverse blocking scheme - fault on the busbar

In this case, the $I_{>>}$ setting of IED 1 will detect the fault current, and after the time expiration $t_{>>}$, will send a trip command to the relevant circuit-breaker CB1, to clear the busbar fault.

However, when the fault is on the outgoing feeder (Figure 3.2), the tripping of the whole busbar system should be prevented, and priority should be given to the outgoing feeder IED to trip its circuit-breaker CB2. In order to achieve that, communication between the IEDs is required. When the $I_{>}$ setting of IED 2 is activated (it is not waited for $t_{>}$ to expire), a blocking signal is sent to the $I_{>>}$ setting of IED 1. In this way, the $I_{>>}$ setting of the incoming feeder IED is blocked throughout the time interval the outgoing feeder detects the fault current. This implies that the outgoing feeder IED will clear the fault, after which the $I_{>>}$ setting of the incoming feeder IED is again put into operational mode.

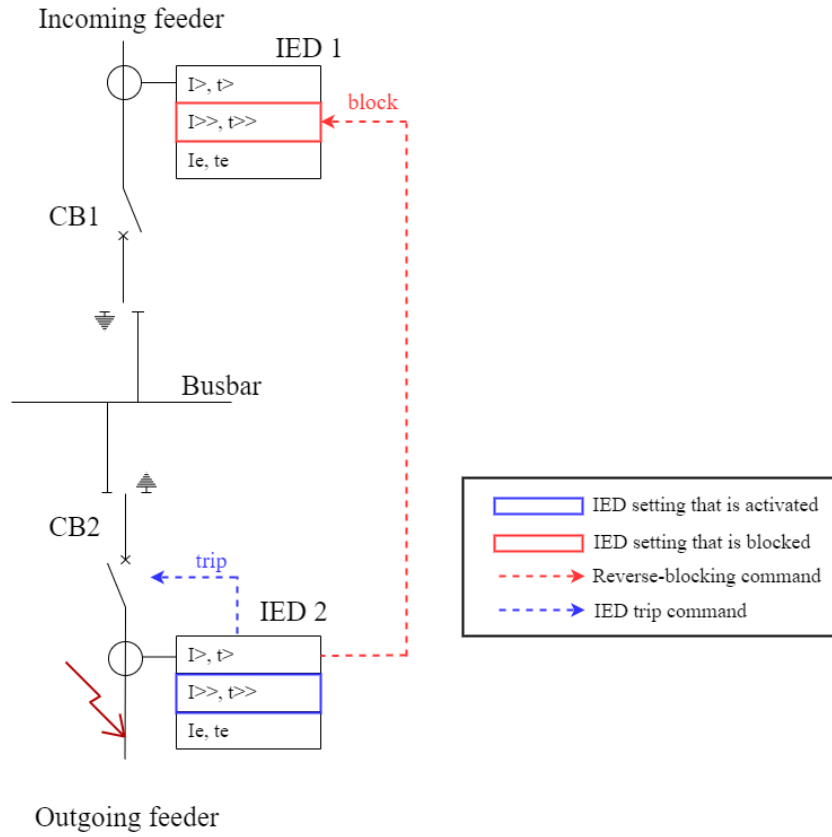


Figure 3.2: Reverse blocking scheme - fault on the outgoing feeder

This is the basic principle behind the operation of the reverse-blocking scheme, which is used to protect and clear busbar faults. However, this protection scheme fails to operate for single-phase-to-ground faults occurring in the impedance earthed medium-voltage distribution network of Stedin. In the following section, the explanation behind the failure of the protection scheme to detect single-phase-to-ground faults is elaborated.

3.2. Single-phase-to-ground busbar fault current distribution

To explain the reasons behind the protection failure, firstly, the current distribution during a single-phase-to-ground fault on the busbar should be investigated. For this purpose, the simplest case is taken, with only one incoming feeder connected and one ZZ transformer ¹, as shown in Figure 3.3. In order to find the symmetrical components of the short-circuit current, the power-invariant transformation is used, and the base power S_b is chosen to be 30MVA. A base voltage U_{b1} of 50kV is used for the external grid and the power transformer, while for the ZZ transformer and the outgoing feeder, a base voltage U_{b2} of 10.5kV. Following that, we have two sets of base currents and base impedances:

$$I_{b1} = \frac{S_b}{U_{b1}} = \frac{30}{50} = 0.6kA, \quad (3.1)$$

$$Z_{b1} = \frac{U_{b1}^2}{S_b} = \frac{50^2}{30} = 83.33\Omega, \quad (3.2)$$

$$I_{b2} = \frac{S_b}{U_{b2}} = 2.857kA, \quad (3.3)$$

$$Z_{b2} = \frac{U_{b2}^2}{S_b} = \frac{10.5^2}{30} = 3.675\Omega. \quad (3.4)$$

¹the overall conclusion does not depend on the grid's topology

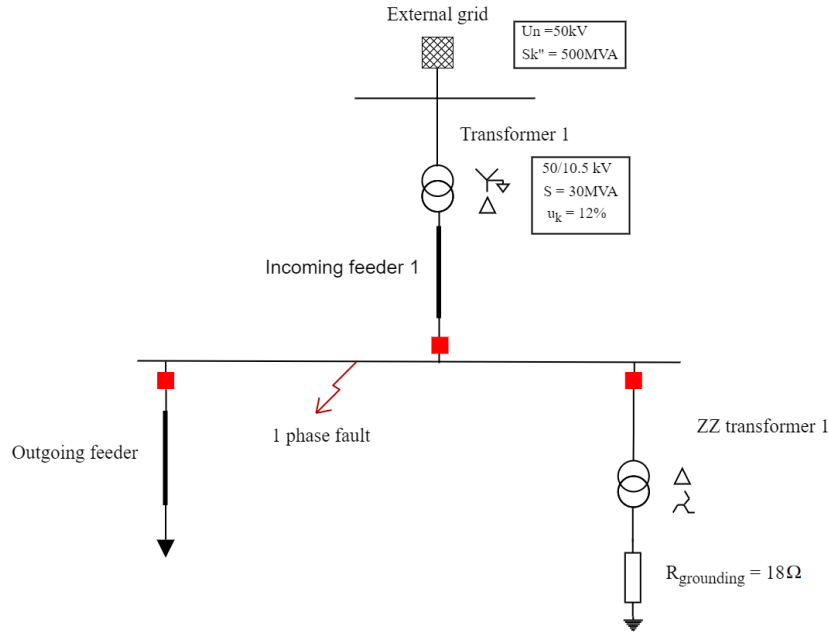


Figure 3.3: Simplified grid topology to explain the current distribution during a single-phase-to-ground busbar fault

According to the data provided by Stedin, the short-circuit power S_k'' of the external grid is 500MVA. Based on this, the impedance X_{eg} that the external grid brings into the network can be computed as:

$$X_{eg} = \frac{U_{b1}^2}{S_k''} = \frac{50^2}{500} = 5\Omega = j0.06p.u. \quad (3.5)$$

For the power transformer, the rated power is $S_{rated} = 30MVA$, the voltage ratio is 50/10.5kV and the short-circuit voltage is $u_k = 12.7\%$. The impedance of the transformer X_{tr} can be calculated as:

$$X_{tr} = u_k(\%) * \frac{U_{b1}^2}{S_b} = \frac{12.7}{100} * \frac{50^2}{30} = 10.583\Omega = j0.127p.u. \quad (3.6)$$

Finally, for the ZZ transformer, the grounding resistance is:

$$R_{grounding} = 18\Omega = 4.898p.u. \quad (3.7)$$

Stedin chooses the value of 18Ω in compliance with their policy for the 10kV level, which states that in a case of a single-phase-to-ground fault, the maximum current that is allowed to flow through the ZZ transformer grounding is 1000A. Since only a zero-sequence current will pass through the grounding resistance, it is evident that all phases will carry the same current. This implies that each phase is allowed to carry a maximum of 333A. Following that requirement, the grounding resistance can be found by simply dividing the phase voltage by the maximum allowed phase current. The winding resistance can be neglected due to its small value compared to the grounding resistance. According to that, Stedin uses the following equation to calculate the required resistance:

$$R_{grounding} = \frac{U_l}{\sqrt{3} * I_0} = \frac{10500}{\sqrt{3} * 333} = 18.2\Omega, \quad (3.8)$$

where U_l is the nominal line-to-line voltage of the busbar where the ZZ transformer is connected.

By applying the theory of symmetrical components, the equivalent positive, negative and zero sequence circuits can be constructed, as shown in Figure 3.4 - 3.6. It is assumed that the positive sequence values are equal to the negative sequence ones, as it is often the practice when working with symmetrical components. As seen in Figure 3.4, in the positive-sequence circuit, we have the positive

impedances of the external grid (X_{eg}), transformer 1 (X_{tr1}), and incoming feeder 1 (X_{in1}). However, $X_{in1} \ll X_{tr1}$, so it can safely be neglected. This means that the positive sequence impedance seen from the fault location can be computed as:

$$Z_1 = X_{eg} + X_{tr} = j0.06 + j0.127 = j0.187 p.u. \quad (3.9)$$

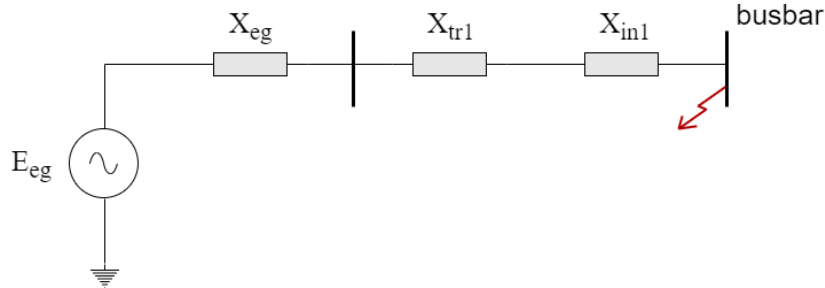


Figure 3.4: Positive-sequence circuit for a single-phase-to-ground busbar fault

The negative-sequence circuit is the same as the positive-sequence circuit, and only the voltage source is omitted from this circuit (Figure 3.5). Again, because of the same reason X_{in1} is neglected. Based on the assumption that the positive and negative sequence parameters are equal for all of the components, we have:

$$Z_2 = Z_1 = j.0187 p.u. \quad (3.10)$$

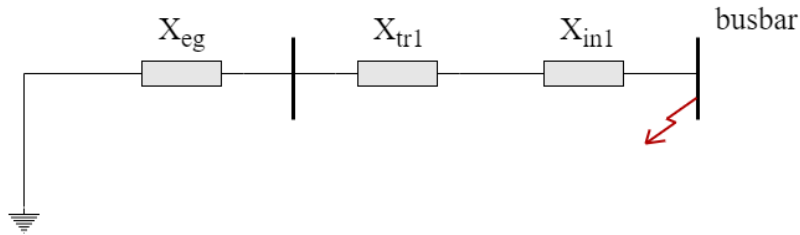


Figure 3.5: Negative-sequence circuit for a single-phase-to-ground busbar fault

Finally, in Figure 3.6, the zero-sequence circuit is shown based on the zero-sequence representation of the transformer groups (Appendix A). It can be seen that only the grounding in the ZZ transformer ($R_{grounding}$) and the impedance of this transformer (X_{0zz_tr}) are being seen as an impedance from the fault location. Again, $X_{0zz_tr} \ll R_{grounding}$, so the zero-sequence impedance of this transformer can be neglected. Consequently, for the zero-sequence impedance, we have:

$$Z_0 = R_{grounding} = 4.898 p.u. \quad (3.11)$$

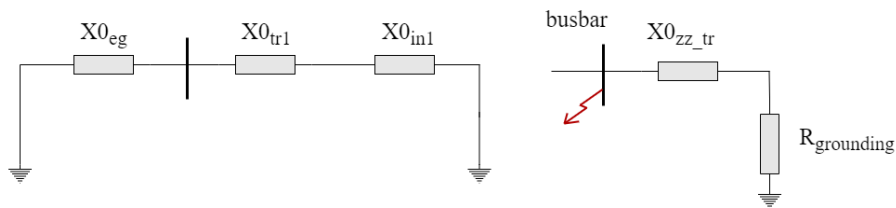


Figure 3.6: Zero-sequence circuit for a single-phase-to-ground busbar fault

From the theory of symmetrical components, we have that to find the total impedance seen from the point of the fault location, the positive, negative, and zero-sequence circuits need to be connected as shown in Figure 3.7. From this, the total impedance can be calculated as :

$$Z_f = Z_1 + Z_2 + Z_0 = 2 * j0.187 + 4.898 = 4.9e^{j4.37} . \quad (3.12)$$

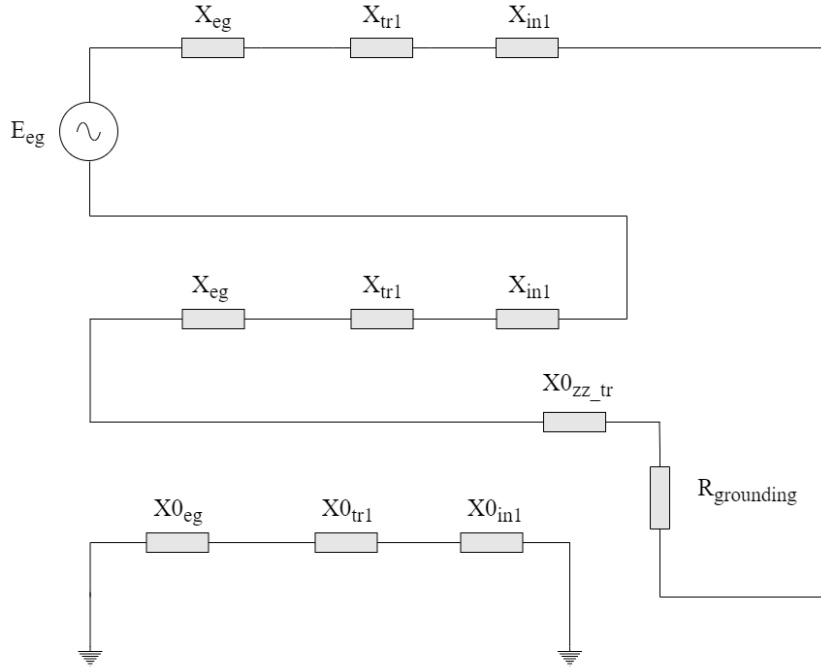


Figure 3.7: Complete circuit for the calculation of a single-phase-to-ground busbar fault

Finally, for the currents it can be derived:

$$I_1 = I_2 = I_0 = \frac{E_{eg}}{Z_f} = \frac{1e^{j30}}{4.9e^{j4.37}} = 0.204e^{j25.63} p.u.^2 \quad (3.13)$$

From this, for the fault current in the faulted phase on the fault location (busbar) we have:

$$I_A = \sqrt{3} * I_0 = 0.3256e^{j25.63} p.u. = 1.007e^{j25.63} kA . \quad (3.14)$$

As seen in Figure 3.7, the zero-sequence impedance of incoming feeder 1 - X_{Oin1} is not connected to the fault circuit, meaning that there is no zero-sequence current component that passes through the incoming feeder. In contrast, current positive and negative sequence components pass through the incoming feeder. From this, by using Equation 1, the current that passes through incoming feeder 1 in the faulty phase can be calculated as:

$$I_{A_(\text{incoming feeder})} = \frac{1}{\sqrt{3}} * (I_1 + I_2) = 0.2356e^{j25.63} = 0.673e^{j25.63} kA . \quad (3.15)$$

As noted, this current is too low to activate the $I_{>>}$ setting on the incoming feeder IED, which explains why the reverse-blocking scheme fails to detect the single-phase-to-ground busbar faults in medium voltage impedance earthed networks.

²the voltage is displaced for a phase of 30° in order to compensate for the transformer ratio - YNd11

3.3. Zero-sequence tripping algorithm

The transformers through which the busbar is connected to the higher voltage level grid (50kV) are in YNd11 connection, with the delta side connected to the busbar in the substation. Based on the theory of symmetrical components, there is no zero-sequence in-feed from the external grid. The only “source” of the zero-sequence component is the ZZ transformer [10] through which the substation is earthed. The fact that there is only one “source” of zero-sequence current, along with the fact that the zero-sequence component can be seen as a “signature” for the single-phase fault, makes the zero-sequence component a suitable choice to serve as the basis for detecting the single-phase-to-ground busbar faults. The distribution of the zero-sequence component of the current in the case of a single-phase-to-ground fault on an outgoing feeder and on the busbar can be seen in Figure 3.8 and 3.9 respectively. The capacitive zero-sequence currents from the cables are neglected because of their low magnitude.

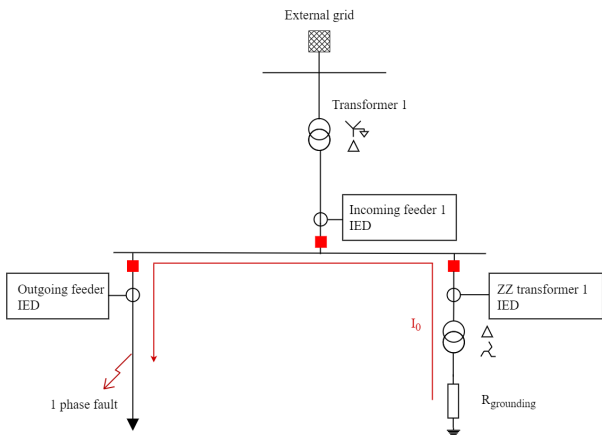


Figure 3.8: Zero-sequence current distribution for a fault on an outgoing feeder

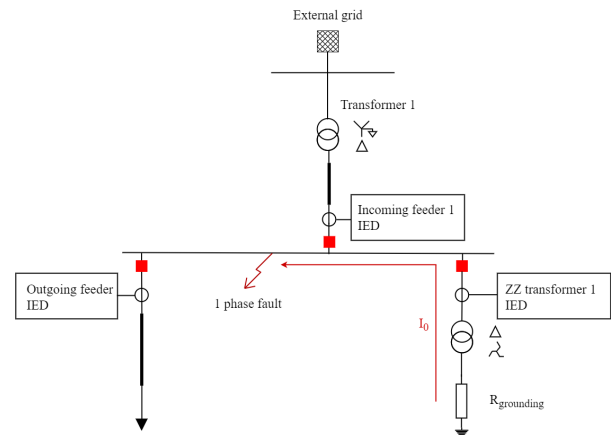


Figure 3.9: Zero-sequence current distribution for a fault on the busbar

As it can be seen, for a fault on the outgoing feeder (Figure 3.8), both the IED on the outgoing feeder and the feeder where the ZZ transformer is connected will detect a zero-sequence component of the current. In contrast, for a single-phase-to-ground fault on the busbar (Figure 3.9), only the ZZ feeder IED will detect a zero-sequence current.³ The new algorithm was based on this knowledge, and it implements the benefits of the IEC 61850 standard.

As discussed, during a single-phase-to-ground fault on an outgoing feeder or a fault on the busbar, a zero-sequence current will be detected by the ZZ transformer IED. As a result, a single-phase-to-ground fault on both the busbar and an outgoing feeder will cause this IED to issue a trip command. However, when a fault occurs on the outgoing feeder, only the IED on that feeder should trip its CB to preserve selectivity. This requires that the trip command from the ZZ transformer IED should be blocked in this case. The signal used to do that is the $I_{e>.Str}$ signal from the outgoing feeder IED. In other words, for a single-phase-to-ground fault on an outgoing feeder, the ZZ feeder IED is prevented from sending its trip command as long as the outgoing feeder IED is detecting a sufficient zero-sequence current. Contrary, when the fault is on the busbar, the outgoing feeder will not detect a zero-sequence current; thus, the ZZ transformer IED will not be blocked. After the time setting $t_{e>>}$ expires, the ZZ IED will issue a trip command. However, the trip command is not sent to its CB but is communicated as a GOOSE message to the incoming feeder IED.

In order to achieve a greater selectivity, in terms of disconnecting only a minimal section of the busbar (when possible), the tripping signal of the ZZ feeder IED is not the only condition necessary for the incoming feeder IED to issue a trip signal to the respective CB. An additional condition will be that the incoming feeder IED will also need to detect a substantial presence of the zero-sequence voltage, set to 30% of the nominal voltage U_n . The check for a zero-sequence voltage presence is added to distinguish between the faulty and the healthy section when the bus coupler is open. This second condition also increases the certainty that an actual single-phase-to-ground fault occurred and that

³a small capacitive current from the cable will also pass through the outgoing feeder IED, but it can safely be neglected because of its small magnitude

the $I_{e_{>>}.Op}$ signal from the ZZ feeder IED is not due to a maloperation or unwanted trip due to maintenance operation. The value of 30% is chosen in such a way that it is high enough so only a single-phase-to-ground fault event would trigger this threshold, but at the same time low enough so even high-impedance faults will be detected. The addition of this second condition in the scheme requires the implementation of a simple AND logic in the incoming feeder IED. This implies that the incoming feeder IED will send a tripping command to the CB only when it receives a trip command from the ZZ IED and, simultaneously, detects a presence of zero-sequence voltage. This way, selectivity of the protection is provided, and the single-phase-to-ground busbar faults can be cleared quickly.

The basic principle of operation and communication in the scheme is presented on the flowchart in Figure 3.10.

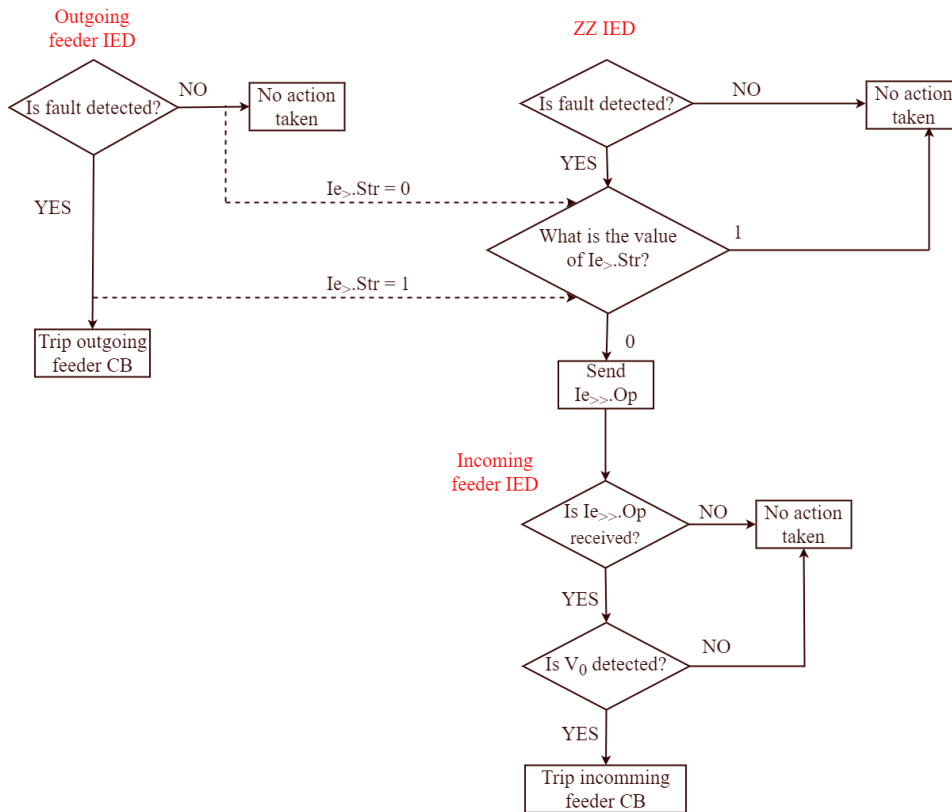


Figure 3.10: Principle of operation of the zero-sequence current tripping scheme

The sequence of operation is as follows:

- A fault on the outgoing feeder causes the $I_{e_{>}.Str}$ signal from this IED to change its value to 1. As a consequence, the operation of the ZZ IED is blocked. After the appropriate time setting expires, the outgoing feeder sends the tripping command ($I_{e_{>}.Op}$) to the CB, which clears the fault.
- A fault on the busbar does not cause a flow of zero-sequence current through the outgoing feeder. As a result, the $I_{e_{>}.Str}$ signal stays at a value of 0, which implies that the ZZ IED will not be prevented from operating. After the appropriate time expires, the ZZ IED sends the $I_{e_{>>}.Op}$ signal to the incoming feeder IED.
- When the incoming feeder IED receives the $I_{e_{>>}.Op}$ signal with a value of 1 from the ZZ IED, a check is done to determine the presence of zero-sequence voltage. If zero-sequence voltage is determined, a tripping signal is sent to the incoming feeder CB. When no zero-sequence voltage is detected, the CB is not tripped.

The performance of the algorithm has been demonstrated on a network topology represented in Figure 3.11.

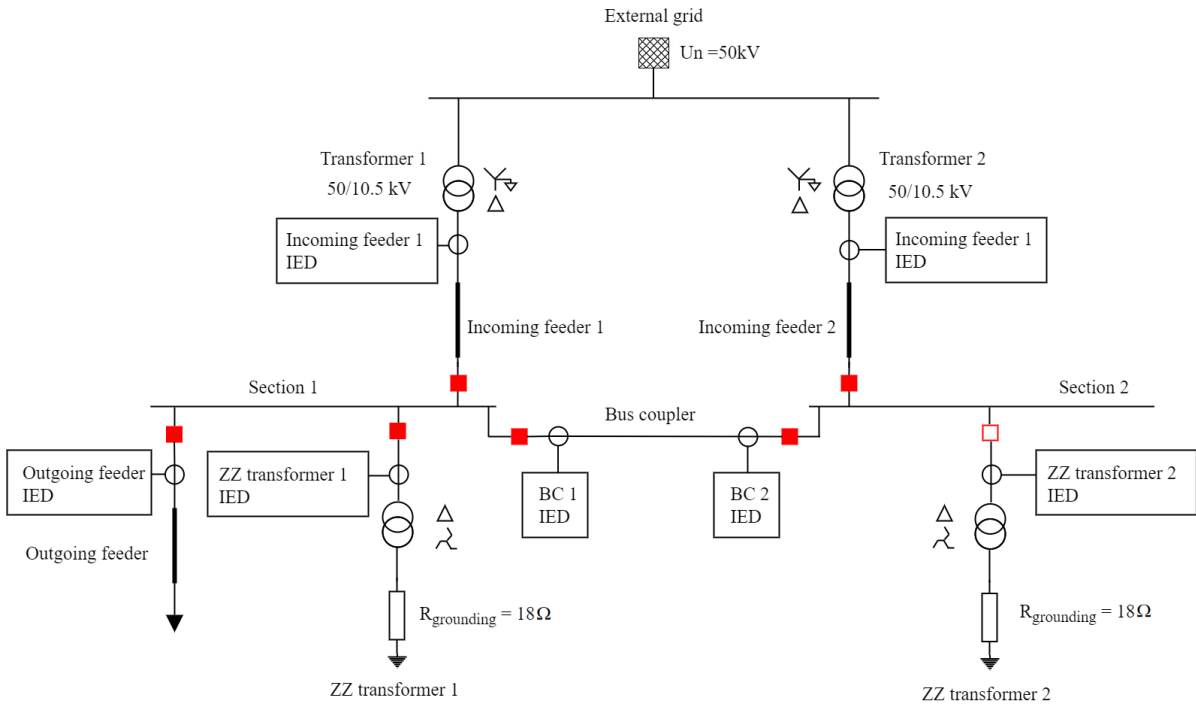


Figure 3.11: Test grid for testing the zero-sequence tripping algorithm

This test network consists of two sections of the busbar system. A ZZ transformer and an incoming feeder are connected to each section, and an outgoing feeder is connected only to Section 1. The bus coupler can be manually operated to connect or disconnect the two sections of the busbar system. Additionally, manual switching of the two ZZ transformers and the two incoming feeders is allowed to create different topologies.

The algorithm works in the same manner as it is explained above, however the $I_{e>>}.Op$ command from the ZZ transformer IED is now sent to the IEDs on both of the incoming feeders. These IEDs detect the presence of the zero-sequence voltage on their respective sections and, based on these two conditions, issue the necessary trip command to their CBs. The selectivity that is provided with the second condition ($U_0 > 0.3 * U_n$) in this case is easily explained with the two following figures. In Figure 3.12, we have the situation when the bus section coupler is closed, meaning that the two busbar sections are connected. When a single-phase-to-ground short circuit takes place on one of the busbar sections, the ZZ IED with its $I_{e>>}$ setting sends a TRIP signal to the IEDs on both of the incoming feeders. Additionally, both IEDs on these bays will detect a zero-sequence voltage, meaning that both conditions are met. According to the above-explained protection scheme, both feeders will be disconnected.

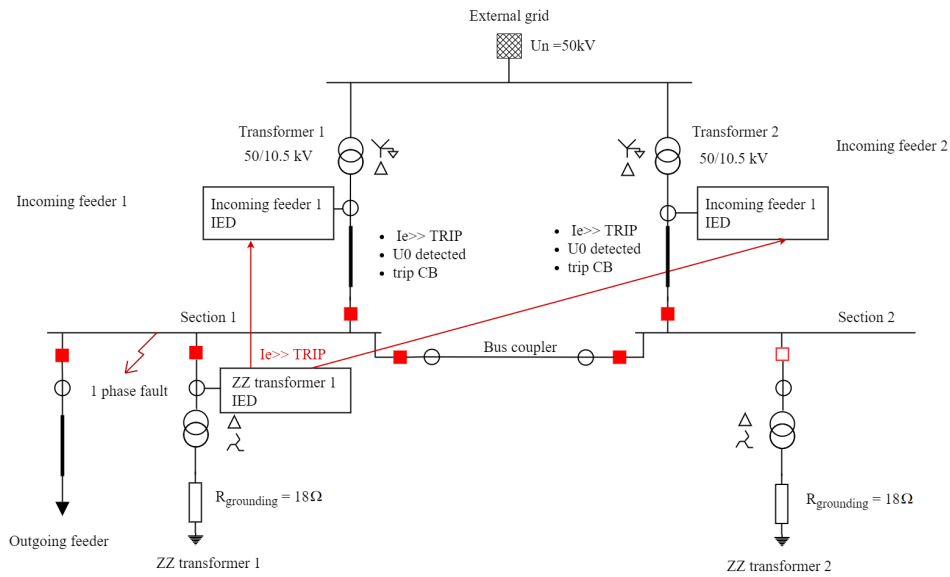


Figure 3.12: Operation of the scheme when the bus section coupler is closed

On the other hand, in Figure 3.13, we have the situation when the bus section coupler is open, meaning that the two sections of the busbar are functioning independently, being powered through the two different power transformers. An assumption is made that a single-phase-to-ground fault occurs in Section 1 of the busbar system. In this case, the IED of the feeder through which the ZZ transformer 1 is connected will detect the zero-sequence current and, after the respective time delay, will send a trip signal to the IEDs on both incoming feeders. However, only for Section 1 the condition about the presence of zero-sequence voltage will be fulfilled, meaning that only Section 1 will be disconnected from the power supply. In contrast, Section 2 would continue to operate uninterrupted. In that sense, the selectivity principle is provided in the case when the two sections of the busbar are operating independently.

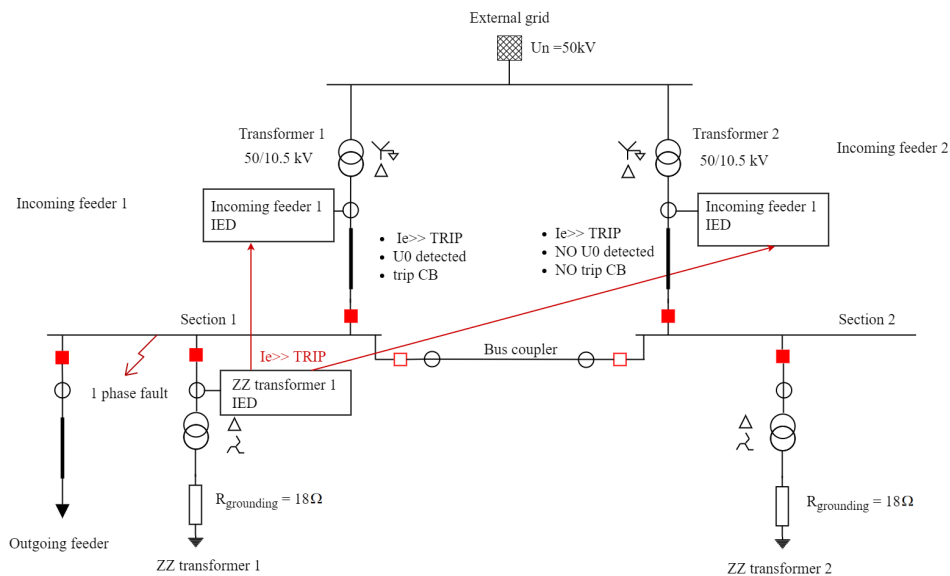


Figure 3.13: Operation of the scheme when the bus section coupler is open

Despite being out of the scope of the original problem, it was found that the ZZ feeder is also not protected in case a single-phase-to-ground fault occurs on it. The reason is that during an event like that, the short-circuit current is too low to be detected by the $I_{>>}$ setting of the IED on that feeder. At the same time, a great part of the current's zero-sequence component originates from the ZZ transformer and

does not pass through the CT whose outputs are used in the IED of this feeder. The only zero-sequence current detected from this IED is the capacitive current being fed from the other outgoing feeders, as shown in Figure 3.14.

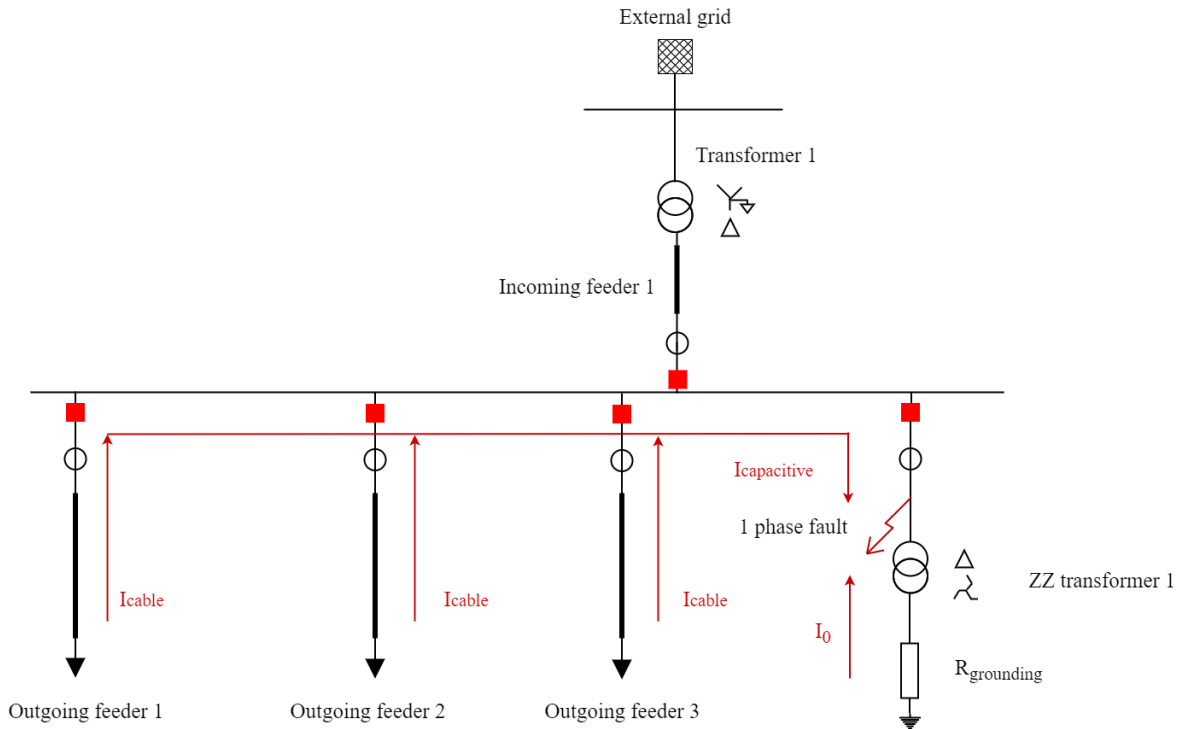


Figure 3.14: Current distribution for a single-phase-to-ground fault on the ZZ feeder

Nevertheless, this current has a very small magnitude (30-40 A⁴) in order to trip the $I_{e>}$ setting of the respective IED. That is why it was decided to use the negative-sequence current component to protect this feeder, which requires the implementation of $I_{neg>}$ setting in the IED.

The settings for the example of a typical substation are shown in Table 3.1, where the newly added settings, along with their operating times, are colored red.

	Outgoing feeder IED	Incoming bay IED	ZZ feeder IED
$I_{>}$ [A] - t[s]	360 - 0.9	2800 - 1.8	/
$I_{>>}$ [A] - t[s]	1500 - 0.3	5200 - 0.2	1500 - 0.3
$I_{e>}$ [A] - t[s]	150 - 0.9	/	150 - 5
$I_{e>>}$ [A] - t[s]	/	/	250 - 0.3
$I_{neg>}$ [A]	/	/	75 - 0.3
V_0 [kV]	/	1.7	/

Table 3.1: Protection settings for a medium-voltage substation

As it can be seen from the table, the only new settings that need to be implemented (on the top of the ones that are already in use in the grid of Stedin) are located in the IED on the feeder connecting the ZZ transformer, namely the $I_{neg>}$ and the $I_{e>>}$ setting. None of the already existing settings or timings were changed, and the time for the newly introduced settings was chosen to be 0.3 seconds. The time for the $I_{neg>}$ was chosen to be 0.3 seconds to correspond to the already used protection for

⁴the magnitude varies with the network topology

that feeder (also, no selectivity issues arise in this part, so the protection setting did not need to be time-graded with the rest of the network). The situation is a bit more complex for the time setting of the $I_{e>>}$ setting, since it effectively trips the busbar, so time-grading and selectivity had to be considered. The first consideration that was taken into account is that even a fault on the 10.5 kV side of Transformer 1, but before CT on the incoming feeder (Figure 3.15) would cause the $I_{e>>}$ setting of the ZZ transformer 1 IED to send a trip command to the Incoming feeder 1 IED.

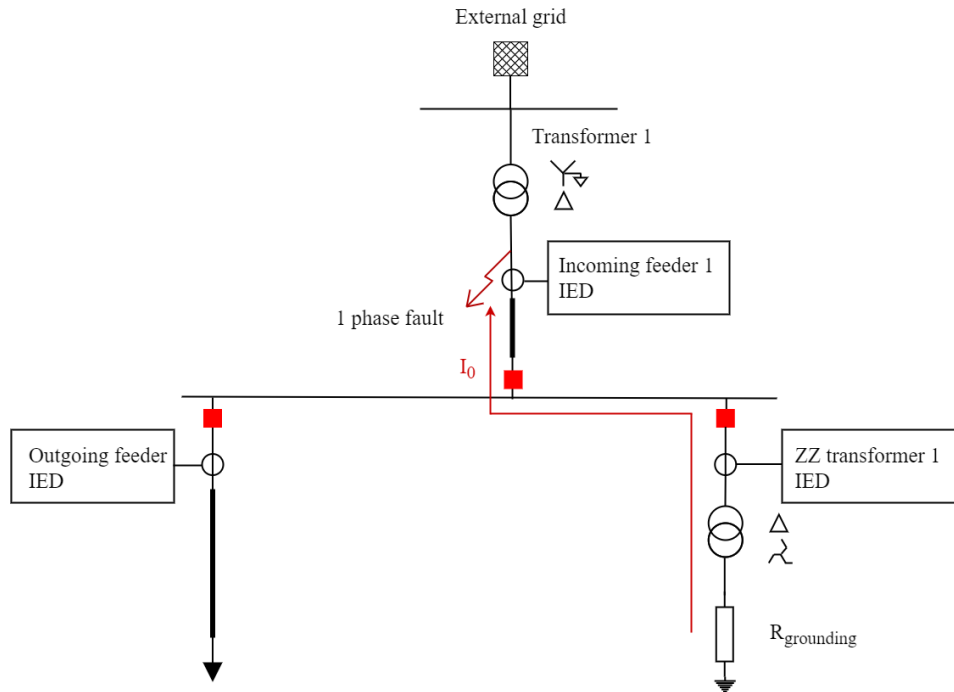


Figure 3.15: Zero-sequence current distribution for a fault between the secondary side of the transformer and the current transformer

However, because of the selectivity principle, the transformer differential protection should clear this fault prior to the busbar protection operation. The transformer differential protection operates in around 50 ms, and taking into account the maximum opening time of the used NX PLUS C CB of 80 ms (Appendix B), results in the fact that the time for the $I_{e>>}$ setting of the ZZ feeder IED can be safely set to 200 ms, and the selectivity upon a fault in the transformer protection zone will still be satisfied. One should note that the zero-sequence component will also appear in the case of a two-phase-to-ground fault that occurs in the substation zone. The two-phase-to-ground fault has a magnitude that is sufficient enough to be detected by the $I_{>>}$ settings of the incoming feeders and bus coupler IEDs. In this case, an advantage should be given to the bus section coupler CBs to separate the two sections and thus provide selectivity to a certain extent between the healthy and the faulty zone. The time of the $I_{>>}$ setting of the bus coupler IEDs is 100 ms, which along with the CB opening time of 80 ms, makes it very close to 200 ms, thus giving a small time margin. Because of this reason, it was decided to increase the time $t_{e>>}$ of the operation of the $I_{e>>}$ setting of the ZZ IED to 300 ms.

3.4. Testing the protection scheme by Omicron RelaySimTest

In order to validate the scheme, initially, it was tested by making use of the Omicron RelaySimTest toolkit. It is a package that allows for simulating short circuit events in a grid, after which the simulated currents and voltages can be passed to Omicron amplifiers, which are afterward used as analog inputs in the IEDs. The IEDs are part of the MOTA⁵ environment, which is Stedin's standardized modular system for designing, testing, and acceptance of protection and control functions. This environment can be seen as a test substation, where all of the standard protection functions and schemes that are

⁵Modulair Ontwerpen, Testen en Accepteren - Modular Design, Test, and Acceptance

being used in Stedin's grid are implemented. All IEDs are connected through Ethernet to the same sub-network, so a GOOSE communication between them is enabled.

The simulated version of the grid is presented in Figure 3.16, and it can be noted that it has the same characteristics as already explained typical 10kV substation of Stedin, where for all of the simulations that are later presented, the ZZ transformer 2 was disconnected.

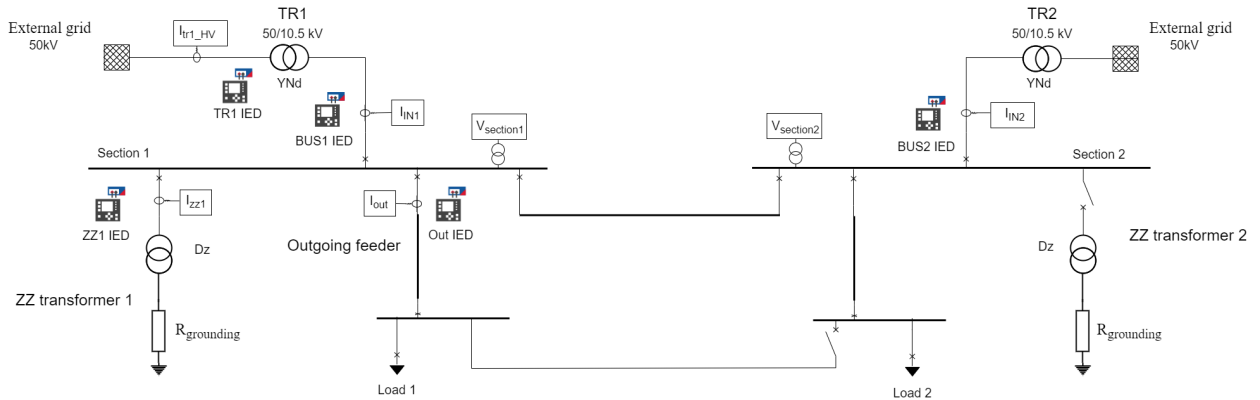


Figure 3.16: Simulated grid in Omicron RelaySimTest

The setup for testing the protection scheme with the Omicron RelaySimTest software and amplifiers is shown in Figure 3.17.

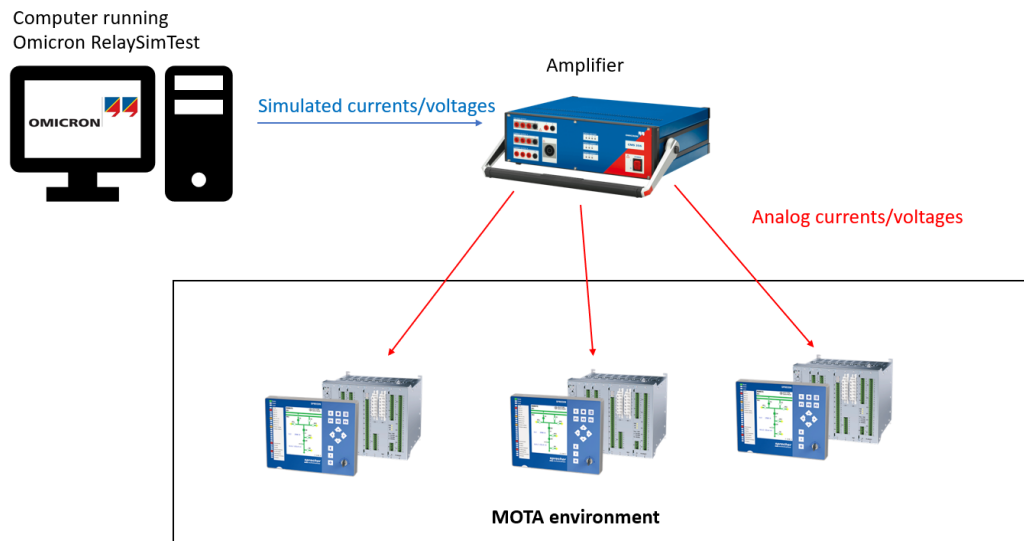


Figure 3.17: Test setup for the offline testing with Omicron in the MOTA environment

Five currents and two voltages from the grid are passed to the Omicron amplifiers, which are then fed into the respective IEDs. The currents that are passed are the currents that pass through both incoming feeders (denoted with I_{IN1} and I_{IN2}), the outgoing feeder (I_{OUT}), ZZ transformer 1 feeder (I_{ZZ1}) and the current that is on the high voltage (50kV) side of Transformer 1 (I_{tr1_HV}). The currents I_{IN1} , I_{IN2} , I_{OUT} , and I_{ZZ1} are fed as inputs to the respective IEDs - BUS1 IED, BUS2 IED, Out IED, and ZZ1 IED. TR1 IED is a transformer differential protection IED, so both currents I_{tr1_HV} and I_{IN1} are fed to it as inputs. The voltage measurements from both sections ($V_{section1}$ and $V_{section2}$) are passed as inputs only to the incoming feeders IEDs (BUS1 IED and BUS2 IED), as only they require voltage inputs for their decision-making.

Several tests were accomplished with this setup, and only a few of them are presented here. Firstly, we have the case when the fault is in the outgoing feeder. As we can see in Table 3.2, the outgoing feeder

IED sends its TRIP signal around 913ms from the fault's appearance, which is in correlation to the set time delay of 900ms⁶.

Table 3.2: Simulation results from Omicron for a fault on the outgoing feeder

Out Ie>start	Out Ie>trip
13.0 ms	912.9 ms

What is also important to note in this figure is that the value of Out Ie> start is only 13ms. This means that the time needed for the outgoing feeder IED to detect the fault and send the block signal to the ZZ transformer feeder IED is 13ms. This is a large time-margin of safety that for an outgoing feeder fault, the ZZ feeder IED will be blocked before it can send its trip command⁷.

In Table 3.3, the tripping times can be seen for a case when the fault is on the busbar, and the bus section breaker is open.

Table 3.3: Simulation results from Omicron for a fault on section 1, when the bus coupler is open

ZZ1 Ie>>	BUS1 trip	BUS2 trip
308.9 ms	312.6 ms	+∞

As it can be seen, the ZZ feeder IED sends its trip command only after 309ms (which means it can detect the fault in just 9ms from its start). The incoming feeder IED sends its trip command after 312.6ms, which shows that there is practically no delay because of the communication. Additionally, it is important to notice that the incoming feeder 2 IED is not sending a trip signal because the second condition of $U_0 > 0.3 * U_n$ is not satisfied, which means that the scheme is operating according to the expectation.

Finally, the case when the fault is between the secondary side of the transformer and the CB on the same feeder is analyzed, which means that the fault is in the transformer protection zone. The tripping times for this simulation case are shown in Table 3.4.

Table 3.4: Simulation results from Omicron for a fault in the transformer protection zone

TR1 trip	BUS1 trip	BUS2 trip	ZZ1 trip
40.1 ms	310.9 ms	312.4 ms	5008.1 ms

The differential protection is the first to be tripped after around 40ms, which means that selectivity is satisfied. The tripping time of the differential protection is short enough to be guaranteed that there will not be any overlapping with the busbar protection trip.

From the last figure, we can see that although the transformer differential protection is the first one to send the trip signal, trip signals are also sent from the incoming transformer feeders (busbar protection scheme) and the ZZ feeder IED ($I_{e>}$ setting). This is because this way of testing is offline, which does not fully replicate the real-life interaction between the grid, the IEDs, and the CBs. This means that this way of testing can serve for testing the protection functions and schemes implemented in the IEDs. However, the tripping signals sent from these IEDs do not influence the rest of the simulation, meaning that the integrity of the grid and the protection scheme cannot be tested simultaneously. In order to have more precise testing of this protection scheme and realize whether it causes some possible problems for the grid integrity, it was decided to perform real-time Hardware-in-the-Loop (HiL) testing of this protection scheme. A HiL testing enables real-time testing to see how the hardware, IED in this case, reacts in real time to realistic virtual inputs. This way of testing allows the protection scheme to be tested to see how it affects the grid and simultaneously test the real physical IEDs. The RTDS (Real-Time Digital Simulator) was chosen for this purpose since it is a tool that allows for this kind of testing.

⁶this is the time for the actual trip command to be sent, the CB operation time is not included

⁷even with the worst-case scenario, with a latency of 4ms for the GOOSE message to reach its destination, the time is less than 20ms

4

Testing the algorithm in RTDS

Testing the protection algorithms by various testing platforms is crucial before being implemented for actual applications. Most simulation packages used for protection testing are normally for offline simulation, which does not consider the interaction between the protection IED and the simulated grid. This means that we can either test the device itself or the grid operation, however, simultaneously both cannot be tested. The RTDS, on the other hand, allows for real-time simulation and HiL testing, in which the interaction between the simulated grid and the connected physical IED is also taken into account. This means that both the physical IED and the integrity of the network can be tested simultaneously. In this section, the complete procedure to prepare the closed-loop testing of the proposed scheme is elaborated. Finally, the simulation scenarios are presented, and the results are discussed.

4.1. Modeling the grid in RSCAD

The power network model and the algorithm were implemented and simulated in RTDS, which allows for simulating real-time power system events. It ensures the accuracy of the testing results, and it allows for hardware-in-the-loop (HiL) testing, at the same time offering the possibility of different communication protocols. In order to run a HiL simulation with the RTDS, the network should firstly be simulated in the RSCAD software, a power system software used for interfacing with the RTDS hardware.

Therefore, the test network was modeled in RSCAD and verified by the one simulated in PowerFactory. The parameters of the cables, the transformers, the external grid, and the ZZ transformer are summarised in Appendix C. CTs on the outgoing feeder, the ZZ transformer feeders and the bus coupler are modeled by a transformer ratio of 600/1, and on the incoming transformer bay, with a ratio of 2500/1. The rest of the parameters of the CTs are left the same as the nominal values of the CT model provided by RTDS library. VT models are also installed on both busbar sections, and their ratios are 10500/110. Figure 4.1 presents the grid's one-line diagram.

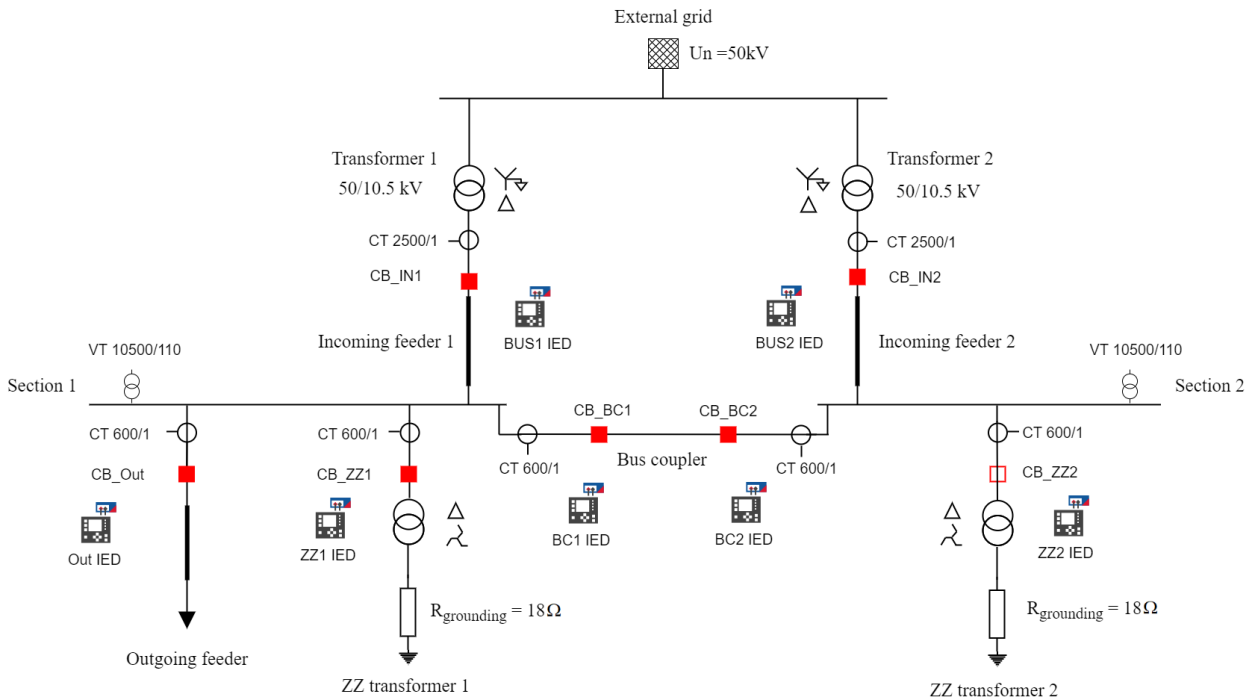


Figure 4.1: Model of the substation in RSCAD

The signals that are later used in the simulations, alongside their explanation, are the following:

- BUS1_TRIP - trip signal from BUS1_IED to trio CB_IN1
- BUS2_TRIP - trip signal from BUS1_IED to trip CB_IN2
- Out_TRIP - trip signal from OUT_IED to trip CB_Out
- Out_Ie>.Str- start signal from the Ie> setting of Out_IED
- ZZ1_Ie>>.Str - start signal from the Ie>> setting of ZZ1_IED
- ZZ1_Ie>>.Op - operating signal from the Ie>> setting of ZZ1_IED
- ZZ1_Ineg>.Str - start signal from the Ineg> setting of ZZ1_IED
- ZZ1_Ineg>.Op - operating signal from the Ineg> setting of ZZ1_IED
- ZZ2_Ie>>.Str - start signal from the Ie>> setting of ZZ2_IED
- ZZ2_Ie>>.Op - operating signal from the Ie>> setting of ZZ2_IED

The protection functions are simulated by the virtual IEDs available in the RSCAD library, which already have the over-current logic implemented. Part of such a virtual IED can be seen in Figure 4.2,

which represents the IED on the outgoing feeders. The part that is shown is used for the earth-fault current protection. As it can be seen, the IED requires the secondary currents from the respective CT connected to the outgoing feeder ($I_{a_outgoing}$, $I_{b_outgoing}$, and $I_{c_outgoing}$). One can see that voltage inputs (VA, VB, and VC) are also required by the default RSCAD over-current IED. However, since the IED operates as non-directional, these voltage inputs are not later used by the IED logic. As outputs, the IED provides the Trip signal, which is used as a command to trip the CB on the outgoing feeder. The Start (pickup) signal is also provided, and it is later used as a blocking signal for the $I_{e>>}$ settings of both ZZ transformer IEDs.

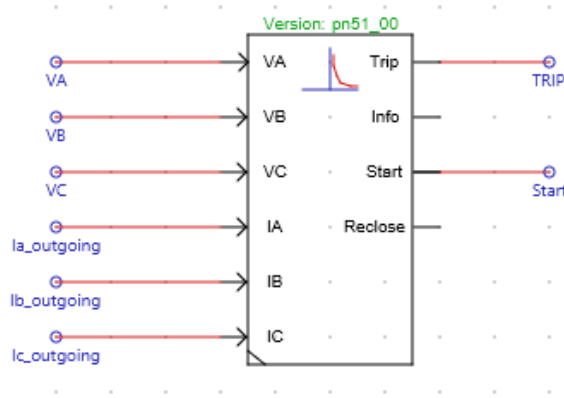


Figure 4.2: Model of the outgoing feeder IED in RSCAD

Table 4.1 shows which settings are entered for this part of the IED (the pickup current is entered in secondary value).

Table 4.1: Settings of the outgoing feeder IED in RSCAD

Directional control	OFF
Operating curve type	DEFINITE
Start Value (pickup)	0.25 A
Operate time delay	900 ms
Reset Time Delay	100 ms

As mentioned before, Stedin's requirements for the operation of their CBs allow for a maximum opening time of 80ms. That is why this time was given as the needed time for the virtual CBs in the RSCAD environment to open their contacts and clear the fault.

For the HiL testing, it was decided that the IED from the type Sprecher C1 placed on the feeder connecting the ZZ transformer 1 to the busbar will be tested. This is because this IED is the one most involved in the whole protection scheme since it is responsible for detecting single-phase faults in the first place and, is also included in sending and receiving the GOOSE messages.

In the following section, the connection of the Sprecher IED to the RTDS and setting up the communication is explained in more detail. The details of setting up the internal logic of the Sprecher IED can be found in Appendix D.

4.2. Communication between the Sprecher IED and the RTDS

Figure 4.3 illustrates the setup through which the HiL testing is supposed to be carried.

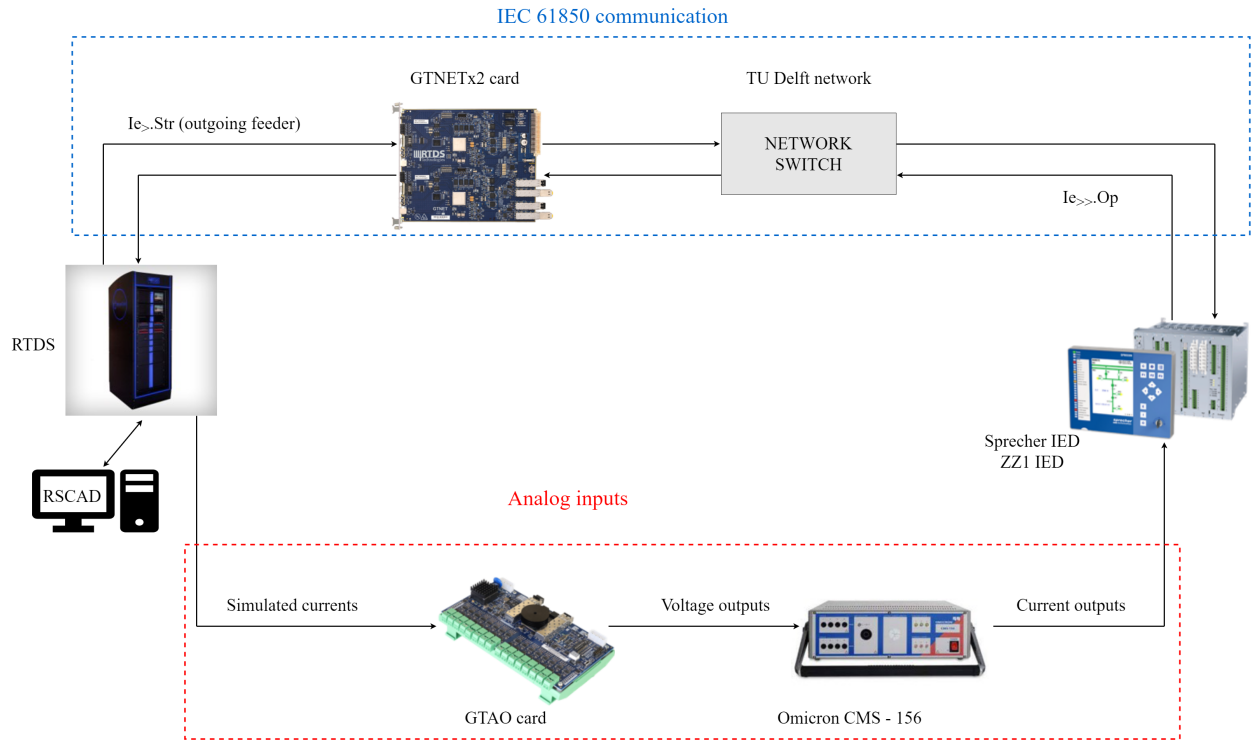


Figure 4.3: Illustration of the HiL test setup for testing the zero-sequence tripping scheme

As it can be seen, the Sprecher IED receives both analog and digital inputs from the RTDS. The analog values that are passed to the IED are, in fact, the secondary currents of the respective CT. These values are sent as analog signals since the applied Sprecher IED (with the current firmware that Stedin uses) is not capable of using Sampled Values (SV). The simulated values from the secondary side of the CT are firstly passed to the GTA0 (Gigabit Transceiver Analogue Output) card. As an output, the GTA0 card produces voltage signals in the +/- 10V range, which are passed as inputs to the Omicron CMS - 156 amplifier. The conversation ratio of the CMS - 156 states that 1 V of input will produce a current output with a magnitude of 5 A (Appendix E). The outputs of the CMS - 156 are then fed as inputs to the Sprecher IED, which then uses them in its internal protection logic. The output currents from the Omicron CMS - 156 must correspond precisely to the simulated secondary currents in the RTDS, as it is explained in [15].

The digital inputs requested from the Sprecher IED (the blocking signal) are communicated as GOOSE messages by utilizing the IEC 61850 standard. The GOOSE communication between the RTDS and the Sprecher IED is achieved through the GNETx2 card, which is the standard component for interfacing an external device with the RTDS [16]. In order to set up this communication properly, the ICT configuration tool must be used.

To communicate GOOSE messages from and back to the RTDS, a virtual component needs to be created in the ICT configuration tool, which is then linked to the RSCAD draft variables by the GNET-GSE component. In this way, it is allowed for draft variables to be sent as GOOSE messages to external devices, for internal use, but also it is possible that GOOSE messages from external devices can be used as draft variables in the RSCAD environment. This virtual component is set to provide blocking GOOSE signal from the outgoing feeder (explained in Section 3). At the same time, this virtual component is subscribed to two tripping signals from the external Sprecher IED ($I_{e>}.Trip$ and $I_{neg>}.Trip$), which are then used as draft variables in the simulation process. Even though, in reality, the publisher and subscriber would be three different devices (outgoing feeder IED, incoming bay IED, and ZZ feeder CB), in the ICT Configuration Tool, we simulate them as one component since it does not have any influence on the simulation itself. The GOOSE messages that are sent or received are linked with their designated draft variable name, so it is not essential from which virtual component in the ICT Configuration Tool they originate. In order to be able to use the GOOSE messages from the external Sprecher IED, the Configured IED Description (CID) file of this IED has to be imported into the ICT

configuration tool. In this way, it is enabled for the external IED GOOSE commands to be published in RTDS environment. One of the crucial parameters that need to be set in the ICT configuration tool is the MAC addresses of the publishing signals, which have to correspond to the address to which the external IED is configured for receiving messages. The explanation of how to properly set the publishers and subscribers in the ICT Configuration Tool is provided in [8] in more detail.

However, due to unforeseen circumstances with the connection of the Sprecher IED to the TU Delft network, the setup had to be adjusted. This adjustment is needed only for the part of the GOOSE communication, meaning that the connections for the analog current inputs to the Sprecher IED remain the same as shown in Figure 4.3. In Figure 4.4, only the adjusted part regarding the GOOSE communication is shown, whilst the part regarding the analog currents is omitted since there is practically no change made in that segment.

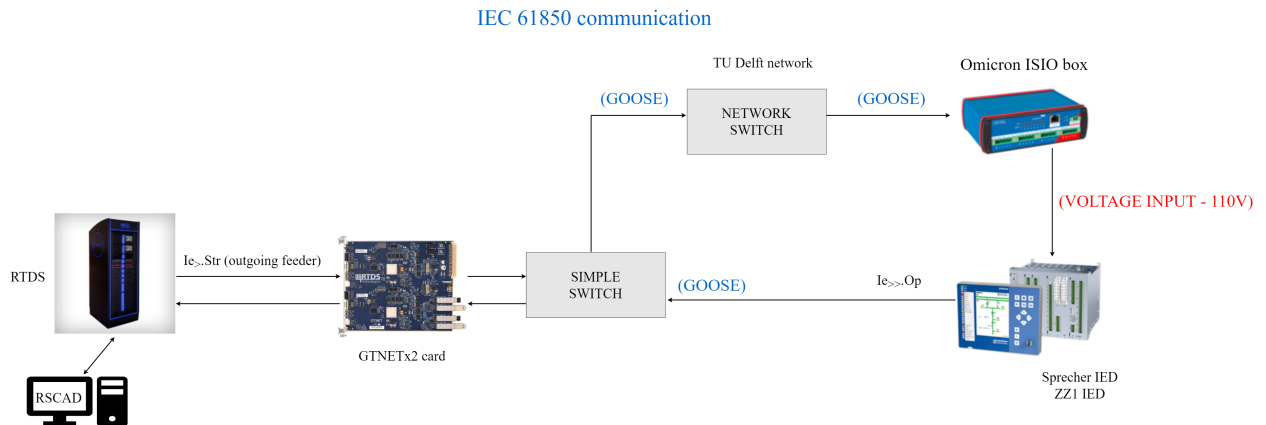


Figure 4.4: Adjustment of the IEC 61850 communication test setup

The first change is that the GOOSE messages from the Sprecher IED are not going through the network switch but are directly connected to the RTDS. Furthermore, the GOOSE messages from the RTDS are still going through the network however, they are now subscribed to Omicron ISIO 200 box instead of the Sprecher IED. The Omicron ISIO 200 box is a flexible binary I/O terminal with an integrated IEC 61850 interface¹. This terminal is subscribed to the GOOSE message published from the RTDS and, based on the value of this message, is passing a binary output (110 V) to the Sprecher IED. This voltage signal is used to block the $I_{e>>.Op}$ command of this IED, substituting effectively the $I_{e>.Str}$ GOOSE signal, which was supposed to be used for blocking. With these minor adjustments, the IEC 61850 GOOSE communication was resolved, and the HiL testing of the scheme was made possible.

4.3. HiL simulation

After the draft file is successfully compiled, the Runtime window from the RSCAD software is where the simulation is run. The simulation process will be explained by making use of Figure 4.5.

¹<https://www.omcronenergy.com/en/products/isio-200/>

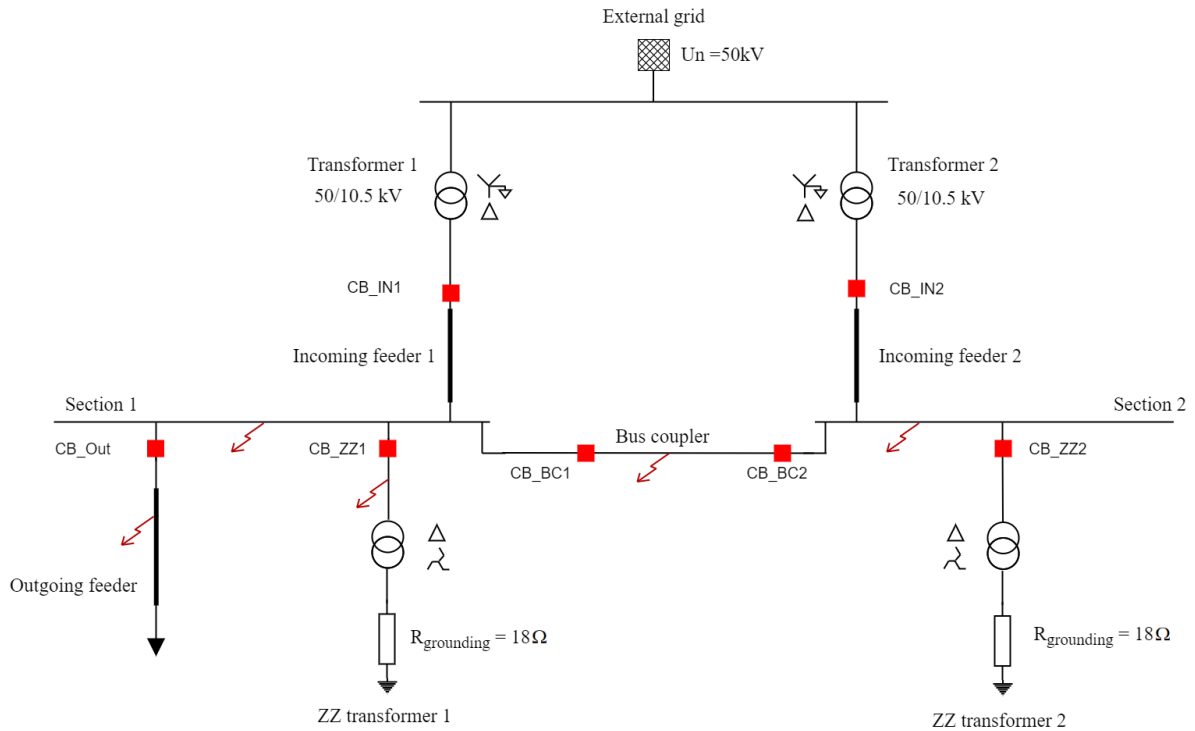


Figure 4.5: One-line diagram of the simulated grid in RSCAD

As it can be seen, for the simulation of the protection scheme faults will be placed on five different locations:

- Section 1
- Section 2
- Bus coupler
- Outgoing feeder
- ZZ transformer 1

They are activated through the respective push buttons placed in the simulation window. Also, through a slider, it is allowed to control at which point on the wave of the sinusoidal voltage the short circuit takes place (e.g., it can be chosen that the fault happens on the zero-crossing of the voltage). The CBs on the incoming feeders 1 and 2, the CBs on the bus coupler, and the CBs on both ZZ transformers can also be manually opened and closed. This possibility allows for creating different operational scenarios in which the algorithm will be tested. As discussed with Stedin, there are four common operational topologies in their grids, as presented in Figure 4.6 -4.9. In all topologies, the red square denotes that the CB is closed, while an empty square represents an open CB.

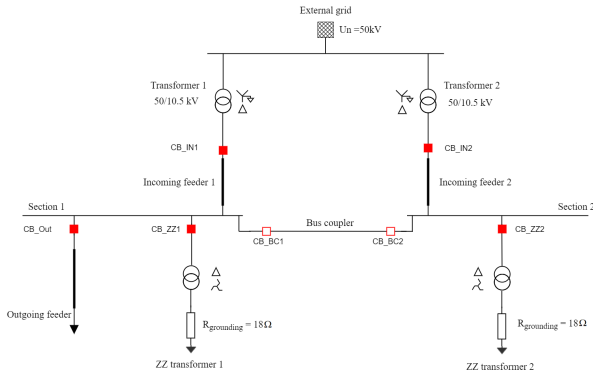


Figure 4.6: Topology 1 - sections disconnected

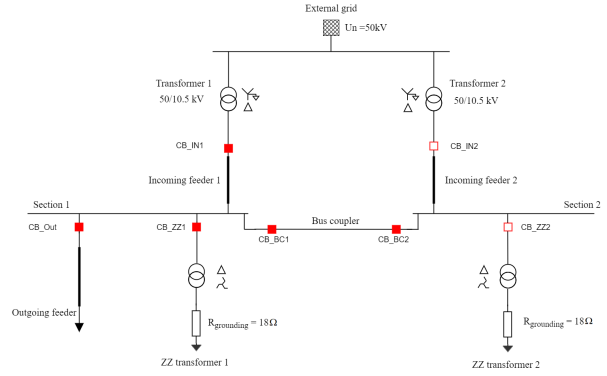


Figure 4.7: Topology 2 - One incoming feeder and one ZZ transformer

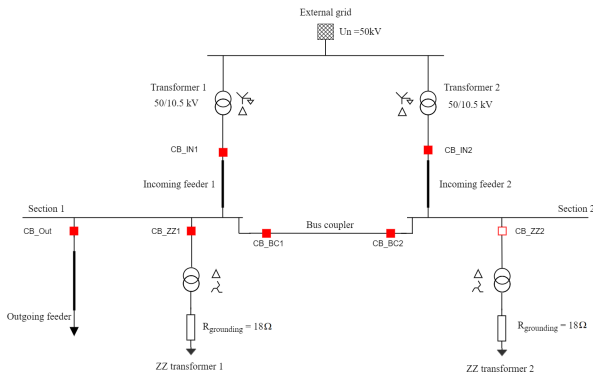


Figure 4.8: Topology 3 - Two incoming feeders and one ZZ transformer

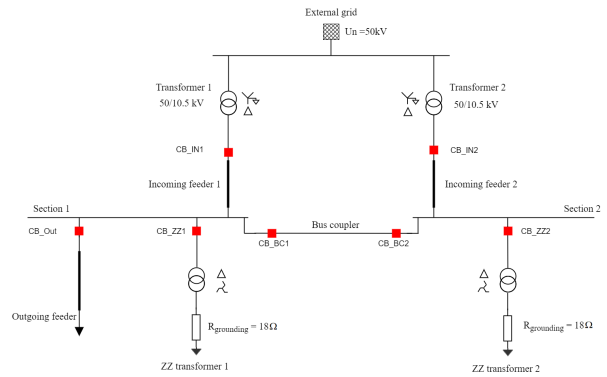


Figure 4.9: Topology 4 - Two incoming feeders and two ZZ transformers

As we can see, cases 1 to 4 differ in whether the bus coupler is closed or not, and on the number of incoming feeders and ZZ transformers that are currently switched in. Topology 1 represents a scenario when both sections of the busbar system work independently, i.e., the bus coupler is open. In all of the other scenarios (Topology 2 to 4), the bus coupler is closed, and the sections are connected. Topology 2 represents an operating scenario where the substation is fed from only one incoming feeder, and the network grounding is provided through only one ZZ transformer. In Figure 4.7, it can be seen that only incoming feeder 1 and ZZ transformer 1 are connected, while the incoming feeder 2 and ZZ transformer 2 are switched off. However, it must be pointed out that the results will be the same for any combination of one incoming feeder and one ZZ transformer. Topology 3 again represents a scenario where only one ZZ transformer is switched in, but the substation is powered through both of the incoming feeders, as shown in Figure 4.8. Once more, the results will be the same regardless whether ZZ transformer 1 or ZZ transformer 2 is switched in. These three cases are the ones in which the 10kV grids are only allowed to operate according to Stedin’s policy.

Nonetheless, sometimes for a short time, the grid topology can be presented as in Figure 4.9, in which both of the incoming feeders are connected, the bus coupler is closed, and both of the ZZ transformers are connected. That is why even though this topology is not in accordance with Stedin’s policy, it was also decided to be part of the investigation. For all of these 4 cases, simulations were carried out with faults simulated on the five locations listed above (one fault at a time). All simulated faults are single-phase-to-ground faults on phase A, with a fault resistance of 0.001Ω , and the results from the simulations are presented in the following section.

4.4. Simulation results

In the following section, the results of some of the simulations are discussed. The presented simulations are chosen in such a way that they offer an insight into the most crucial aspects of this algorithm.

Case 1 : Fault on an outgoing feeder

The first simulation results discussed are for the case of a single-phase-to-ground fault on the outgoing feeder when the grid is operating as described in Topology 3, as presented in Figure 4.10.

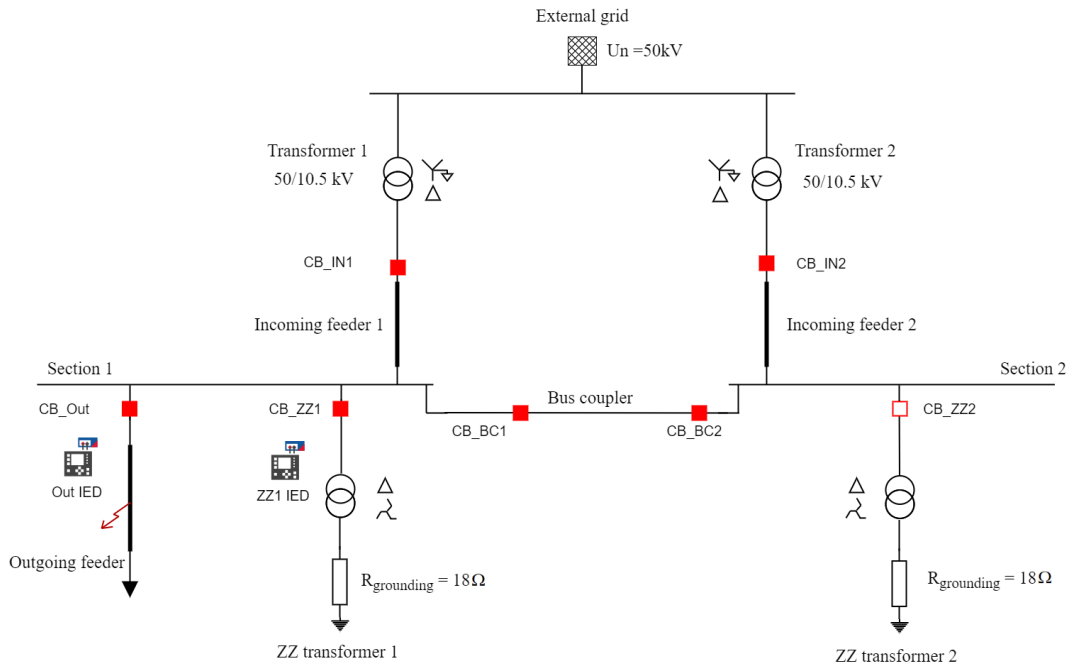


Figure 4.10: Case 1: Fault on an outgoing feeder in Topology 3

Figure 4.11 presents the simulation results for this case. As seen in the figure, the fault occurs at the time instance of 20.6 ms. It can be noted that the current in phase A, as discussed, has an insufficient magnitude in order to activate the over-current protection of the IED on the outgoing feeder - Out IED. However, it can be seen that the zero-sequence current that passes through this IED is sufficient enough to activate the earth-fault protection setting. The IED requires around 7ms to detect the fault, after which the 'Out_Ie>.Str' signal is activated. At this time, a timer starts, which is compared to the time delay $t_e >$, which for this IED is 900ms. After the time expiration, the Out IED sends the tripping command, as shown in Figure 4.11. The fault is finally cleared around 970ms from its beginning. The signal 'Out_Ie>.Str' is sent as a GOOSE message to the ZZ1 IED to prevent the operation of its $I_{e>>}$ setting. One can notice that the blocking is done successfully, as the $ZZ1_{I_{e>>}.Op$ signal remains at a value of zero during the entire fault duration. These simulation results prove the selectivity and the desired operation of this protection scheme in the case of a single-phase-to-ground fault on the outgoing feeder.

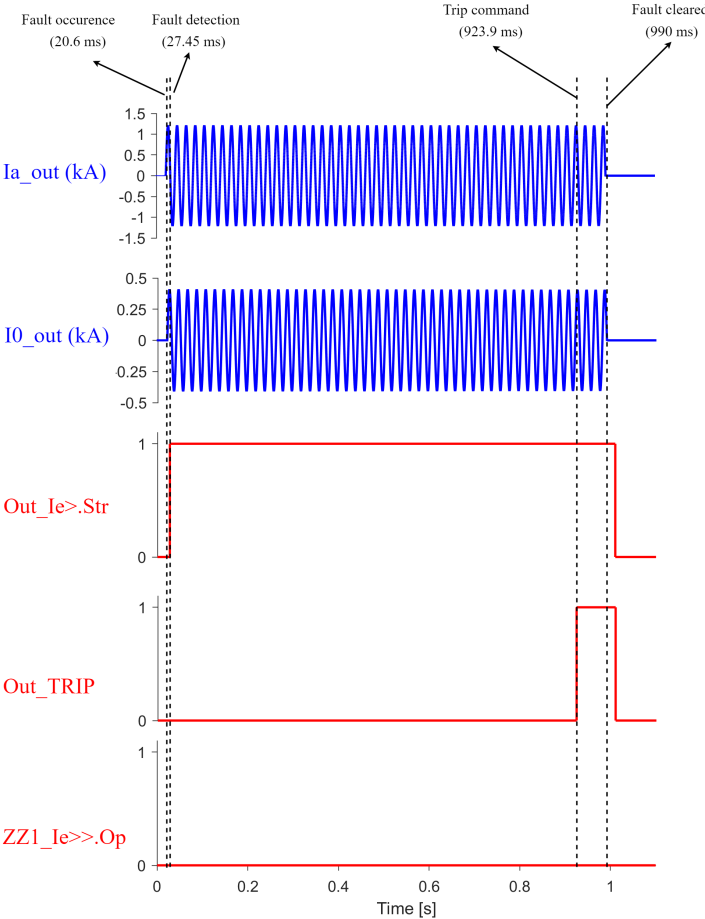


Figure 4.11: Simulation results for a fault on an outgoing feeder in Topology 3

Case 2: Fault on Section 1 of the busbar system, with the bus bus section breaker being opened

The second case discussed here is when a fault occurs on Section 1 of the busbar system when the network is operating according to Topology 1. A schematic of this scenario is presented on Figure 4.12.

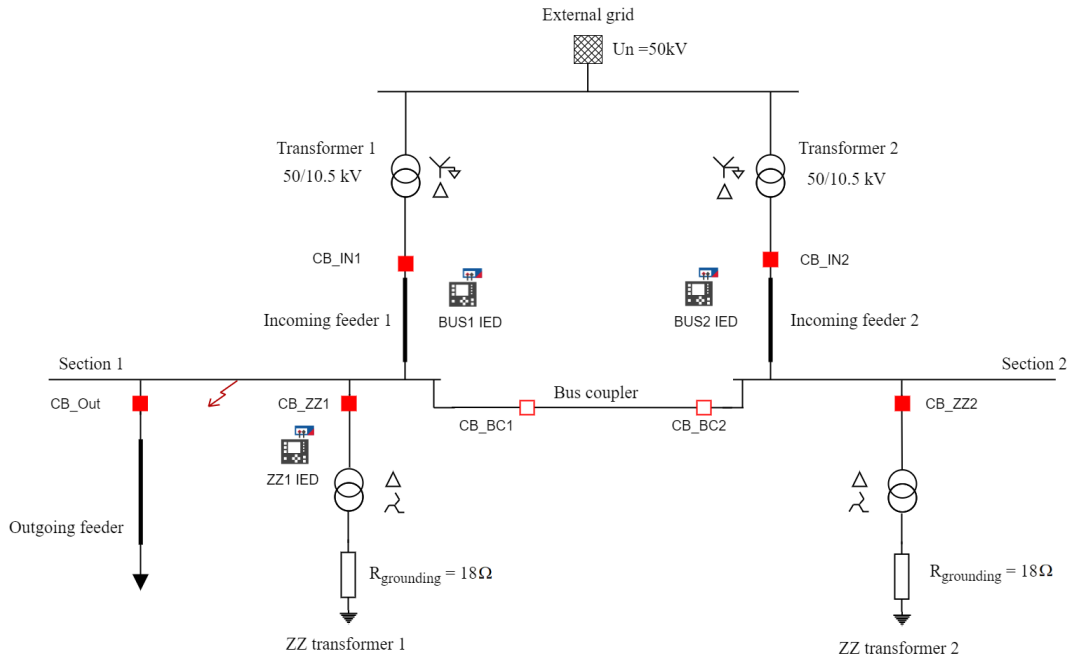


Figure 4.12: Case 2: Fault on Section 1 in Topology 1

The results from this simulation can be observed in Figure 4.13, where only the necessary signals for the observations are included. The single-phase-to-ground fault occurs at time $t=9.95\text{ms}$. As discussed, the current I_{a_in1} , that is, the current flowing through incoming feeder 1, is too low to trip the $I >>$ setting of BUS1 IED. The fault current is picked up by the ZZ1 IED after around 5 ms. After the time $t_{e>>}$ expiration, ZZ1 IED sends the tripping command to BUS1 and BUS2 IED, which happens at time $t=318.95\text{s}$. However, as seen in Figure 4.13, only in section 1 there is a sufficient presence of a zero-sequence voltage, while in section 2, the magnitude of the zero-sequence voltage is almost zero. As a result, the second condition is only satisfied for BUS1 IED, and it issues a trip signal to its CB (CB_IN1). In contrast, no trip command is sent by the BUS2 IED as the zero-sequence over-voltage condition is not satisfied. The fault is finally cleared after around 390ms from its appearance.

It should be noted that the timings for the signals $ZZ1_I_{e>>}$ and $BUS1_TRIP$ are the same since the GOOSE messages (according to the previously explained test setup) from the Sprecher IED are directly connected to the RTDS. This means that no network latency is introduced. In reality, there will be some small latency, but according to the standards, it is limited to 4ms, which means that that delay will not influence the basic principle of operation of this scheme.

This simulation case proves the selectivity brought to the scheme by adding the second condition $U_0 > 0.3 * U_n$. The same results are obtained in the case when the fault is taking place on Section 2 of the busbar system.

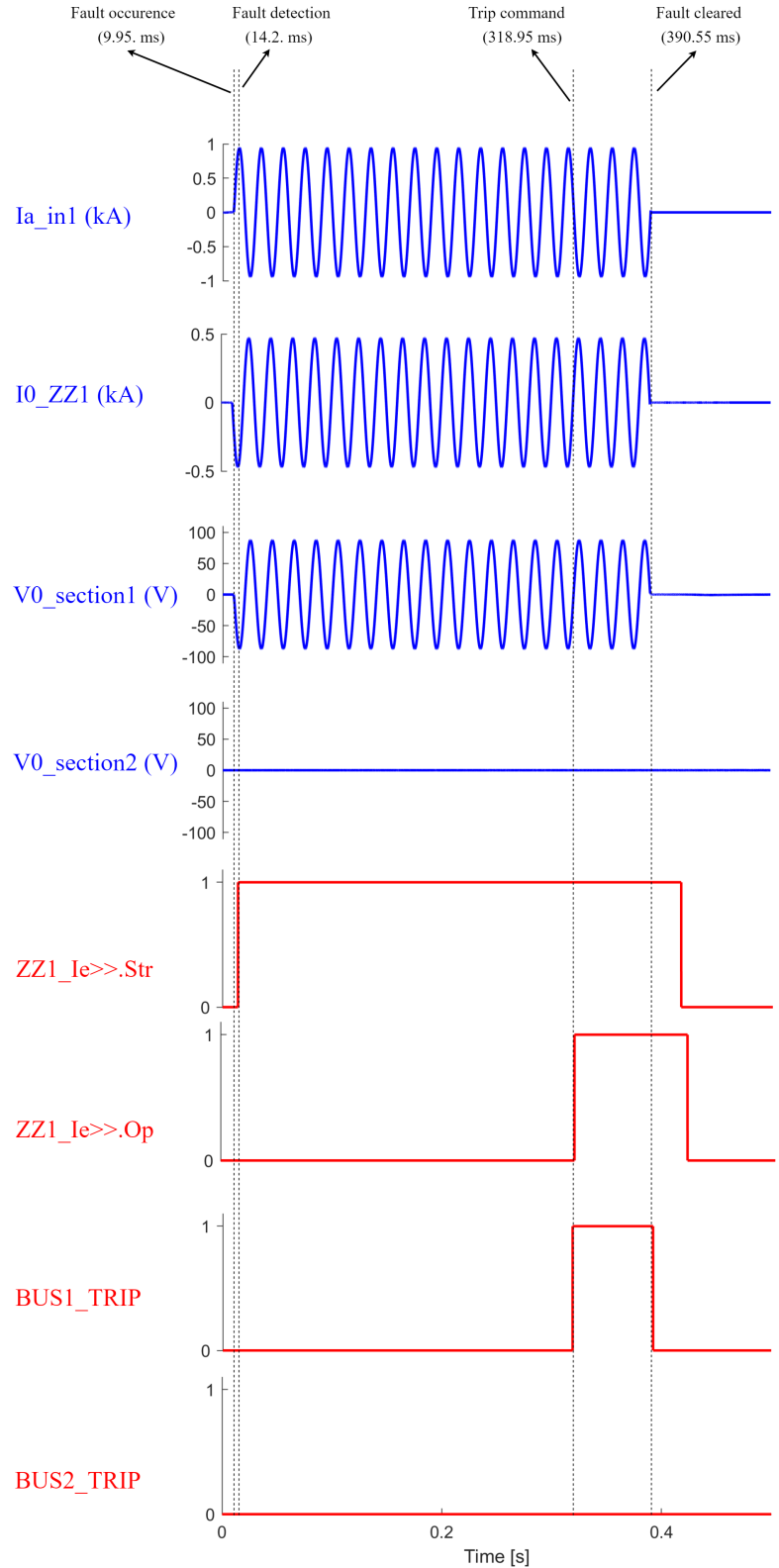


Figure 4.13: Simulation results for a fault on Section 1 in Topology 1

Case 3: Fault on Section 1 of the busbar system, with the bus bus section breaker being closed

The following case is again when a fault occurs on Section 1 of the busbar system. However, the bus coupler is now closed, meaning that the network operates according to Topology 3 - Figure 4.14, and the results from it are accordingly presented in Figure 4.15.

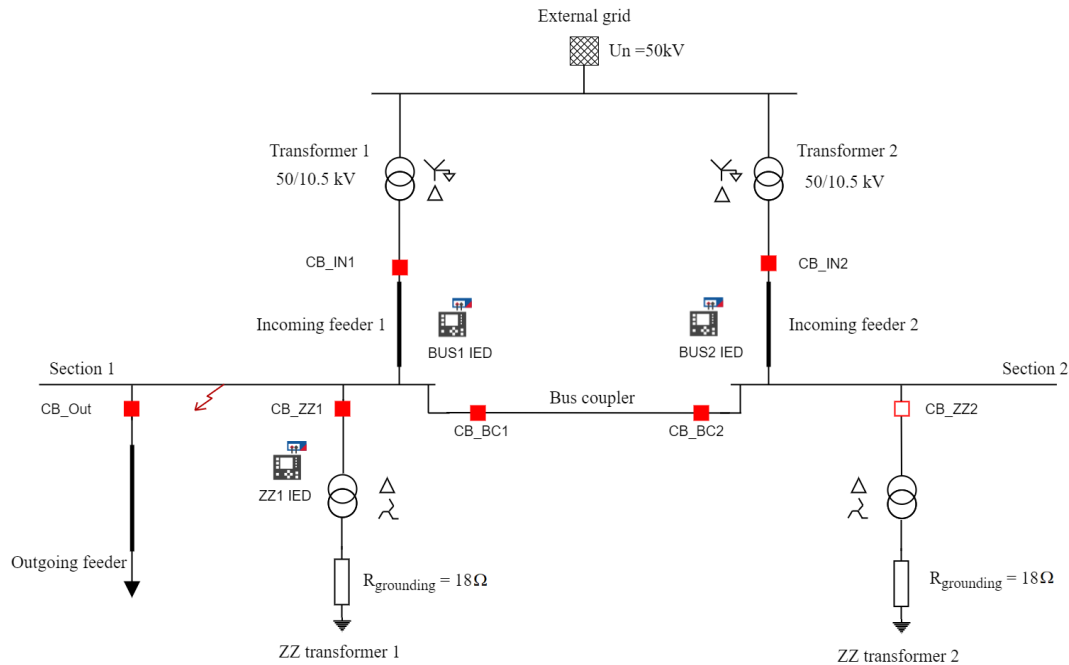


Figure 4.14: Case 3: Fault on Section 1 in Topology 3

Similar to the previous case, the fault occurs at time $t = 20.1$ ms and is picked up by the ZZ1 IED after around 4 ms. After the time $te_{>>}$ expiration, ZZ1 IED sends the tripping command to BUS1 and BUS2 IED, which happens at time $t = 329.9$ s. As seen in Figure 4.15, now on both sections, there is a zero-sequence voltage detected by BUS1 IED and BUS2 IED, respectively. This means that the two conditions are satisfied for both BUS1 IED and BUS2 IED, which results in both of the IEDs sending tripping commands. This implies that both of the incoming feeders will be disconnected at time $t = 400,6$ ms. A similar conclusion is drawn from the results when the fault occurs on Section 2 and the bus coupler, respectively. The same behavior is obtained in the case when the ZZ transformer 2 is switched in while ZZ transformer 1 is disconnected.

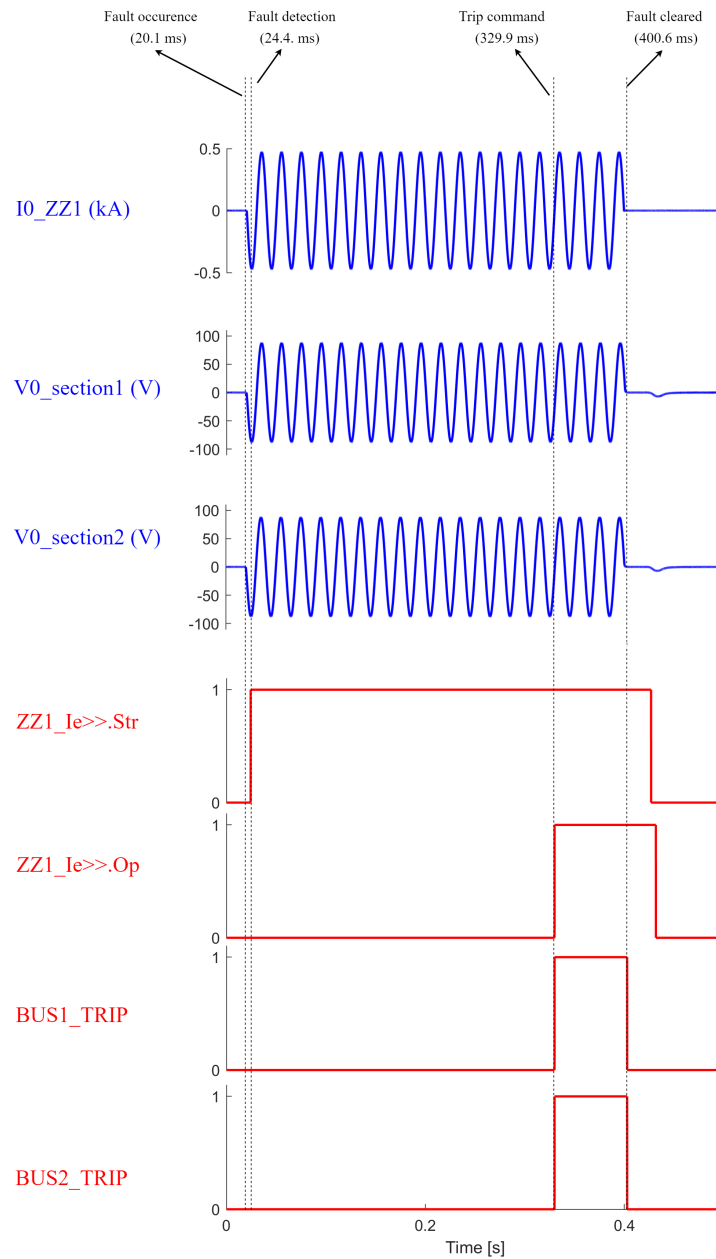


Figure 4.15: Simulation results for a fault on Section 1 in Topology 3

It can be seen that the scheme is not fully selective in terms of disconnecting only the faulted section. However, the tripping of both incoming feeders in situations like these was decided in consultation with Stedin as a stakeholder. The reason is that creating a fully selective algorithm with the decentralized protection of IEDs will require a much more complicated logic than the one presented before, which will be more error-prone. That is why, to prevent mall operations of the protection scheme during normal conditions and during maintenance, it was decided that the safer option is to fully de-energize the whole busbar system in case of a fault on any of the sections.

Case 4: Fault on the feeder connecting the ZZ transformer 1 in Topology 3

The following case is when the grid operates according to Topology 3, and a single-phase-to-ground fault occurs on the ZZ transformer 1 feeder (after the CT). The described situation is shown in Figure 4.16. This case's results are presented in Figure 4.17.

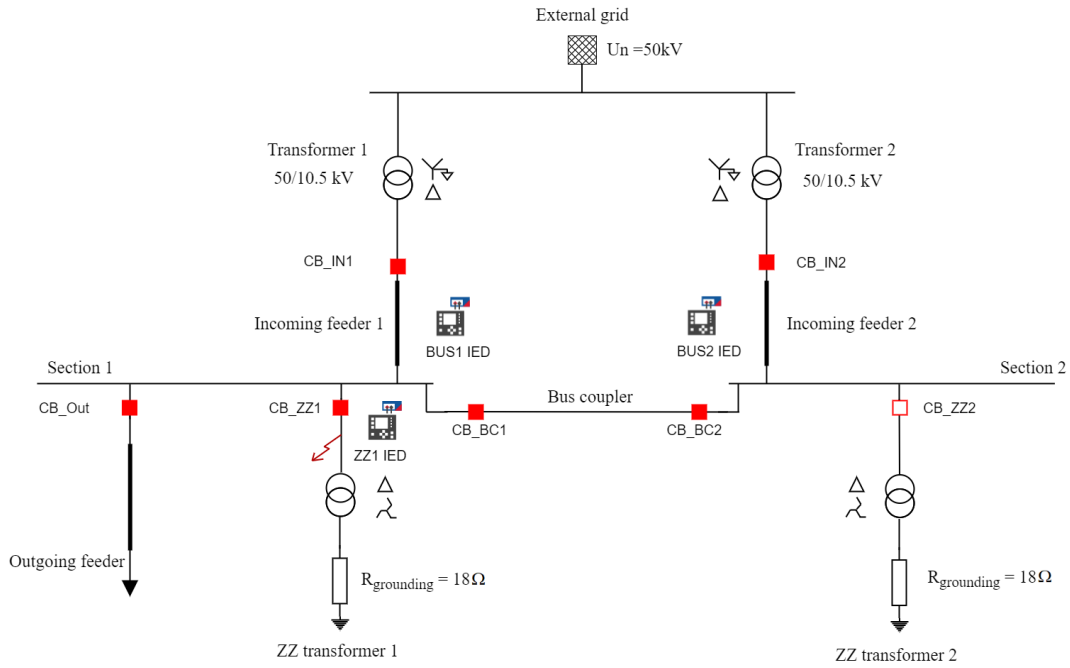


Figure 4.16: Case 4: Fault on ZZ transformer 1 feeder in Topology 3

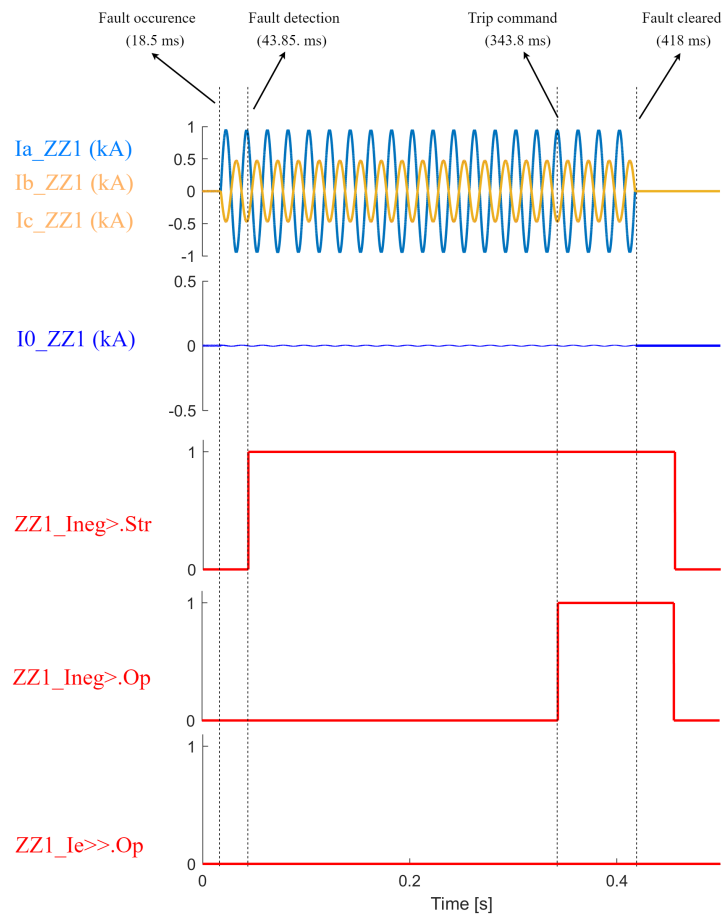


Figure 4.17: Simulation results for a fault on the ZZ transformer 1 feeder in Topology 3

As shown in Figure 4.17, the fault occurs at time $t = 18.5\text{ms}$. As expected, in this case, the $I_{e>>.Op}$

signal from the ZZ1 IED is not activated since that IED detects practically no zero-sequence current. This implies that no tripping commands will be issued by BUS1 IED and BUS2 IED. However, from the shape of the phase currents presented in Figure 4.17, it is evident that the system of currents is not symmetrical. As a result, there is a sufficient magnitude of the negative-sequence current to activate the $I_{neg>}$ setting. One can see that the fault is picked up around 20ms after its occurrence. After the expiration of approximately 300ms (time according to the settings explained in Table 3.1), the $I_{neg>}.Op$ command is activated, and a trip signal is sent to the respective CB_ZZ1. The fault is selectively cleared at time $t = 418$ ms. The same results are obtained for all Topologies 1 to 3, regardless of which ZZ transformer is connected.

Case 5: Fault on the feeder connecting the ZZ transformer 1 in Topology 4

Finally, the case when the grid is operating according to Topology 4, and a fault occurs on the feeder connecting the ZZ transformer 1, as shown in Figure 4.18 is presented. Even though this topology is not in compliance with Stedin's policy, for a brief time, it can happen that the grid will be working according to this topology. That is why it was considered when evaluating the algorithm, and the results from this test case are shown in Figure 4.19.

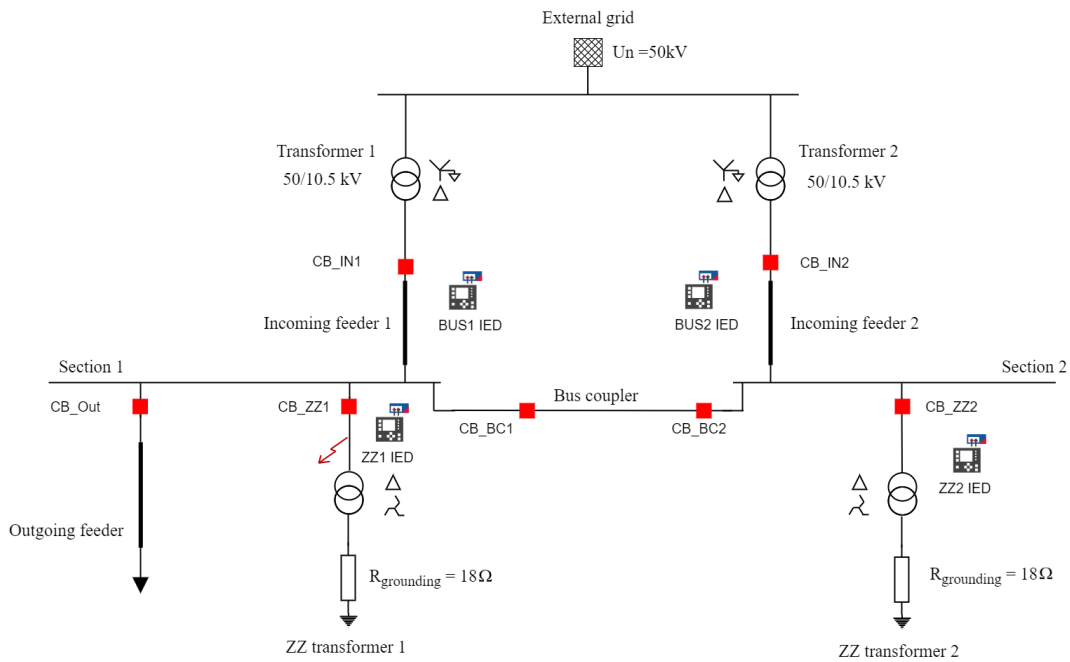


Figure 4.18: Case 5: Fault on ZZ transformer 1 feeder in Topology 4

The single-phase-to-ground fault takes place at time $t = 22.4$ ms. In contrast to the above-mentioned case, both a zero-sequence component and a negative-sequence component of the current are detected from the ZZ1 IED, as seen in Figure 4.19. The same zero-sequence current is seen by ZZ2 IED also, as ZZ transformer 2 is the "source". The negative-sequence current activates the $I_{neg>}$ setting of ZZ1 IED after around 4 ms, while the zero-sequence current activates the $I_{e>>}$ setting of both ZZ1 and ZZ2 IED after around 7ms. After the respective time settings expire, the tripping commands are sent from ZZ1 and ZZ2 IEDs. The $I_{neg>}.Op$ trip from ZZ1 IED is sent at time $t=323.25$ ms to the CB_ZZ1. Almost simultaneously, with a delay of just 2.5 ms, ZZ1 and ZZ2 IED send the trip command to BUS1 and BUS2 IED. As both of these IEDs detect a zero-sequence voltage, tripping commands are given to CB_IN1 and CB_IN2, respectively. As a result, non-selective tripping of the busbar system is taking place, and the algorithm is not working as desired. The reason for this undesired operation can be explained by observing the distribution of the negative and the zero-sequence components of the fault currents, as presented in Figure 4.20. The positive-sequence component is omitted from the single-line diagram as it does not play any role in the algorithm's explanation and operation.

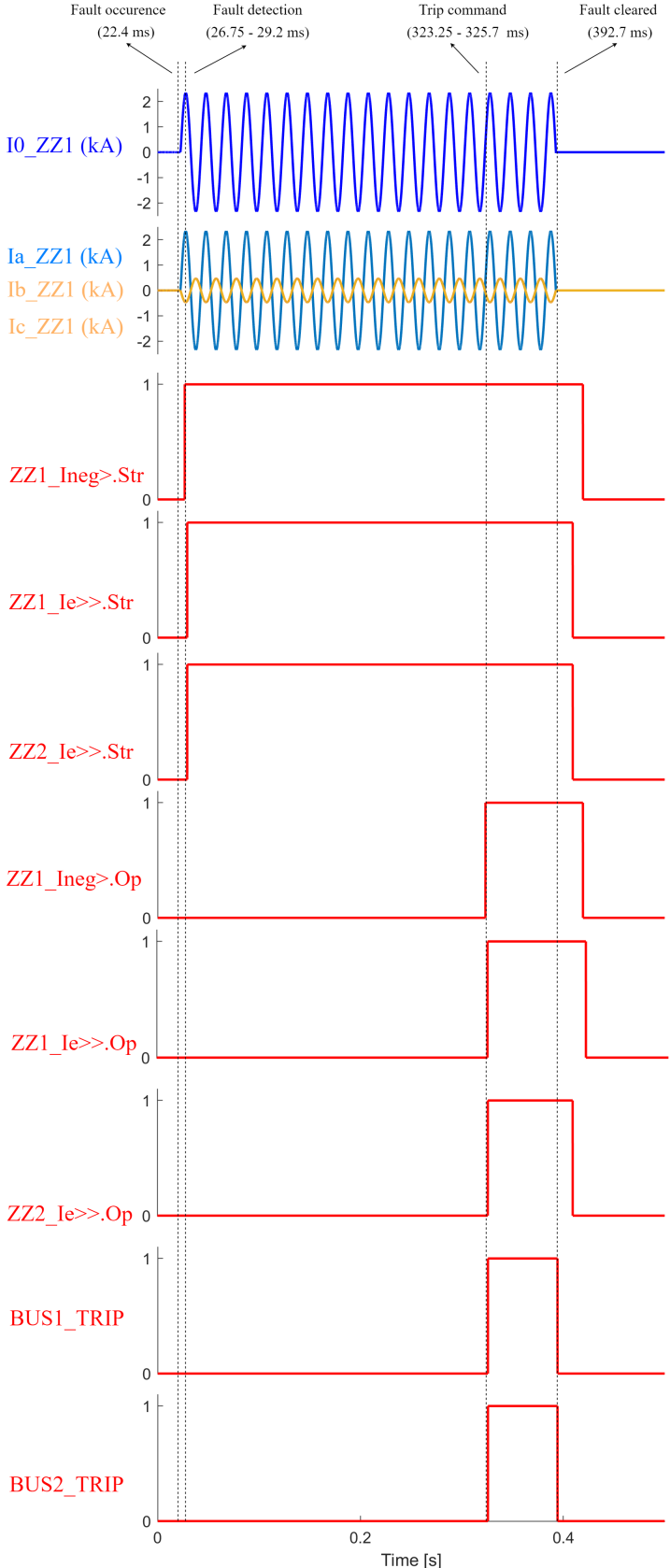


Figure 4.19: Simulation results for a fault on the ZZ feeder in Topology 4

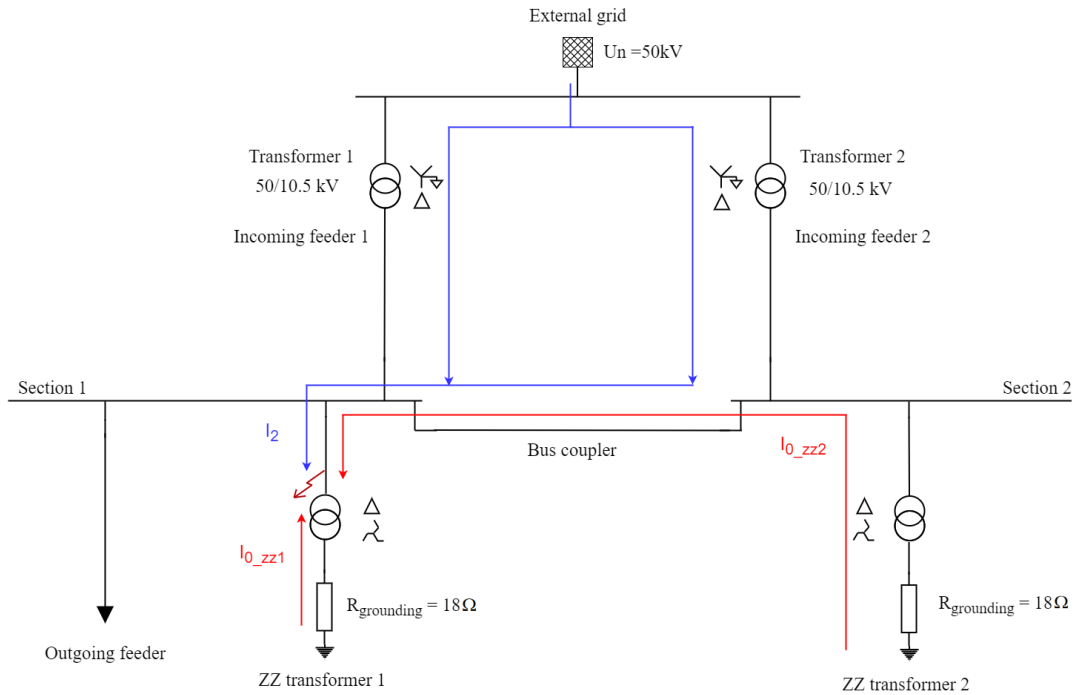


Figure 4.20: Current distribution for a fault on the ZZ feeder in Topology 4

As it can be seen, the negative-sequence component of the current (I_2) is being fed from the two incoming feeders, passing through the IED that is connected to the ZZ transformer feeder 1, which explains the activation of the command $Ineg_{>}.Op$ from the same IED. The zero-sequence component of the current (I_0) is fed from two different sources: ZZ transformer 1 and ZZ transformer 2. The zero-sequence current being fed from the ZZ transformer 1 is not passing through any of the CTs on its way to the fault location; thus, it is not responsible for tripping any of the IEDs. On the other hand, the zero-sequence current, whose source is the ZZ transformer 2, is passing both through the CT on the ZZ transformer 2 feeder and through the CT on the ZZ transformer 1 feeder on its way to the fault location. This means that this current is activating the command $Ie_{>>}.Op$ from the IEDs on the ZZ transformer feeder 1 and ZZ transformer feeder 2. As a result of that, both the incoming feeders are tripped. Even though this grid topology can be in service only for a short time, the chaotic behavior of the protection scheme if a single-phase fault on the ZZ transformer feeder occurs in that situation can pose a considerable problem for Stedin.

One way of solving this problem is to block the tripping command sent to the incoming feeders IEDs on both of the ZZ transformer feeder IEDs whenever one of them detects a negative-sequence current above the set threshold. This means that when the $Ineg_{>}.Str$ is activated; it will block the $Ie_{>>}.Op$ on ZZ transformer feeders 1 and 2 IED, providing selectivity as shown in Figure 4.21. As seen in this figure, for the same fault, now only ZZ1 IED is sending a tripping signal, which selectively clears the fault.

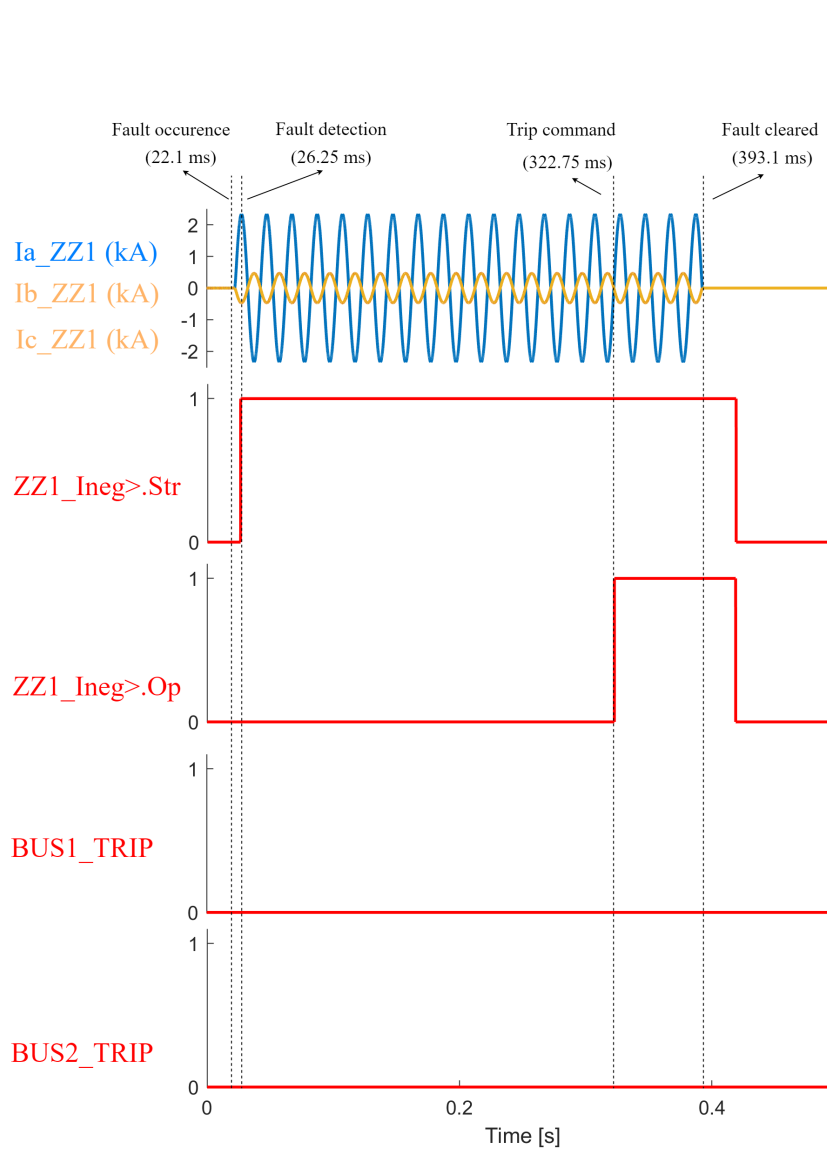


Figure 4.21: Simulation results for a fault on the ZZ feeder in Topology 4, after the improvement of the protection scheme

This would require that the logic for blocking the $I_{e>>}.Op$ of the ZZ transformer IED should be expanded with one more element in parallel. In other words, an $I_{e>}.Str$ signal of any of the outgoing feeders or an $Ineg>.Str$ signal of a ZZ transformer will be used to block the $I_{e>>}.Op$ of the ZZ transformer IED. From a technical aspect, this would require expanding the already used OR logic, so it should not pose a challenge.

Another possible solution is to time grade the $Ineg>.Op$ and the $I_{e>>}.Op$ of the ZZ feeder IED. This would mean the time-setting for the $Ineg>.Op$ could remain to be 300ms, but the time-setting for the $I_{e>>}.Op$ will need to be increased to 600ms. This would mean that for the above-discussed situation, the ZZ feeder $Ineg>.Op$ setting will have a priority in clearing this fault, and selectivity will be provided. Although this is a more straightforward solution from a technical point of view, it is worsening (longer clearing times) the overall operation of the protection scheme. Because of this long operating time, a decision was made that the first presented option is the better solution to solve this problem.

4.5. Conclusion

After discussing and explaining some of the more characteristic cases in this chapter, some conclusions are drawn from the simulation results. In Table 4.2, the operation of the proposed algorithm in the different topologies and for various fault locations is presented. The different columns of this table

represent the different fault locations, while the different grid topologies are assessed in the rows. With the letter 'S' it is denoted that the scheme is operating selectively, meaning that only the minimal faulty part of the grid is disconnected. On the other hand, with 'O', it is denoted that the algorithm performs according to the desired scheme, but the disconnecting of the faulty elements is not fully selective. Nevertheless, this is expected and acceptable for Stedin at the current time. Finally, the notation 'S*' for a ZZ feeder fault in Topology 4 denotes that the algorithm will be selective only with the necessary adjustment explained in Case 5. However, as a fault on the ZZ feeder in Topology 4 is highly unlikely, this adjustment can be considered unnecessary by Stedin. In that case, the notation will have to be changed to 'X', meaning that the algorithm is not operating according to the desired tripping scheme. The notation 'NA' denotes that this fault location is not applicable in the given topology.

Table 4.2: Operation of the zero-sequence tripping algorithm for different fault locations in different grid topologies

Fault location / Network Topology	Section 1	Section 2	Bus coupler	Outgoing feeder	ZZ feeder
Topology 1	S	S	NA	S	S
Topology 2	O	O	O	S	S
Topology 3	O	O	O	S	S
Topology 4	O	O	O	S	S*

Extensive simulations were carried out with varying the inception point of the fault, which proved that the inception angle is not playing any significant role in this protection scheme. The fault resistance was also varied, and it was observed that every fault on the busbar could be detected in the range of 13Ω . Faults with higher resistance are not being detected. That is not a problem since 13Ω is a very high value for fault resistance, and Stedin is usually not experiencing that kind of faults in their cable networks. However, if high resistance faults are to be expected, the criteria for detecting the zero-sequence over-voltage can be lowered, which will make the protection scheme more sensitive. When this condition is lowered to $0.2 * U_n$, this scheme detects the faults until the 18Ω resistance, which is a substantially high fault resistance. The tripping results for the IEDs were closely correlated to those obtained with the offline testing using the Omicron RelaySimTest. Furthermore, it is noticed that this protection scheme is not causing any bottlenecks or endangering the system integrity since all faults are cleared as intended, without causing any unwanted CB trips (after the necessary adjustments of the algorithm).

It is worth pointing out that selectivity between the different sections is provided only in the case when the bus section coupler is opened (Topology 1). This means that when the bus section coupler is closed, and both sections are connected, selectivity is not provided in terms of disconnecting only the faulty section, but the whole busbar is disconnected instead. In theory, an algorithm can be implemented which will also consider the grid topology and the currents that are "entering" and "leaving" the bus section breaker and, in that way, know exactly where the fault is located - on Section 1 or Section 2. This will require an operation of the IEDs based on logic tables, where multiple conditions will have to be examined. This added logic can cause trouble for the installation and/or the maintenance team, resulting in unnecessary trips from this protection scheme. This can pose a bigger problem than non-selectively tripping off both the sections since it will be uncontrolled and thus present a more significant challenge for the grid and the grid operator itself. That is why it is proposed to allow the non-selective² clearing of the fault to prevent possible more extensive damage.

For the time being, this way of clearing the busbar faults is acceptable for Stedin, and it is not expected to be causing any problems in the grid operation. However, in the future, the trend is that the currently passive distribution networks will change to operate as active distribution networks [17], which means that greater reliability will be required from the distribution networks in general. This will require a bigger selectivity in clearing the faults, meaning that the non-selective approach between faults on a different section of the busbar system will no longer be the desired practice. Along with that, the requirements for the protection will become more extensive, meaning that the backup protection

²the non-selectivity applies only to the sections itself and not to the busbar as the element

will also have to react in shorter times than what is used now. Additionally, the fault current levels can decrease. They will depend on the grid topologies and the power output from the intermittent Distributed Energy Resources (DERs), meaning that the decentralized protection will become more challenging to coordinate. Centralized protection is becoming a hot topic these days as a possible solution that can outcome this kind of problem. As part of this thesis, further investigation was done in the domain of centralized protection, which is presented in the following section.

5

Centralized protection

For the past decades, the decentralized protection systems were the system of choice for all the power system utilities. This was on a grand scale influenced by the lack of adequate communication and processing capabilities of the used devices. The grid was also not prone to drastic shifts in its operation, so the utilities did not find an incentive to change a scheme that was already operating adequately. Nonetheless, with the significant increase in the processing and communication powers of the new generation of numerical IEDs and the fact that the grids tend to be more active in the future, meaning that a faster and more reliable operation of the protection schemes will be required, the centralized protection principle is a highlight in the power system world these days. Contrary to the traditional way of operating the distribution networks, with the additional increase of Distributed Energy Resources (DERs), the distribution systems will also tend to operate as active networks so that the centralized protection concept will become of interest to them too. This chapter firstly explains a definition of the centralized protection system and some possible architectures on how to achieve it. Furthermore, two proposals are made for a centralized scheme for busbar protection against single-phase faults in medium voltage impedance earthed substations. The principle of operation of this scheme is explained in this section, along with requirements that would need to be implemented in real life for a centralized protection scheme like this to work properly.

5.1. Background

The idea of a centralized protection and control (CPC) system dates back to the 1970s. It coincides with the beginning of the wide use of computers for business purposes [18]. However, it has not been widely applied and/or investigated due to the lack of hardware, software, and communications technologies [19]. In recent years, the signal processing capabilities of the IEDs and Merging Units (MUs)¹ are rapidly increasing and, along with that, acceptable communication standards (e.g. IEC 61850, IEEE 1588) are available for substations, which contributes to making the centralized protection a popular topic again.

Centralized protection and control is a concept that combines several IEDs in a single hardware platform, which should allow for more efficient use of the processing power, but at the same time, will not compromise the stability and reliability of the conventional decentralized solution ²[20].

As explained in [21], there are multiple ways in which a CPC architecture can be achieved, along with the redundancy of the system.³ The most straightforward way is to have a fully centralized and redundant CPC, as shown in Figure 5.1 and Figure 5.2.

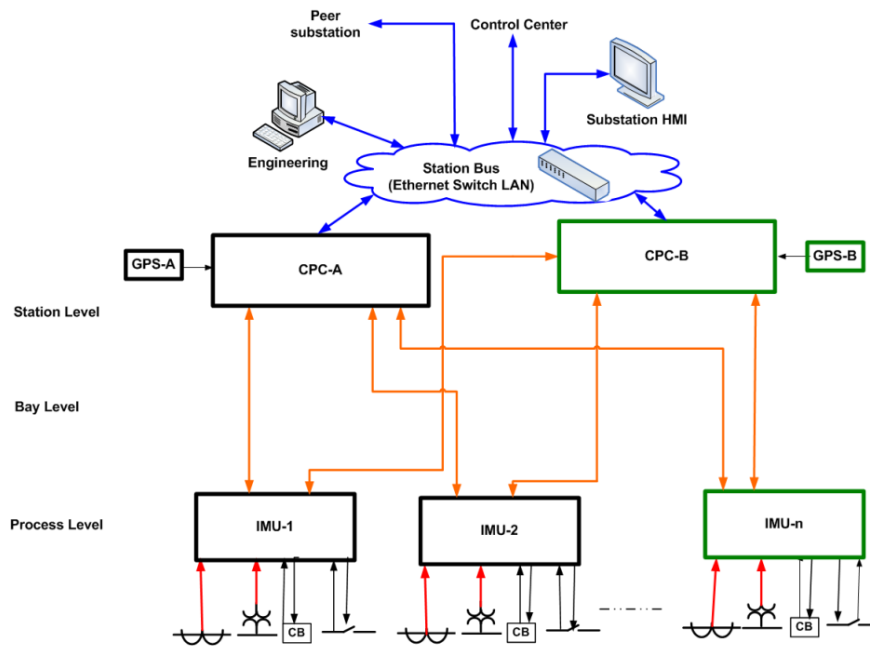


Figure 5.1: CPC connected with MUs directly through point-to-point process bus architecture [21]

¹Merging Units are devices that are digitizing the analog outputs from the CTs and VTs

²separate IEDs for every component

³a remark has to be made that this redundancy is in terms of hardware/device redundancy and not communication redundancy

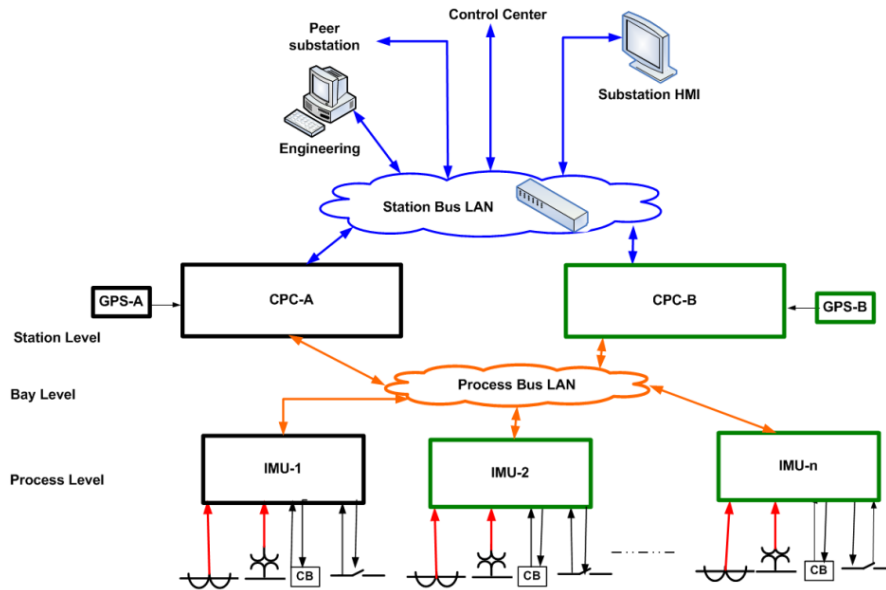


Figure 5.2: CPC connected to MUs through Ethernet LAN architecture [21]

In both of these architectures, the CPC has the role of both primary and backup protection, and depending on the substation, more than two CPC are possible. The current and/or voltage values are measured from the respective CTs and VTs (MUs) and then handed to the CPC, which, based on its programmed logic, decides whether protection actions are needed. The only difference is how these values are sent to the CPC. In the first case (Figure 5.1), the MUs are directly connected to the CPC, and the connection is a Point-to-Point connection. On the other hand, in the architecture shown in Figure 5.2, the communication between the MUs and the CPC is achieved over a process bus LAN network, which means that the MUs are multicasting SV and GOOSE messages, and the CPC is subscribed to those messages. Similarly, the CPC is multicasting its GOOSE messages (tripping commands), and the respective IEDs are subscribed to the relevant messages. This fully utilizes the implementation of the IEC 61850 standard. However, fully switching to completely centralized protection is a step that is too big for the utility companies at this point. This is because the current protection operation relies entirely on the IEDs, which serve as a backbone for decentralized protection. This implies that entirely replacing the already existing protection architecture will be an expensive and time-costly process. Furthermore, what is more important is that it will also require time for the protection engineers to develop new methods of testing and maintaining this new protection architecture since the already existing ways will not be able to be fully implemented. As it is a relatively new technology, it also requires extensive testing and time for the engineers to fully trust its implementation and work.

That is why implementing a hybrid protection scheme is proposed for the initial stage of the shift towards centralized protection, consisting of the already used decentralized protection schemes and IEDs in addition to the new CPC concept. Possible examples of this hybrid substation protection scheme are shown on Figure 5.3 and 5.4.

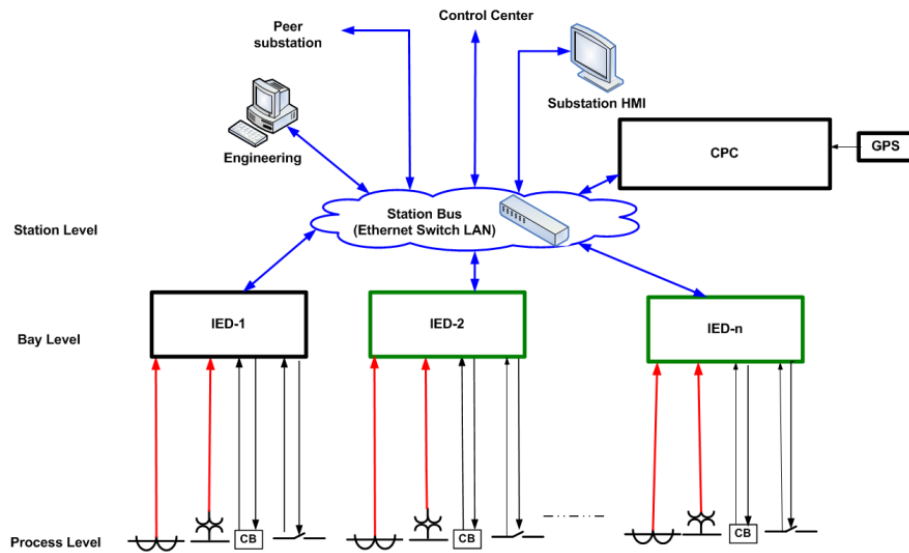


Figure 5.3: IEDs take values through copper wires and are interfaced with the CPC [21]

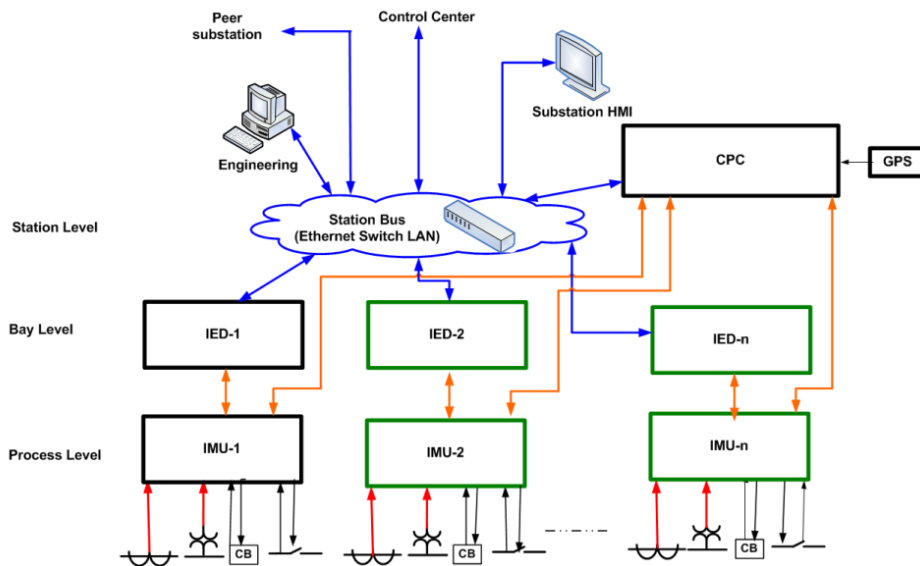


Figure 5.4: IEDs and CPC connected to MUs over point-to-point process bus architecture [21]

In both cases, the IEDs function as primary protection (in the same manner as they are operating now), and the CPC is used to provide backup protection. The difference between the schemes consists in the way the information (current and voltage values, CB status, tripping signals) is conveyed between the IEDs and the CPC. In the architecture presented in Figure 5.3, the IEDs are connected with the process level equipment (instrument transformers and switching devices) over copper wires and then communicate SV and GOOSE messages to the CPC. On the other hand, the architecture presented in Figure 5.4 uses the concept of MUs, which digitize the current and voltage measurements and then transmit them to both the IEDs and the CPC through a dedicated point-to-point connection. An alternative to this architecture is presented in Figure 5.5, where the data from the MUs is communicated to the IEDs and the CPC over Ethernet LAN connection via the so-called process bus, which requires that a publisher-subscriber communication is established.

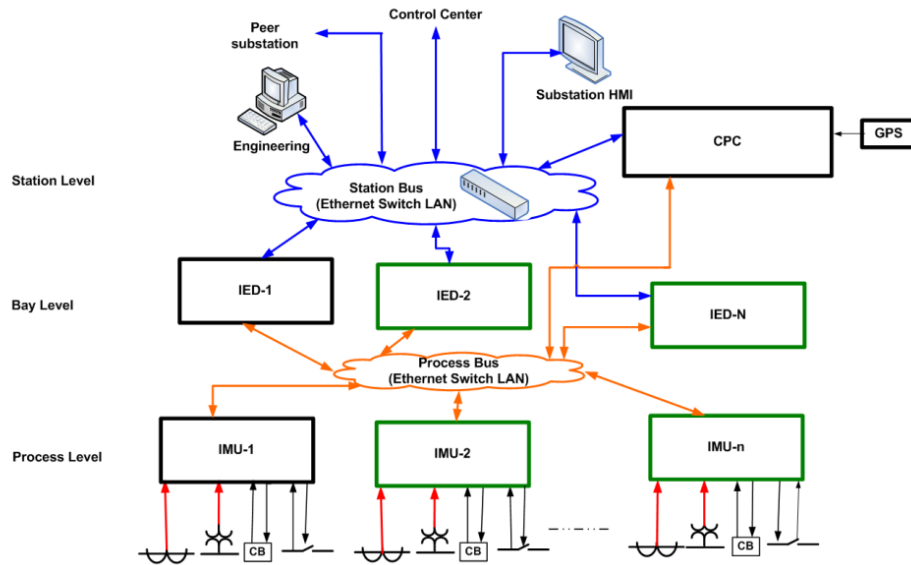


Figure 5.5: IEDs and CPC connected to MUs over Ethernet LAN connection [21]

5.2. Design of a centralized protection

As part of this thesis project, a design for centralized protection is also proposed and tested. The proposed design is based on the hybrid architecture, where the already installed IEDs play the role of the primary protection, while the centralized platform provides the backup protection. As explained later, the centralized platform also adds some extended functionalities for the protection schemes. The current and voltage transformers pass the currents/voltages via copper wires to the MUs, where this data is digitized and passed to the IED and the centralized platform. The process bus communicates the current and voltage measurements to the CPC. Additionally, GOOSE messages are communicated between the IEDs and the centralized platform in two-way communication. This design intends to test whether a setup like this can provide the backup busbar protection faster than the already applied one, without any influence on the IEDs that will serve as the primary protection. Also, the possibility of overcoming the selectivity problem (explained in Section 4.5) with the centralized approach is examined.

The proposed centralized protection schematic is presented in Figure 5.6. Two of the seven IEDs used for the simulation testing will be physical IEDs - Siemens 7SA86, while the rest are virtual over-current IEDs from the RSCAD library. The two Siemens 7SA86 IEDs are used to simulate their primary task of the feeder protection, as well as to stream SV and/or GOOSE messages to the centralized protection. It was decided that the two Siemens IEDs will represent the IEDs connected to the ZZ transformer 1 feeder and the incoming feeder 1. Further explanation of how to properly set the Siemens IEDs can be found in Appendix F.

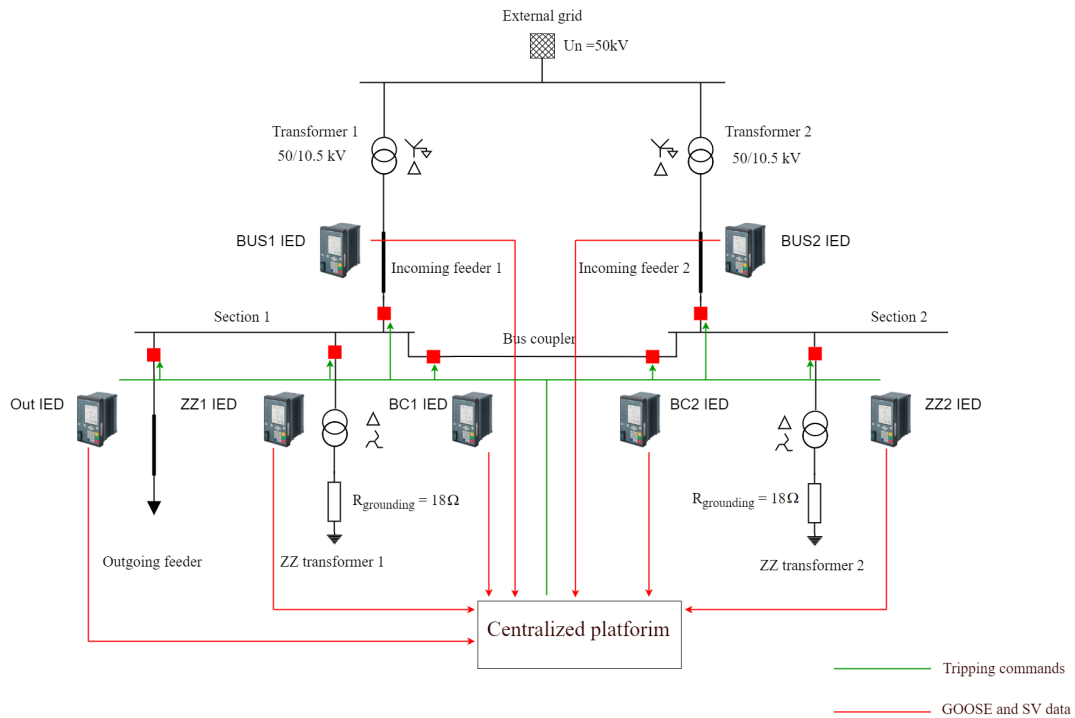


Figure 5.6: Proposed hybrid centralized protection scheme

The algorithm for the centralized protection is implemented in MATLAB, which is then run as a Software-in-the-Loop (SiL) simulation in combination with RTDS, in a similar manner as explained in [22]. This requires the PC, where the MATLAB code is being run, and the RTDS to be connected through the local area network (LAN). Then, using the TCP socket protocol, the data from the RSCAD software is transmitted to the MATLAB script, where the algorithm is run, and the appropriate tripping commands will be transmitted back from MATLAB to RSCAD. Graphically, this is presented in Figure 5.7.

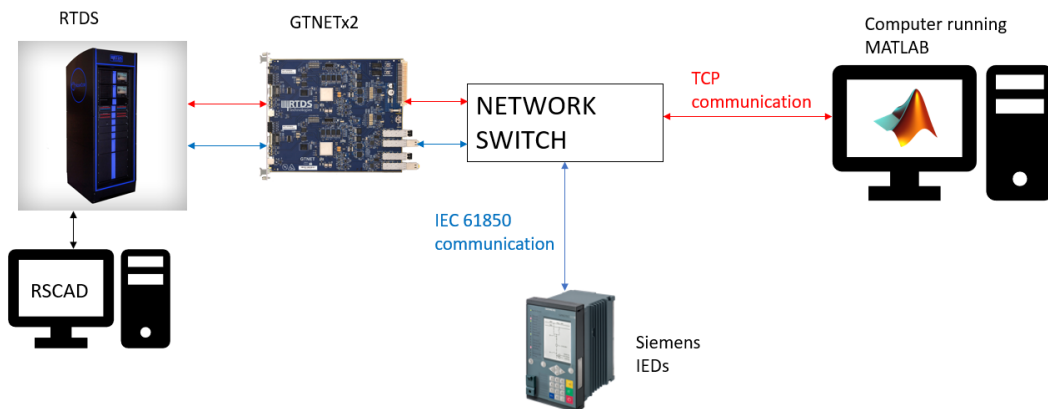


Figure 5.7: Communication setup for testing the centralized protection algorithms

The backup protection functionalities of the centralized protection are related to the protection of the busbar sections. Since this centralized protection will initially serve only as a backup, it has to be time-graded with the primary protection, in this case, the reverse-blocking scheme with the addition of the newly proposed zero-sequence tripping scheme. As mentioned in Chapter 3, the current requirements for opening the CBs are 85 ms, meaning that a time margin of 300ms will guarantee time-selectivity between the primary and backup protection. That is why for the operation time of the

busbar backup protection, a time of 600ms was decided to be set.

Furthermore, an added functionality in the centralized busbar protection will be detecting a fault on the section coupler. By providing this functionality, for a single-phase-to-ground fault on this location, only the bus coupler CBs will be tripped off. In contrast, the bus section(s)⁴ will continue to be energized. In this case, the centralized protection cannot be seen as the backup protection, but as the primary one, in the sense that it has to operate before the de-centralized protection can trip the whole busbar system. This is why a time delay of 100ms was chosen, allowing a time margin of 200ms for the CB to trip, again guaranteeing the selectivity principle.

Two algorithms for detecting single-phase-to-ground faults on the busbar system in a centralized manner were designed and tested using the above-explained setup. The difference between the algorithms is mainly based on the data they use to detect the fault. The first algorithm is based solely on GOOSE messages from the IEDs, which means that the IEDs need to detect the disturbance in the system, and the centralized protection based on their messages is being able to locate the fault⁵. The second algorithm is based solely on the SV messages gained from the IEDs/MUs, which means that it is the algorithm's task to detect whether there is a fault occurrence and, based on the current and/or voltage measurements, to issue the appropriate tripping signals. The principle of operation of these algorithms is explained in the following sections.

5.3. GOOSE based algorithm

5.3.1. Principle of operation

The first algorithm that is explained is the one that operates based on the GOOSE messages received from the IEDs. The MATLAB code for the operation of this algorithm, alongside its explanation, can be found in Appendix G. This algorithm is operating on the $I_{e>}.Str$ signals of all of the IEDs (i.e., it takes into account which of the IEDs are detecting a zero-sequence current) and, based on that, determines the location of the fault. Additionally, the detection of a zero-sequence over-voltage at the busbar IEDs is also taken into account, as well as the negative-sequence current detection from the IEDs on both of the ZZ transformers.

This means that it operates on the same basis as the zero-sequence tripping distributed protection scheme explained in Section 3, with the difference that the decision is made on a centralized level instead of on a decentralized level. Using a centralized platform to make the tripping decisions makes it much easier to achieve selectivity between a fault on the different sections and a fault on the bus section coupler. The test case network is shown in Figure 5.8. As noted from the figure, the network consists of one outgoing feeder, two incoming transformer feeders, and two zig-zag transformers, which can be switched in and out manually with a push button, thus enabling the four topologies that were previously described in Chapter 4.3. The fault is again simulated in five different locations.

The first thing that needs to be mentioned is that if the outgoing feeder detects a zero-sequence current (i.e., the signal from the outgoing feeder IED $I_{e>}.Str$ is equal to 1), the tripping signal to both of the incoming feeders' CBs (on Section 1 and 2) is disallowed until the signal changes its value to zero. In this way, priority is provided to the IED on the outgoing feeder to clear the fault in its zone.

Similarly, if a ZZ transformer IED detects a negative-sequence current ($I_{neg>}.Str$ is equal to 1), the tripping signal to both incoming feeders CBs is disallowed. This is done to prevent false tripping when the two ZZ transformers are switched in, and a fault occurs on the feeder connecting one of them to the busbar, as explained in 4.4.

Finally, when the $V_{0>}.Str$ signal of the IED on Section 1 is equal to zero (meaning that the busbar IED is not detecting the presence of zero-sequence voltage), the CB on Section 1 is prevented from tripping, and the same logic is applied to Section 2 also. This again serves as a safety mechanism to prevent false trips from the protection scheme due to maintenance or maloperation.

Three locations are possible for a fault on the busbar system: a fault on Section 1, a fault on Section 2, and a fault between the bus section CBs. The zero-sequence current distribution for a fault on the bus coupler (when only ZZ transformer 1 is switched in) can be seen in Figure 5.9. The zero-sequence current is detected by only one of the bus coupler IEDs (the one closer to section 1), while the other one is not detecting it. In case of the ZZ transformer 2 being switched in (while ZZ transformer 1 is

⁴depends on the network's topology

⁵the location is meant in terms of element and not in terms of the exact location on a specific element

disconnected), the situation will be almost the same, with the difference that now the bus coupler IED that is closer to section 2 would detect a presence of a zero-sequence current, while the other would not.

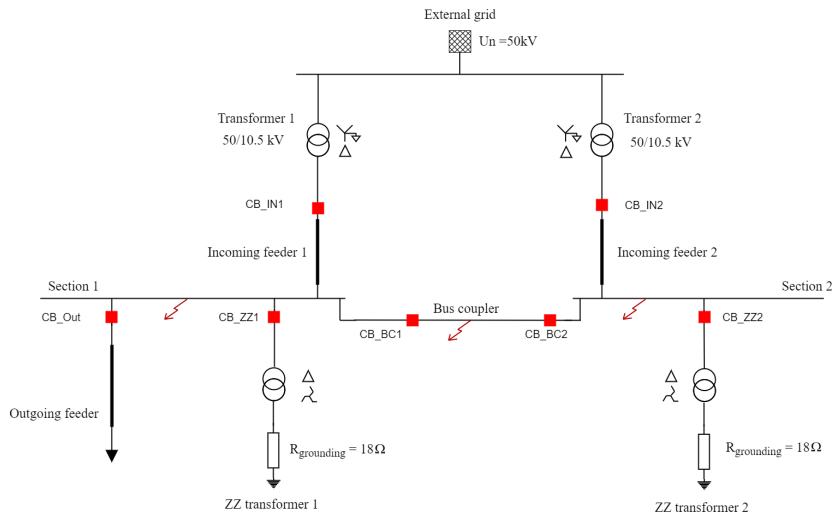


Figure 5.8: Test case network for the centralized protection

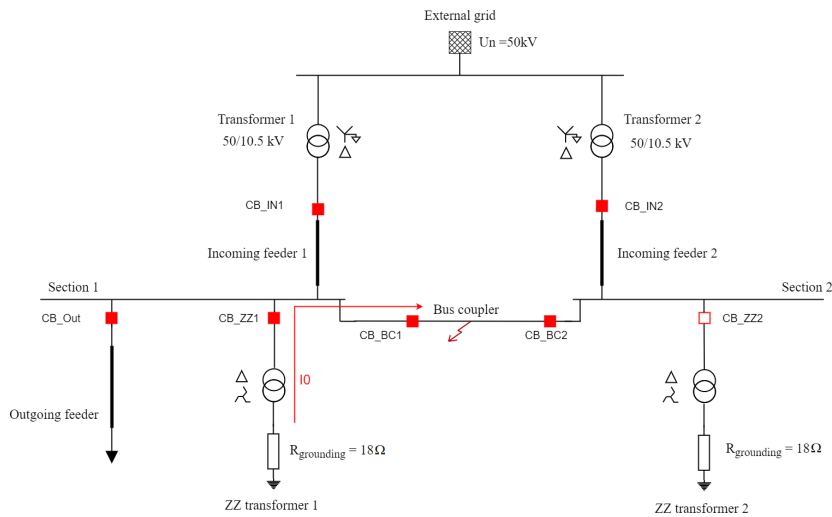


Figure 5.9: Distribution of the zero-sequence current for a fault on the bus coupler in Topology 3

This means that the necessary condition for detecting a single-phase-to-ground fault in this location is that only one of the bus coupler IEDs must detect a presence of a zero-sequence current. This criterion requires that for the GOOSE signals from these two IEDs, an XOR logic must be implemented, as shown in Table 5.1. The signal ‘Cent_BC_TRIP’ is the tripping signal issued from the centralized platform and serves to open the bus coupler CBs.

Table 5.1: Logic table for the GOOSE algorithm when a fault occurs on the bus coupler, with only one ZZ transformer switched in

Incoming GOOSE messages		
Ie>.Str (Out IED)	0	0
Ineg>.Str (ZZ1 IED)	0	0
Ie>.Str (ZZ1 IED)	1	0
Ie>.Str (ZZ2 IED)	0	1
Ie>.Str (BC1 IED)	1	0
Ie>.Str (BC2 IED)	0	1
V0>.Str (BUS1 IED)	1	1
V0>.Str (BUS2 IED)	1	1
Outgoing commands		
Cent_BC_TRIP	TRIP	TRIP
Cent_BUS1_TRIP	NO TRIP	NO TRIP
Cent_BUS2_TRIP	NO TRIP	NO TRIP

As explained before, the centralized protection algorithm is the primary protection for this fault location. Hence the reaction time should be as fast as possible, and for the above-explained reasons was chosen to be 100ms. The results for a simulated single-phase-to-ground fault on the bus coupler in Topology 3 (both incoming feeders connected and only one ZZ transformer switched in) are presented in Figure 5.10.

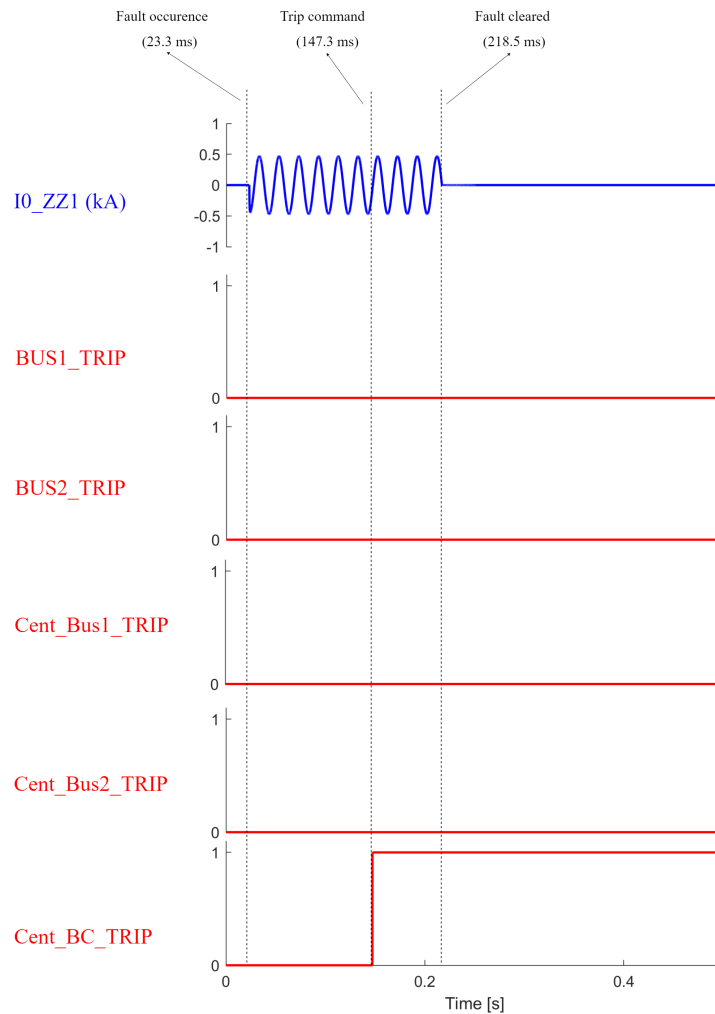


Figure 5.10: Tripping times from the centralized GOOSE algorithm for a fault on the bus coupler in Topology 3

As it is seen, the fault happens at time $t = 23.3\text{ms}$. The centralized protection sends the tripping command to the bus coupler CBs ('Cent_BC_TRIP') at time $t = 147.3\text{ms}$, while the tripping commands to the incoming feeder IEDs ('Cent_BUS1_TRIP' and 'Cent_BUS2_TRIP') are both with a value of zero, meaning no tripping action is being taken. This shows that the centralized protection successfully distinguishes between a fault on one of the sections and the fault on the bus section coupler. The fault is selectively cleared by opening the bus coupler CBs at $t = 218.5\text{ms}$. What is worth mentioning is also that the bus coupler CBs are tripped before the primary protection of the incoming feeders ('BUS1_TRIP' and 'BUS2_TRIP') has enough time to react. This proves that centralized protection can be the primary protection for a fault on the bus section coupler to provide complete selectivity and prevent tripping the whole busbar system.

The next cases analyzed are when a single-phase-to-ground fault occurs in Section 1 or Section 2 of the busbar system, assuming the bus coupler is closed, and only one ZZ transformer is switched in. First, the case when only the ZZ transformer 1 is connected is examined. On Figure 5.11 and 5.12, the distribution of the zero-sequence component for both of the fault locations is given.

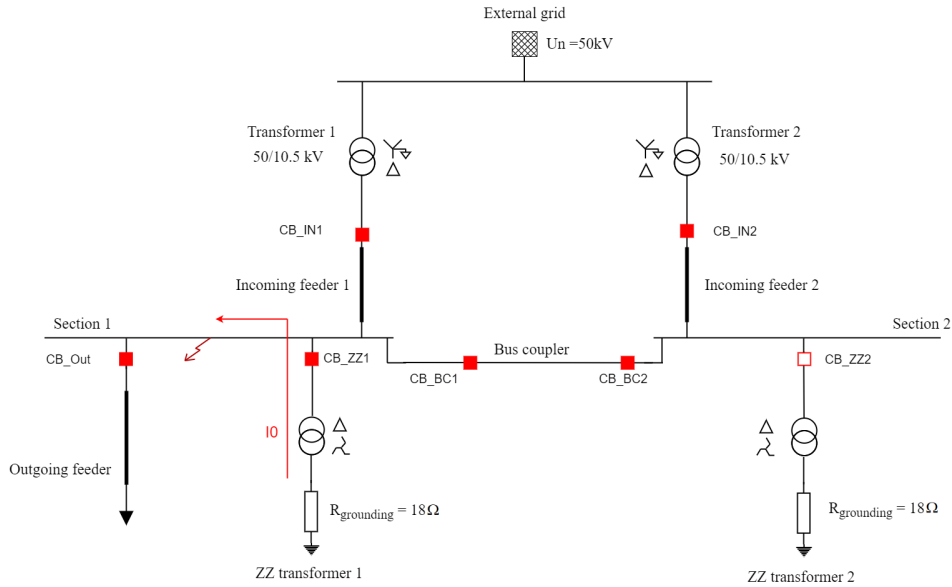


Figure 5.11: Distribution of the zero-sequence current for a fault on Section 1, with only ZZ transformer 1 connected

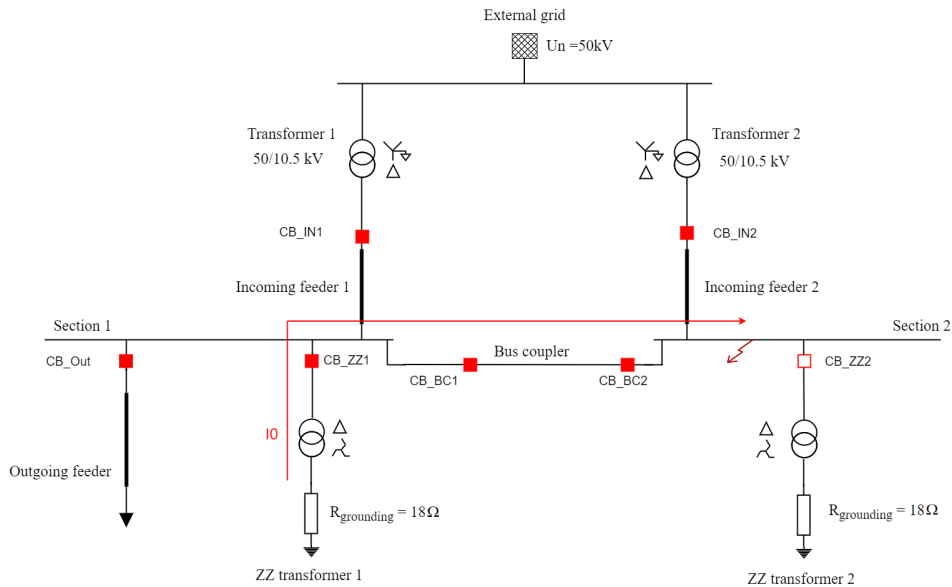


Figure 5.12: Distribution of the zero-sequence current for a fault on Section 2, with only ZZ transformer 1 connected

As shown in Figure 5.11, for a fault in section 1, when only ZZ transformer 1 is connected, only the IED on the ZZ transformer 1 feeder is detecting a zero-sequence current, while none of the other IEDs are detecting it. On the other hand, from Figure 5.12, it can be noted that when the fault is on section 2, the ZZ transformer 1 IED detects a zero-sequence current, but also both of the IEDs on the bus coupler will be detecting it. As explained above, when the outgoing feeder IED is detecting a zero-sequence current or the ZZ feeder is detecting a negative-sequence current, the tripping of the incoming feeders will be prevented. Accordingly to the previously explained logic, when only one of the bus coupler IEDs detects a zero-sequence current, only the bus coupler will be switched off. The merging of these conditions about the tripping signals to the bus coupler and/or incoming feeders CBs, in the case when ZZ transformer 1 is connected, can be seen in Table 5.2.

Table 5.2: Logic table for the GOOSE algorithm when the ZZ transformer is connected on Section 1

INCOMING GOOSE MESSAGES					
Ie>.Str (Out IED)	1	0	0	0	0
Ineg>.Str (ZZ1 IED)	0	1	0	0	0
Ie>.Str (ZZ1 IED)	1	0	1	1	1
Ie>.Str (ZZ2 IED)	0	0	0	0	0
Ie>.Str (BC1 IED)	0	0	1	0	1
Ie>.Str (BC2 IED)	0	0	0	0	1
V0>.Str (BUS1 IED)	1	1	1	1	1
OUTGOING COMMANDS					
Cent_BUS1_TRIP	NO TRIP	NO TRIP	NO TRIP	TRIP	NO TRIP
Cent_BUS2_TRIP	NO TRIP	NO TRIP	NO TRIP	NO TRIP	TRIP
Cent_BC_TRIP	NO TRIP	NO TRIP	TRIP	TRIP	TRIP

This logic was validated by running simulations in RTDS. The results for a fault in Section 1 and Section 2 are shown in Figure 5.13 and Figure 5.14 respectively, where the signals 'Cent_BUS1_TRIP' and 'Cent_BUS2_TRIP' are the centralized signals to trip incoming feeder 1 and incoming feeder 2 respectively. The signal 'Cent_BC_TRIP' is the trip that is sent to the bus coupler CBs. The first thing that must be pointed out is that centralized protection operates as backup protection for the bus sections. As explained before, the operational timings are set to 600ms, which corresponds to what we see in the figures. This time setting implies that the tripping signals from the IEDs ('BUS1_TRIP' and 'BUS2_TRIP') operate faster than the centralized protection. That is why these tripping signals are indeed being sent from the IEDs but are not connected as tripping commands to any CB. As it can be seen from Figure 5.13, the centralized protection is successful in detecting that the fault is happening in Section 1. As expected, tripping commands are sent only to the incoming feeder 1 CB and the bus coupler CBs to fully disconnect section 1 from any power supply. We can see that without the centralized protection, both of the incoming feeders would have been tripped.

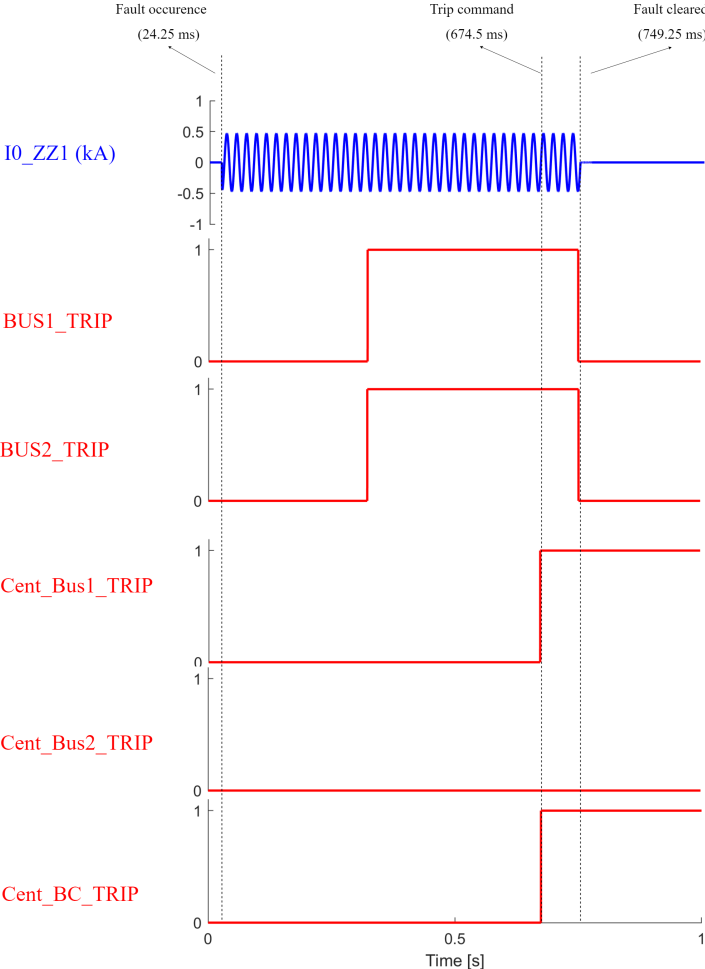


Figure 5.13: Tripping times from the centralized GOOSE algorithm for a fault on Section 1 in Topology 3

The same conclusion can be drawn for a fault in Section 2 by looking at the results from Figure 5.14.

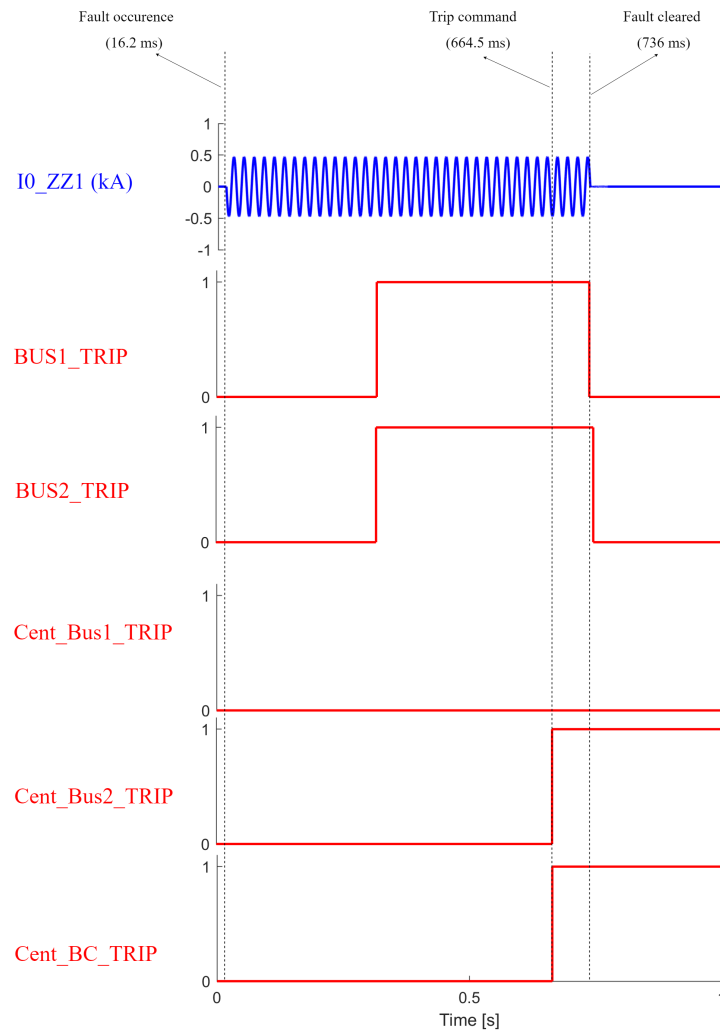


Figure 5.14: Tripping times from the centralized GOOSE algorithm for a fault on Section 2 in Topology 3

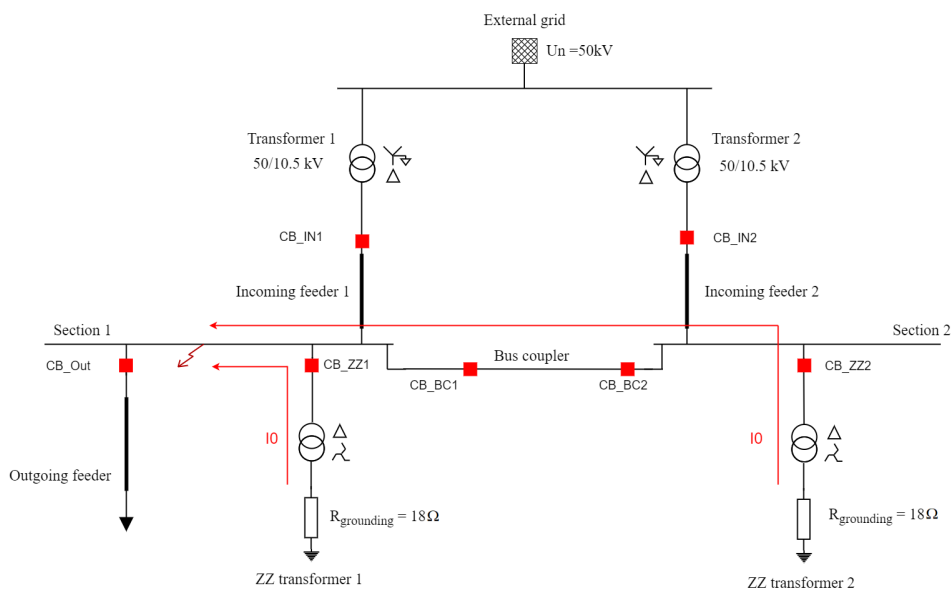
If the ZZ transformer is connected to Section 2, the logic for tripping the bus section CBs remains the same, while the logic for tripping the separate sections must be reversed. In other words, when the IED on this ZZ feeder detects a sufficient magnitude of the zero-sequence current, and both of the bus section IEDs also detect the zero-sequence current - the conclusion is that the fault is in Section 1. On the other hand, if the ZZ feeder IED is again detecting the zero-sequence current, but none of the bus section IEDs are detecting it, the conclusion is that the fault is in Section 2. This logic is presented in Table 5.3.

Table 5.3: Logic table for the algorithm when the ZZ transformer is connected on Section 2

INCOMING GOOSE MESSAGES					
Ie>.Str (Out IED)	1	0	0	0	0
Ineg>.Str (ZZ2 IED)	0	1	0	0	0
Ie>.Str (ZZ1 IED)	0	0	0	0	0
Ie>.Str (ZZ2 IED)	1	0	1	1	1
Ie>.Str (BC1 IED)	1	0	0	1	0
Ie>.Str (BC2 IED)	1	0	1	1	0
V0>.Str (BUS1 IED)	1	1	1	1	1
V0>.Str (BUS2 IED)	1	1	1	1	1
OUTGOING COMMANDS					
Cent_BUS1_TRIP	NO TRIP	NO TRIP	NO TRIP	TRIP	NO TRIP
Cent_BUS2_TRIP	NO TRIP	NO TRIP	NO TRIP	NO TRIP	TRIP
Cent_BC_TRIP	NO TRIP	NO TRIP	TRIP	TRIP	TRIP

By combining the logic schemes for the two ZZ feeders in the centralized algorithm, selective tripping can be achieved regardless of which section the ZZ transformer is connected to. This was tested by simulating all the different combinations with one ZZ transformer switched in, and one or two incoming transformers switched in, with the bus section CBs closed in all the simulation cases. For all of the cases, selectivity was achieved.

Again, a case that needs special attention is the case when both of the ZZ transformers are switched in, meaning that the grid is operating according to topology 4, which is a case in which a selectivity issue can arise. In Figure 5.15, the distribution of the zero-sequence current during a single-phase-to-ground fault in section 1, when the grid is operating according to topology 4, can be seen. In this case, both the ZZ transformers' IEDs and the bus coupler IEDs detect a presence of a zero-sequence current.

**Figure 5.15:** Distribution of the zero-sequence current for a fault on Section 1, with both ZZ transformers connected

It can easily be deduced that regardless of the fault location (Section 1, Section 2, or on the bus section coupler), all four abovementioned IEDs will still be detecting the zero-sequence current. That makes it practically impossible to achieve selectivity between a fault on the sections and the bus coupler

(when the grid operates in this topology) based on the $I_{e>.Str}$ signals of the IEDs. That is why, for this case, an extra logic was implemented in this algorithm to trip both the incoming feeders CBs and the bus coupler CBs when the fault occurs anywhere on the busbar system. Namely, if both the ZZ transformer IEDs are detecting a zero-sequence current (meaning that both of them are switched in) and both of the bus coupler IEDs are also detecting the zero-sequence current (meaning that the bus coupler CBs are closed and the two sections of the busbar systems are connected), a simultaneous tripping command is being sent to both of the incoming feeders CBs and the bus sections coupler CBs. The test results for the case when both of the ZZ transformers are switched in and the bus coupler CBs are closed, and a fault occurs on the bus coupler are shown in Figure 5.16. As it can be seen, the scheme is working according to the expectations and is tripping off the whole busbar system ('Cent_BUS1_TRIP', 'Cent_BUS2_TRIP' and 'Cent_BC_TRIP' are all changing their value to 1 simultaneously). Further notice is that even without the centralized protection scheme, the IEDs would send a tripping command to both of the incoming feeders ('BUS1_TRIP' and 'BUS2_TRIP'), and again the whole busbar system would be left de-energized. This means that even though the centralized scheme is not fully selective in this situation, it is not degrading the already existing busbar protection scheme.

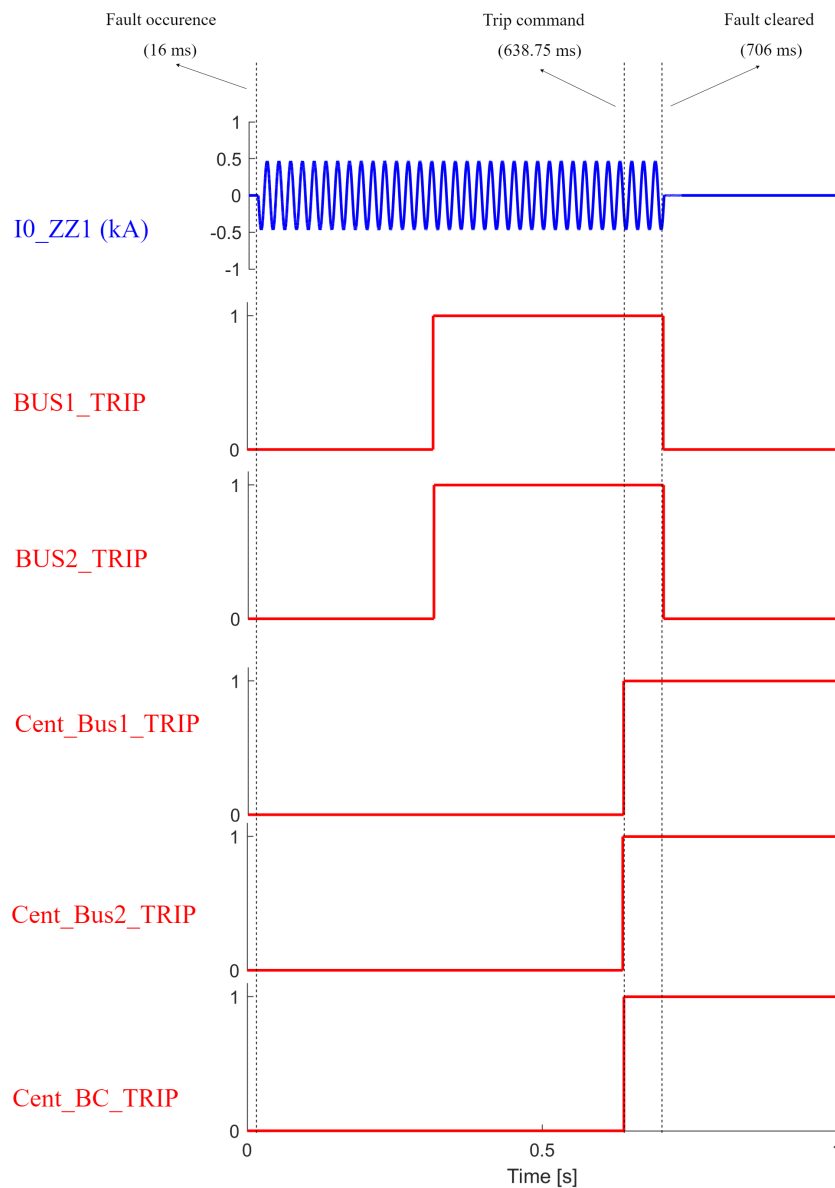


Figure 5.16: Tripping times from the centralized GOOSE algorithm for a fault on the bus coupler in Topology 4

Finally, a critical case to be examined is when the grid functions according to topology 4 again. However, now the single-phase-to-ground fault is taking place on the feeder connecting ZZ transformer 1 to the busbar. As shown in Figure 4.20, in this case, both of the incoming feeders IEDs and both of the bus coupler IEDs are detecting zero-sequence current. However, in this case, the $I_{neg>.Str}$ from the ZZ transformer feeder IED where the fault occurs will prevent sending of the tripping commands to the incoming feeders and the bus coupler CBs. An additional safety margin is that the ZZ transformer operates on the negative-sequence over-current setting ($I_{neg>.Op}$) with a time delay of 300ms. In comparison, the time delay of the tripping commands to the incoming feeders from the centralized protection scheme is 600ms. This insinuates that even time selectivity is achieved in this case. This means that the fault will be cleared only by the ZZ transformer IED, while the centralized protection algorithm will not send any unwanted trips, as seen in Figure 5.17. It is noticeable that only the ZZ transformer 1 sends a tripping signal to its respective CB, while the rest of the signals remain at zero.

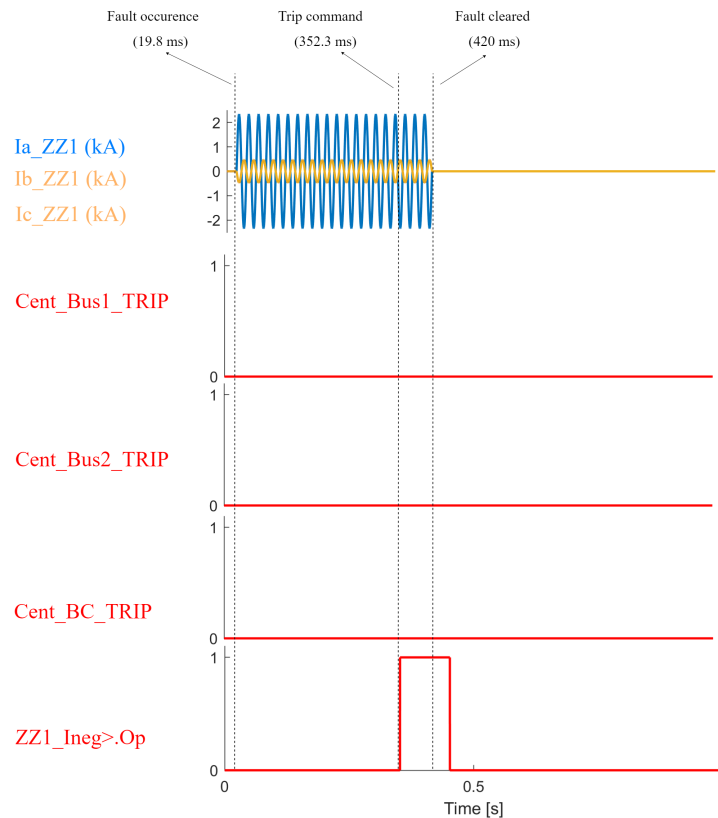


Figure 5.17: Tripping times from the centralized GOOSE algorithm for a fault on ZZ transformer 1 feeder in Topology 4

5.3.2. Conclusion for the GOOSE-based centralized algorithm

Table 5.4 presents the results obtained after the extensive simulations of single-phase-to-ground faults on different fault locations while the grid operates according to different operational topologies. Again, all simulated faults are single-phase-to-ground faults occurring in phase A with a resistance of 0.01Ω . The table's layout is exactly the same as explained for Table 4.2.

Table 5.4: Operation of the GOOSE based centralized algorithm for different fault locations in different grid topologies

Fault location / Network Topology	Section 1	Section 2	Bus coupler	Outgoing feeder	ZZ feeder
Topology 1	S	S	NA	S	S
Topology 2	S	S	S	S	S
Topology 3	S	S	S	S	S
Topology 4	O	O	O	S	S

As seen from the table, when the grid is operating according to topology 1 (the bus coupler being switched off and the sections disconnected), there is a fully selective algorithm, just as the one presented in Section 3.3. However, during the active topologies 2 and 3 (only one ZZ transformer switched in and the bus coupler closed), it was concluded that the centralized algorithm based on GOOSE messages is fully selective, meaning that it can fully distinguish between a fault on Section 1, Section 2 and the bus coupler. This, compared to the zero-sequence tripping algorithm, improves the protection scheme, as only the faulty part of the busbar is getting disconnected, and the rest of the grid can continue to have a power supply. The only selectivity problem can arise when both zig-zag transformers are in operation (topology 4), as seen in Table 5.4. In this case, as explained above, the algorithm cannot distinguish between a fault on Section 1, Section 2 or the bus coupler, so a tripping signal is sent to both the incoming feeders CBs and the bus coupler CBs. Even though this behavior is not fully selective, its operation is like the zero-sequence tripping scheme, meaning that no downgrading is introduced with this algorithm. Furthermore, it is intended that the centralized protection will initially function only as backup protection, so the criteria for selectivity can also be looser. From the results presented, it is evident that by using GOOSE messages from the already existing IEDs and centralized platform to run an algorithm that would process these messages and, based on that, make the necessary tripping decisions, much greater selectivity can be achieved than with the decentralized algorithm based on the zero-sequence tripping scheme. Furthermore, let us consider the centralized protection only as backup protection initially. It is noticeable that faster response times can be obtained than the currently necessary time for the backup protection to act.

It must be noted that this centralized protection cannot be defined as centralized backup protection in terms of independently detecting and clearing the faults. It is still dependent on the proper functioning of the already existing IEDs. However, it can be used more effectively as a centralized platform for running distributed protection schemes. It was proven that it could improve the overall busbar protection scheme and, at the same time, serve as an initial step for Stedin towards its learning experience with centralized protection. The reason for this is that this centralized protection is working explicitly by using GOOSE messages. This data type is already standard in Stedin's operation of the grids and for which the communication network is already suited. This means that in a case where Stedin requires a greater selectivity for the busbar faults, this algorithm can be implemented more quickly than a fully centralized protection scheme with only SV as inputs. In practice, this would require a processor/centralized platform that is IEC 61850 compatible and tested, without much processing capability since the algorithm runs on simple mathematical calculations. Special attention will have to be paid to configuring that the tripping messages from the centralized controller will be adequately mapped to the substation network, so a proper operation of the protection scheme can be guaranteed. A recommendation would also be that in a case of a GOOSE communication failure (one or more GOOSE messages are not being sent/received), the centralized algorithm would have to be disabled, thus providing greater security against unwanted trips.

5.4. SV based central protection

A genuine (centralized) backup protection should not rely on the proper operation of the primary protection (the IEDs) and must operate independently. This requires that the backup protection will be getting the current and/or voltage measurements from the instrument transformers and, solely based on its protection logic, will be issuing the correct tripping commands. In compliance with the IEC 61850 standard, the centralized protection will be subscribed to the SV messages published from the

respective MUs. As part of the thesis research, an algorithm based on this principle was developed.

The test case grid is again the same as the one used for the GOOSE-based centralized algorithm. However, this time instead of the GOOSE messages from the IEDs, the currents from all the current transformers are being communicated to the centralized platform. The SV rate is chosen to be the standard rate of 80 samples/cycle, which in the 50Hz systems would translate to a rate of 4000Hz. The SVs from the virtual devices were created by sampling the analog values of the CTs at a rate of 4000Hz.

However, due to technical limitations of the GTNETx2 card, sending the data with a rate of 4000Hz from the RTDS to MATLAB is not possible. Additionally, most relays use the 4000Hz rate only for fault and disturbance recording. In contrast, the protection algorithms operate at a much slower rate, usually in the vicinity of 4 to 8 samples per cycle [23]. Following this logic, it was decided that streaming the SV to the centralized MATLAB platform at 400Hz is sufficient. This requires that the SV data should first be pre-processed in RTDS and down-sampled to 400Hz. Only afterward the RTDS sends this data to MATLAB. The pre-processing of the data is shown in Figure 5.18.

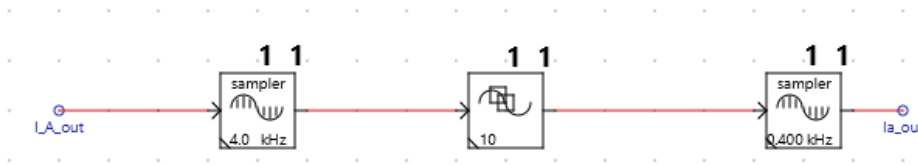


Figure 5.18: Pre-processing of the data for the SV-based centralized algorithm

The example shown in this figure is for the current in phase A of the outgoing feeder; however, the procedure is the same for all currents. The signal 'I_A_out' is the analog current on the secondary side of the CT on the outgoing feeder for phase A. As seen, this analog current is passed to a sampler, which samples the current at a rate of 4000Hz, thus, effectively creating SV data. For the SV messages from the Siemens IEDs, this step is skipped, as they are already sampled at 4000Hz. Before being sent to the MATLAB centralized algorithm, this data needs to be further processed. First, the SV data is buffered into a moving average filter, which creates an average value from ten consecutive data points. After that, the output of this average filter is down-sampled at a rate of 400Hz. The value of 400Hz corresponds to 8 samples/cycle for the power system frequency of 50Hz. After the final processing of the data, it is passed to the MATLAB code which runs the algorithm. The code of the algorithm is explained in Appendix H.

The algorithm, in its basics, operates on the same principle as differential protection. Three zones of protection were created: section 1, section 2, and the bus coupler. For every zone, it is detected whether the sum of the currents entering the zone equals the currents leaving the zone. If the sum difference is above an established threshold, a decision is made that a fault has occurred in the respective zone, and appropriate trip signals are sent. The threshold has to be set so that the protection will be sensitive enough to detect a fault in its zone but not over-sensitive to cause maloperations. The threshold was set to 200A (primary value), as it is a value that guarantees the sensitivity of the algorithm. Zone 1 covers section 1, which means that the sum of the currents from the incoming feeder 1, ZZ transformer 1, the outgoing feeder, and the bus coupler must be considered ⁶. Similarly, for Zone 2, the currents from the incoming feeder 2, ZZ transformer 2, and the bus coupler must be considered. Finally, for Zone 3, the currents on both sides of the bus coupler are considered. The CTs polarity is considered when calculating the difference in the currents for each zone. The three different zones, alongside the currents taken into account, are shown in Figures 5.19 - 5.21.

⁶the current from the CT that is on the side where the bus coupler is connected to section 1

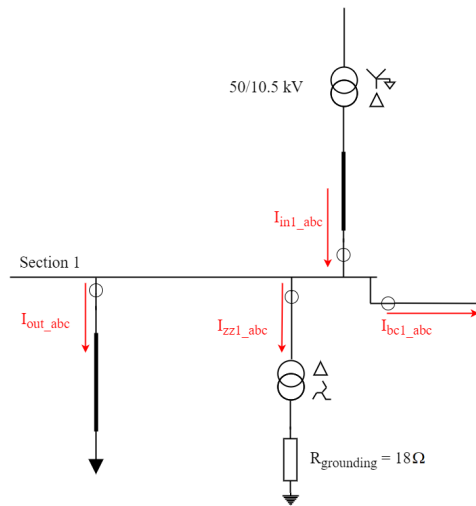


Figure 5.19: Zone 1 of the SV-based centralized algorithm

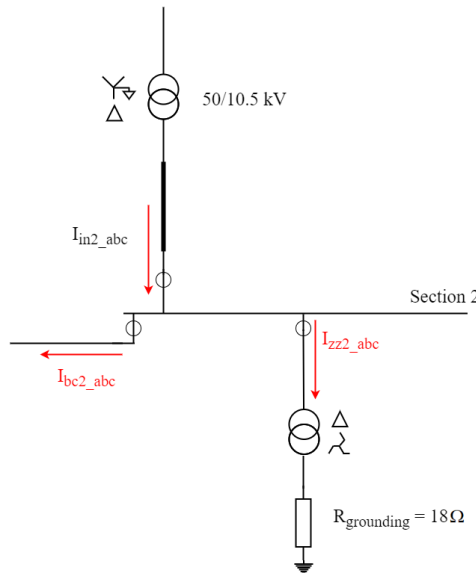


Figure 5.20: Zone 2 of the SV-based centralized algorithm

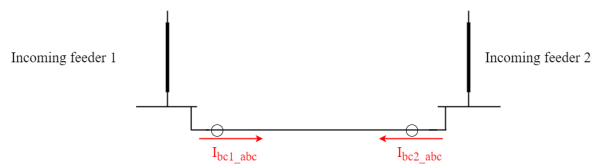


Figure 5.21: Zone 3 of the SV-based centralized algorithm

Again, this centralized protection is devised as backup protection with some added functionalities. In accordance with the previous centralized algorithm, the times for zone 1 and zone 2 are set to 600ms, while the operating time for a fault in zone 3 is set to 100ms. The fault locations and the possible network topologies are the same as the previously described ones. When the network operates according to topologies 1-3 (only one ZZ transformer is connected), full selectivity is provided with this algorithm. The results for single-phase faults when the network operates according to these three topologies are not further described here. The reasoning is that the same selectivity is achieved with the GOOSE-based algorithm, so no improvement is introduced for these topologies in terms of selectivity. However,

improvement is achieved when the network operates per topology 4 - both ZZ transformers are switched in. In this case, selectivity between faults in different zones can be achieved with this SV-based algorithm, which is an improvement compared to the GOOSE-based centralized algorithm. Figure 5.22 shows the results for a fault on the bus coupler when the network operates according to topology 4.

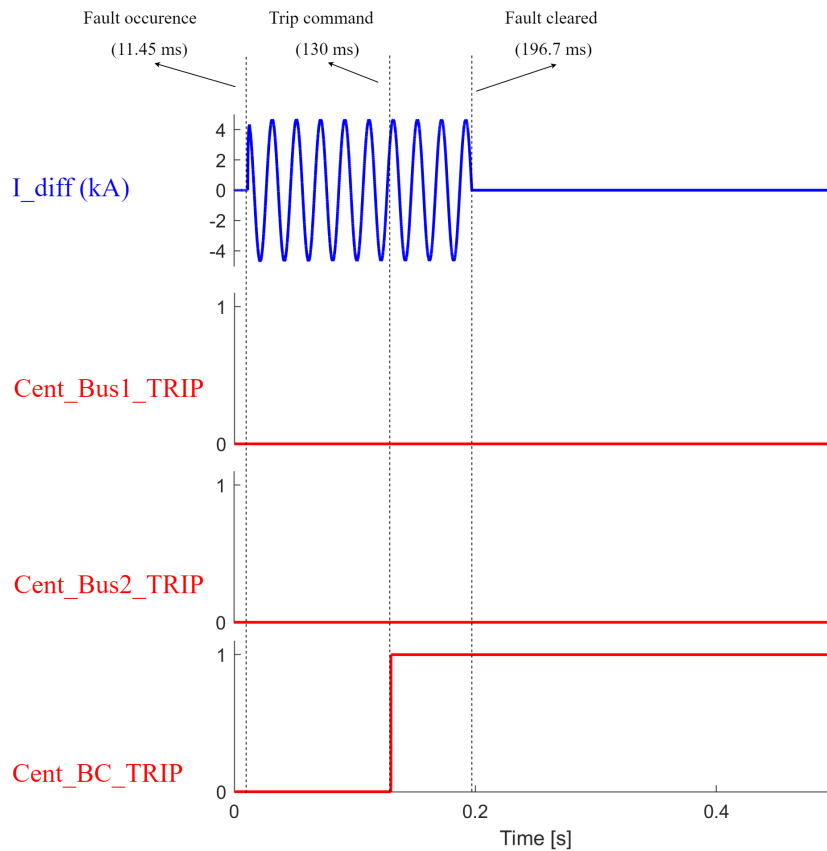


Figure 5.22: Tripping times from the SV-based algorithm for a fault on the bus coupler in Topology 4

As seen, the fault occurs at time $t = 11.45$ ms. A fault on the bus coupler will result in inequality of the currents that “enter” and “leave” the bus coupler. The directions of whether a current “enters” or “leaves” the protected zone are arbitrary, as only the magnitude of the difference is of interest. This inequality is presented in Figure 5.22, where ‘ I_{diff} ’ represents the difference of the currents seen by BC1 and BC2 IED, respectively. It has to be pointed out that this difference will have a value different than zero only in the case of a fault on the bus coupler. In every other case, the difference will be zero as the same current would pass through both the IEDs. One can notice that the magnitude of this difference is higher than the defined threshold, which means that the fault will be detected. A tripping signal is sent after approximately 120 ms from the fault occurrence. Because of the selectivity provided with this method, we can see that the tripping signal is sent only to the bus coupler CBs. Around 180ms after the occurrence of the fault, the fault is cleared. The same behavior is observed for a fault in sections 1 and 2. It can be concluded that the algorithm is entirely selective for all fault locations during all network topologies.

5.4.1. Conclusion for the SV-based centralized algorithm

Table 5.5 shows the results from the operation of the SV-based centralized algorithm for faults on different fault locations during different network topologies.

Table 5.5: Operation of the SV based centralized algorithm for different fault locations in different grid topologies

Fault location / Network Topology	Section 1	Section 2	Bus coupler	Outgoing feeder	ZZ feeder
Topology 1	S	S	NA	S	S
Topology 2	S	S	S	S	S
Topology 3	S	S	S	S	S
Topology 4	S	S	S	S	S

As explained, full selectivity is achieved with this kind of algorithm. Additionally, it functions entirely independently from the primary protection and the IEDs. This means that it does not depend on the proper operation of the protection IEDs. Thus, it can act as proper backup protection if they fail to operate. However, the implementation of this kind of centralized protection is technically more challenging for Stedin (and other DSOs). There are several reasons behind this statement.

Firstly, SV streaming should be possible for the protection devices in the substation if an algorithm like this is operational. This requires using MUs or IEDs with MUs capabilities, which are not standard equipment types in the Stedin network. Furthermore, a process bus network is necessary to support this data type communication. An implication is that further investment and expansion in the communication network will be needed. Another difference is that SV messages are streamed continuously, and unlike GOOSE messages, they are not prioritized. Based on the number of devices streaming the SV data, the data can get buffered, and packets can get lost, as shown in [24]. The possibility of lost data and the latency limit has to be accounted for, as it may cause an improper algorithm operation. Further research in this direction will be required to assess the risks from this problem and possible solutions for its mitigation.

A proprietary consequence of using SV messages is the substation time-synchronization with increased accuracy. The method for time synchronization of the SV data uses the IEEE 1588 PTP protocol over the communication network [20]. By using a PTP time synchronization, a time-stamping that is synchronized for all substation devices can be achieved. This means that a PTP time-synchronization will be crucial in the network if SV-based centralized protection is to operate.⁷ Furthermore, if the PTP synchronization fails, the algorithm will no longer be operational. This implies that redundancy in the PTP time-synchronization should be considered a possibility. This will prevent the SV data from being completely blocked in case of the PTP clock failure, as there will be another PTP clock to substitute it.

Another consideration that needs to be taken into account is CT saturation. This phenomenon occurs when a very high current passes through the CT, which saturates the CT core to its maximum point. This implies that the secondary current of the CT does not match the primary current input (divided by the CT ratio) once the CT gets saturated [25]. As a result, the IED will register a current smaller than the actual one, which can cause possible protection maloperations. The currents that pass through the CTs in the case of single-phase faults are too low to cause CT saturation. However, in a case of a two-phase or three-phase fault, the currents can reach a magnitude that could cause CT saturation. As this algorithm depends on the accurate detection of currents, the CT saturation can pose a big problem for its proper operation. A solution is to use the principle already implemented in the state-of-the-art IEDs. The modern IEDs⁸ are required to detect a presence of fault before the minimum time to saturation of the CT expires. The minimum time to saturation of a CT is the time for which it is guaranteed that no saturation happens in the CT. They can also have a saturation detector, requiring the CT only to transform until saturation is detected [26]. If the centralized platform detects the fault according to this principle, then the saturation should not threaten the proper operation of the protection. In this direction, faster and smarter fault detection algorithms would have to be investigated and developed. Another possibility is that in the future, to utilize the IEC 61850 standard more efficiently, conventional CTs can be replaced by non-conventional instrument transformers. An example of such a non-conventional instrument transformer is the Rogowsky Coil. As the Rogowsky Coil is constructed over a nonmagnetic core, as a result of the linearity of the core, it does not experience saturation [27]. Using Rogowsky Coil as an

⁷local time synchronization is sufficient for the busbar protection scheme, and absolute synchronization is not required

⁸saturation is mainly a problem for the differential and distance protection

instrument transformer can make the saturation problem neglectable and improve the efficiency of this algorithm.

All of the considerations mentioned above make the implementation of the SV-based centralized algorithm a trickier task for the DSOs. Additionally, new testing and maintenance methods will have to be developed, as well as preparing the personnel for the logic behind the protection operation. However, the benefits of a more selective and faster protection algorithm, along with more optimal utilization of digital data, outweigh the challenges and make the concept of centralized protection worth exploring.

6

Conclusions and Recommendations

6.1. Conclusions

This thesis presents the implementation of a novel busbar protection scheme, which fully implements the IEC 61850 standard. This busbar protection scheme serves to protect against single-phase-to-ground faults in impedance earthed distribution grids. The first part of the thesis focuses on a protection scheme that uses the already available Stedin's infrastructure. The part of the grid under investigation is modeled in RTDS. A HiL simulations were carried out with a Sprecher IED. From the simulation results, the following conclusions can be made:

- The IEC 61850 communication protocol enables more efficient utilization of distributed protection schemes. In this way, protection problems or protection blinding can be tackled with the currently available IED infrastructure.
- The proposed zero-sequence tripping scheme can properly detect and switch off single-phase-to-ground busbar faults. No false trips were experienced during the simulation runs.
- The selectivity that can be achieved with the current IED infrastructure of Stedin is limited. This limitation does not allow for a distinction between a fault in section 1 and section 2 in some of the grid topologies. However, it is not considered a significant drawback according to the current needs of Stedin as a stakeholder.
- The simulations show that the operation of this protection scheme does not endanger the system's integrity.
- The delay introduced in the scheme's operation as a result of the communication between the IEDs is negligible. This results from the strict time latency allowed for GOOSE messages according to the IEC 61850 standard.
- The solution is ready to be implemented as a plug-and-play solution in Stedin's network in order to solve the problem of the current busbar protection blinding for single-phase-to-ground faults.

The second part of the thesis explores the possibilities for a centralized approach to achieve busbar protection. The same RTDS network is used, and two Siemens IEDs are utilized for the HiL simulation. The algorithm for running the centralized protection is implemented in MATLAB, and is then run as a SiL simulation with RTDS. Two centralized approaches are discussed, operating on GOOSE and SV data. From the simulation results, it could be seen that the centralized approach has an increased performance compared to the decentralized approach. The conclusion obtained from running simulations with the centralized approach are the following :

- Implementing the logic behind the zero-sequence tripping scheme at a centralized level increases the selectivity of the algorithm. This requires only the communication of GOOSE messages; thus, no significant communication latency is introduced in the protection scheme.
- The infrastructure of Stedin is already adjusted for the communication of GOOSE messages, which means that no significant investments in the communication network are required. This centralized approach can provide a good learning experience for DSOs such as Stedin to understand the possibilities and problems of centralized protection.

- Utilizing centralized protection as backup protection in the initial stage of its implementation can significantly decrease the operational times compared to the currently used backup protection.
- A centralized protection that operates only on the grid measurement (SV messages) is entirely independent of the IEDs and offers complete selectivity.
- The SV-based centralized approach requires further investment in the communication network and the measuring devices. Further research is needed to thoroughly understand this approach's risks and how to mitigate them.
- Communication is a discipline that is becoming increasingly entangled with power system protection.

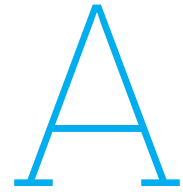
6.2. Recommendations

The zero-sequence tripping scheme can be tested against intermittent faults, which usually occur in cable networks. Systematic testing could be carried out by varying the frequency and duration of the impulses to detect any false operation of the protection scheme when an intermittent earth fault occurs on one of the outgoing feeders. Further study should be carried out in the domain of communication reliability in power system protection, as it will play a vital role if a centralized protection concept is implemented. For that purpose, a more in-depth analysis could be carried out to see the best communication practices and how to optimally achieve communication network redundancy in the substation. Research should be conducted to determine how to fully implement the IEC 61850 standard resilient and robustly in the distribution substations. The interoperability of devices from different vendors can be tested to see whether it complies with the IEC 61850 standard. Additionally, it should be tested whether the MUs and IEDs from different vendors react in the same manner to data and/or time-synchronization loss. New, more intelligent algorithms for fault detection and localization based on SV data are also encouraged to be investigated. This could help to utilize the digital data optimally and produce more selective and faster clearing of the faults.

References

- [1] Alstom Grid, *Network Protection & Automation Guide*. Alstom Grid, 2011.
- [2] J. G. John and D. S. J. William, *Power System Analysis*. McGraw-Hill Inc., 1994.
- [3] R. Rifaat, S. McFetridge, and J. Hong, "Considerations in applying symmetrical components for fault current evaluation of an islanded neutral resistance-grounded system," in *2017 Petroleum and Chemical Industry Technical Conference (PCIC)*, 2017, pp. 469–476. doi: [10.1109/PCICON.2017.8188769](https://doi.org/10.1109/PCICON.2017.8188769).
- [4] M. S. Thomas, A. Prakash, and Nizamuddin, "Modeling and Testing of Protection Relay IED," in *2008 Joint International Conference on Power System Technology and IEEE Power India Conference*, 2008, pp. 1–5. doi: [10.1109/ICPST.2008.4745389](https://doi.org/10.1109/ICPST.2008.4745389).
- [5] C. Brunner, "IEC 61850 for power system communication," pp. 1–6, 2008. doi: [10.1109/TDC.2008.4517287](https://doi.org/10.1109/TDC.2008.4517287).
- [6] K.-P. Brand, "The standard IEC 61850 as prerequisite for intelligent applications in substations," 714–718 Vol.1, 2004. doi: [10.1109/PES.2004.1372909](https://doi.org/10.1109/PES.2004.1372909).
- [7] R. Mackiewicz, "Overview of IEC 61850 and Benefits," in *2006 IEEE PES Power Systems Conference and Exposition*, 2006, pp. 623–630. doi: [10.1109/PSCE.2006.296392](https://doi.org/10.1109/PSCE.2006.296392).
- [8] Y. Mi, "Closed-loop Testing of Distance Relay Based on IEC 61850 and RTDS," M.S. thesis, Delft University of Technology, 2021.
- [9] P. van Oirsouw, *Netten voor distributie van elektriciteit*. Phase to phase, 2011.
- [10] H.-L. Jou, J.-C. Wu, K.-D. Wu, W.-J. Chiang, and Y.-H. Chen, "Analysis of zig-zag transformer applying in the three-phase four-wire distribution power system," *IEEE Transactions on Power Delivery*, vol. 20, no. 2, pp. 1168–1173, 2005. doi: [10.1109/TPWRD.2005.844281](https://doi.org/10.1109/TPWRD.2005.844281).
- [11] M. Jankovski, "Proposing different possibilities for the detection of phase to earth faults on busbars systems in impedance grounded distribution networks," Internship report, 2021 - not available publicly.
- [12] Z. Gajić, H. Faramawy, L. He, K. Koppari, L. Max, and M. Kockott, "Modern design principles for numerical busbar differential protection," in *2019 72nd Conference for Protective Relay Engineers (CPRE)*, 2019, pp. 1–16. doi: [10.1109/CPRE.2019.8765881](https://doi.org/10.1109/CPRE.2019.8765881).
- [13] E. J. H. Juan M. Gers, *Protection of electricity distribution networks*. The Institution of Electrical Engineers, London, United Kingdom, 1999.
- [14] E. Parabirsing, "Analysis of Protection Malfunctioning in Meshed Distribution Grids," M.S. thesis, Delft University of Technology, 2010.
- [15] A. Novikov, "Testing and evaluation of distance protection in system with high PV sources penetration," M.S. thesis, Delft University of Technology, 2018.
- [16] RTDS Technologies, "RTDS Hardware Manual," User's manual.
- [17] R. Hidalgo, C. Abbey, and G. Joós, "A review of active distribution networks enabling technologies," in *IEEE PES General Meeting*, 2010, pp. 1–9. doi: [10.1109/PES.2010.5590051](https://doi.org/10.1109/PES.2010.5590051).
- [18] Working Group on Centralized Substation Protection and Control, IEEE Power System Relaying Committee, "Advancements in centralized protection and control within a substation," *IEEE Transactions on Power Delivery*, vol. 31, no. 4, pp. 1945–1952, 2016. doi: [10.1109/TPWRD.2016.2528958](https://doi.org/10.1109/TPWRD.2016.2528958).
- [19] ABB, "Centralized protection and control," White paper.
- [20] C. P. Teoh, R. Hunt, and G. Lloyd, "A centralized protection and control system using a well proven transmission class protection relay," in *15th International Conference on Developments in Power System Protection (DPSP 2020)*, 2020, pp. 1–6. doi: [10.1049/cp.2020.0088](https://doi.org/10.1049/cp.2020.0088).

- [21] Substation Protection Subcommittee, "Centralized substation protection and control," Report, 2015.
- [22] J. J. Chavez, N. V. Kumar, S. Azizi, J. L. Guardado, J. Rueda, P. Palensky, V. Terzija, and M. Popov, "PMU-voltage drop based fault locator for transmission backup protection," vol. 196, 2021, p. 107188. doi: <https://doi.org/10.1016/j.epsr.2021.107188>. [Online]. Available: <https://www.sciencedirect.com/science/article/pii/S0378779621001693>.
- [23] RTDS Technologies, "Protection and Automation Tutorial," User's manual.
- [24] D. M. E. Ingram, P. Schaub, R. R. Taylor, and D. A. Campbell, "Performance Analysis of IEC 61850 Sampled Value Process Bus Networks," *IEEE Transactions on Industrial Informatics*, vol. 9, no. 3, pp. 1445–1454, 2013. doi: [10.1109/TII.2012.2228874](https://doi.org/10.1109/TII.2012.2228874).
- [25] A. Hargrave, M. J. Thompson, and B. Heilman, "Beyond the knee point: A practical guide to CT saturation," in *2018 71st Annual Conference for Protective Relay Engineers (CPRE)*, 2018, pp. 1–23. doi: [10.1109/CPRE.2018.8349779](https://doi.org/10.1109/CPRE.2018.8349779).
- [26] G. Ziegler, *Numerical differential protection*. Publicis Publishing, Erlangen, 2012.
- [27] A. Bagheri, M. Allahbakhshi, D. Behi, and M. Tajdinian, "Utilizing Rogowski y coil for saturation detection and compensation in iron core current transformer," in *2017 Iranian Conference on Electrical Engineering (ICEE)*, 2017, pp. 1066–1071. doi: [10.1109/IranianCEE.2017.7985199](https://doi.org/10.1109/IranianCEE.2017.7985199).
- [28] J. Wang and R. Lascu, "Zero sequence circuit of three-legged core type transformers," in *2009 62nd Annual Conference for Protective Relay Engineers*, 2009, pp. 188–213. doi: [10.1109/CPRE.2009.4982513](https://doi.org/10.1109/CPRE.2009.4982513).



Transformer groups in zero-sequence representation

Representation of the different transformer groups in the zero-sequence equivalent circuits [28].

CASE	SYMBOLS	CONNECTION DIAGRAMS	ZERO-SEQUENCE EQUIVALENT CIRCUITS
1			
2			
3			
4			
5			

B

NX PLUS C datasheet

STEDIN™

SIEMENS

1 Leveranciersgegevens

1.1 Opstelling	
Vloerbelasting (kg/m ²):	1200
Ventilatie:	N.V.T.
Vochtigheid:	≤98%
Verwarming:	-5C° t/m +55C°
Rijmogelijkheid, vijzels, ...	Hijsogen, pompwagen
1.2 Motoren	
Vermogen (W):	600
Opgenomen stroom (A)	5,5
Aanloopstroom gedurende (A/s):	6,8/3
Aanloopstroom volgens oscillogram:	6,8
1.3 Hulpspanning	
Gemiddeld opgenomen vermogen per veld voor bediening en signalering (W):	25
1.4 Vermogensschakelaars	
Type schakelaar:	3AH55
Opgenomen vermogen inschakelspoel (W):	140
Opgenomen vermogen uitschakelspoel (W):	140
Maximale inschakeltijd (ms):	75
Uitschakeltijd (som van de mechanische openingstijd en de maximale boogtijd, gemeten bij 60% en 100% van het uitschakelvermogen) (ms):	80
Poolongelijkheid (ms):	2



Network parameters

External grid

f (Hz)	50
Z1 (Ohm)	5
phi1 (degrees)	84.3
Z0 (Ohm)	5
phi0 (degrees)	84.3

Power transformer

f (Hz)	50
Rated power (MVA)	30
Transformation ratio (kV/kV)	50/10.5
Connection ratio	Ynd11
Leakage inductance (p.u)	0.1269
Copper losses (p.u)	0.0056
phi0 (degrees)	84.3

Cables

f (Hz)	50
R1 (Ohm)	0.194
X1 (Ohm)	0.083
Xc1 (MegaOhms)	0.0096
R0 (Ohm)	2.46
X0 (Ohm)	0.13
Xc0 (MegaOhms)	0.0159

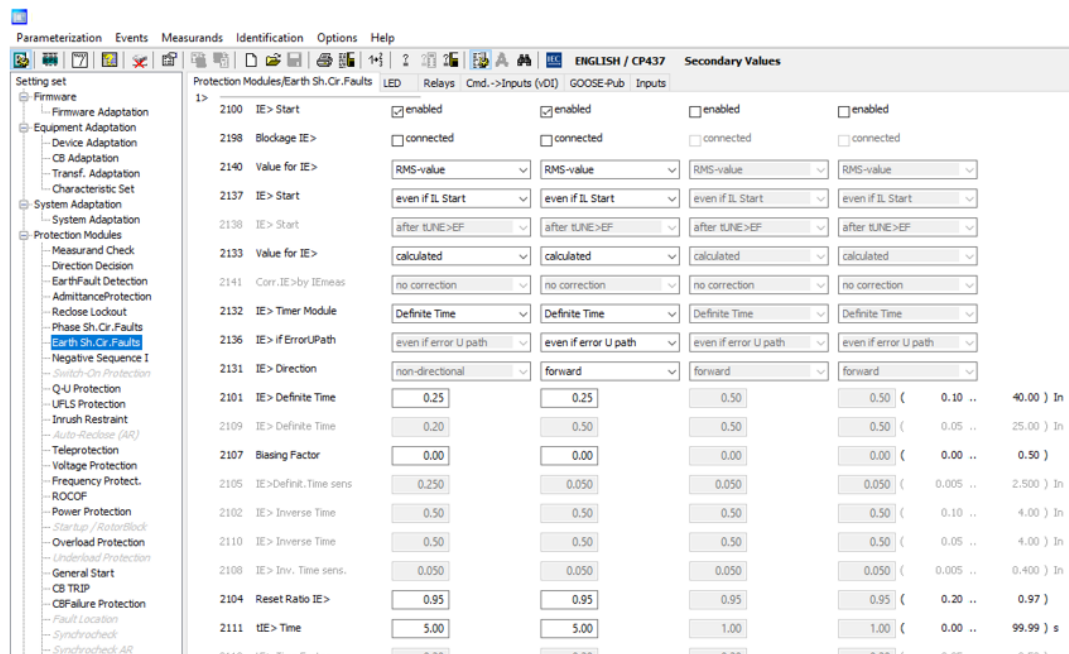
ZZ transformer

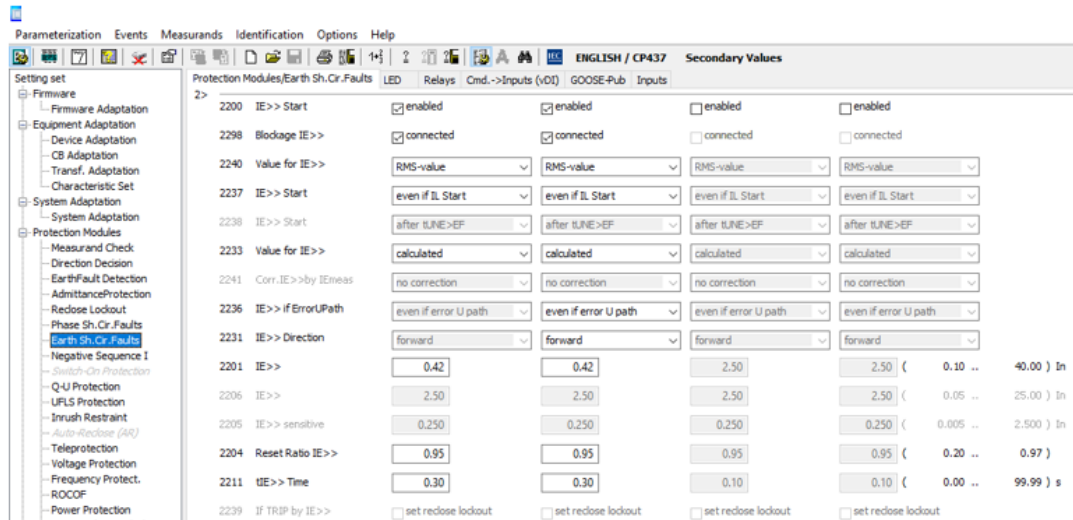
R0 (Ohm)	18
L0 (Henry)	0.001

D

Sprecher IED setting

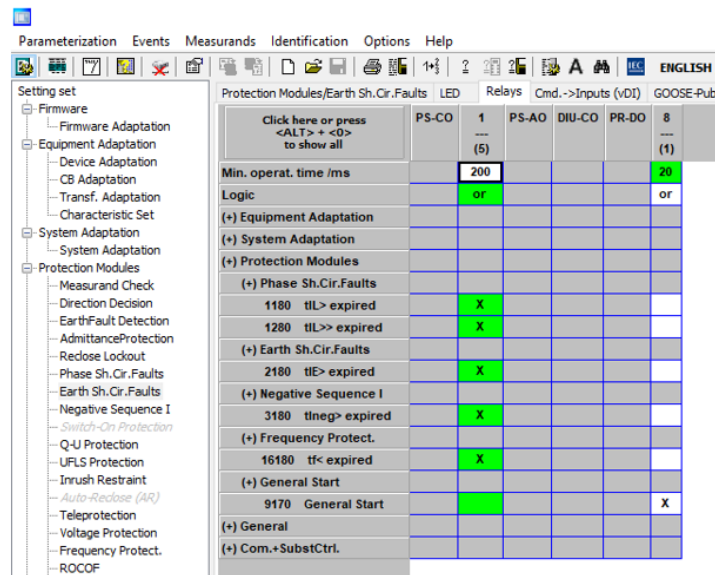
Firstly, the correct settings need to be implemented in the IED, which is done through the Sprecon E-engineering software, as shown in the following figures.





Important to be noted while filling in these parameters are that the timings are entered in seconds, while the standard entries for the operating currents are in secondary values (with the CT having a ratio of 600/1, as explained before). The next thing is to configure the trip signals in the IED, i.e., under which conditions should the IED send a tripping signal to the respective CB.

As seen, the OR logic is applied, meaning a trip signal will be sent regardless of which condition is fulfilled.



It is also important to notice that the $I_{e>>}$ is missing from this list because it is not used to trip the CB on the ZZ feeder but only passes as information to the IED on the incoming bay. This information still needs to be communicated as a GOOSE message, so it must be set in the GOOSE publishing tab.

Click here or press <ALT> + <G> to show all	LED	Description text
Min. operat. time /ms	100	
(+) Equipment Adaptation		
(+) Characteristic Set		
271 Char. Set 1 act.	*	Char. Set 1 act.
272 Char. Set 2 act.	*	Char. Set 2 act.
273 Char. Set 3 act.	*	Char. Set 3 act.
274 Char. Set 4 act.	*	Char. Set 4 act.
(+) System Adaptation		
(+) Protection Modules		
(+) Direction Decision		
1990 Sh.C.Direct FctOn	*	Sh.C.Direct FctOn
2990 EarthSCDirectFctOn	*	EarthSCDirectFctOn
(+) Phase Sh.Cir.Faults		
1152 IL> Start	*	IL> Start
1252 IL>> Start	*	IL>> Start
(+) Earth Sh.Cir.Faults		
2170 IE> Start	*	IE> Start
(+) Negative Sequence I		
3170 Ineg> Start	*	Ineg> Start
(+) Frequency Protect.		
16199 Blockage f<	*	Blockage f<
16170 f< Start	*	f< Start
(+) General Start		
9170 General Start	*	General Start
9171 Start IL1	*	Start IL1
9172 Start IL2	*	Start IL2
9173 Start IL3	*	Start IL3
(+) CB TRIP		
9202 General TRIP	*	General TRIP
9207 TRIP IL>	*	TRIP IL>
9208 TRIP IL>>	*	TRIP IL>>
9211 TRIP IE>	*	TRIP IE>
9212 TRIP IE>>	*	TRIP IE>>
9216 TRIP Ineg>	*	TRIP Ineg>
9235 TRIP f<	*	TRIP f<
(+) General		
(+) Prot.Device On/Off		
51171 Protection ready	*	Protection ready
(+) Relays		
32401 PS-C01	*	PS-C01
(+) Com.+SubstCtrl.		

Finally, the subscribing GOOSE messages need to be configured for the IED. As explained, the $I_{e>>}$ of this IED is blocked upon receiving the appropriate signal from any of the outgoing feeders. The logic is set to OR since any of the outgoing feeders' inputs will block this overcurrent setting. A GOOSE message from only one outgoing feeder is presented to point out that the blocking command is the $I_{e>}$ start of the outgoing feeder.

General/GOOSE	LED	Relays	Cmd.->Inputs (V0)	GOOSE-Pub	Inputs
44101 Oper.Time GOOSE-Pub1					0 .. 500) ms
45101 Text GOOSE-Sub1			Veld 203 Ie> Str		RDM_NOTA_010_veld203_C_PROT/BEPTOC16T85tr [general + q + 1]
45301 On Delay GOOSE-Sub1			0		0 .. 65000) ms
45501 Off Delay GOOSE-Sub1			0		0 .. 65000) ms
45102 Text GOOSE-Sub2					



CMS - 156 Datasheet

Technical Data¹

Voltage amplifiers	
Setting range	3-phase AC (L-N) 3 x 0 ... 250 V 1-phase AC (L-L) 1 x 0 ... 500 V DC (L-N) 3 x 0 ... ±250 V
Power	3-phase AC (L-N) 3 x 75 VA at 75 ... 250 V 1-phase AC (L-N) 1 x 150 VA at 75 ... 250 V 1-phase AC (L-L) 1 x 150 VA at 150 ... 500 V DC (L-N) 1 x 212 W at ±(150 ... 250 V)
Accuracy	error < 0.03 % typ., < 0.1 % guar.
Distortion (THD+N) ²	< 0.03 % typ., < 0.1 % guar.
Bandwidth (-3dB)	> 6 kHz
Phase lag at 50/60 Hz (autom. corrected by a CMC)	1.95°/2.34°
Input voltage	0 ... 5 V
Amplification	50 V / V
Current amplifiers	
Setting range	3-phase AC (L-N) 3 x 0 ... 25 A 1-phase AC (L-N) 1 x 0 ... 75 A DC (L-N) 1 x 0 ... ±25 A
Power	3-phase AC (L-N) 3 x 70 VA at 7.5 A 1-phase AC (3L-N) 1 x 210 VA at 22.5 A 1-phase AC (L-L) 1 x 140 VA at 7.5 A DC (L-N) 1 x 140 W at ±10.5 A
3/6 phase operation	
single phase operation	

Current amplifiers (cont.)	
Accuracy	error < 0.03 % typ., < 0.1 % guar.
Distortion (THD+N) ²	< 0.1 % typ., < 0.3 % guar.
Bandwidth (-3dB)	> 6 kHz
Phase lag at 50/60 Hz	1.88°/2.26°
Input voltage	0 ... 5 V
Amplification	5 A / V
Max. compliance voltage (L-N)/(L-L)	15 Vpk / 30 Vpk
Amplifiers, general ³	
Input impedance	> 40 kΩ
Galvanic isolation Input/Output	1.5 kVDC
Galvanic isolation amplifier groups	1.5 kVDC
Connection	4 mm (0.16 in) banana sockets/comb. socket
Amplifiers, if controlled by a CMC	
Frequency	range sine signals 10 ... 1000 Hz range transient signals DC ... 3.1 kHz
	accuracy/-drift ±0.5 ppm / ±1 ppm resolution 5 μHz
Phase	angle range -360° ... +360° resolution 0.001° error at 50/60 Hz < 0.02° typ., < 0.1° guar.
Output voltage resolution	12 mV
Output current resolution	1 mA
Power supply	
Nominal input voltage	110 ... 240 VAC, 1-phase
Permissible input voltage	99 ... 264 VAC
Nominal frequency	50/60 Hz
Permissible frequency range	45 ... 65 Hz
Power consumption	< 1000 VA
Connection	Standard AC socket (IEC 60320)
Environmental conditions	
Operation temperature	0 ... +50 °C (+32 ... +122 °F)
Storage temperature	-25 ... +70 °C (-13 ... +158 °F)
Humidity range	Relative humidity 5 ... 95 %, non-cond.
Vibration	IEC 60068-2-6 (20 m/s ² at 10 ... 150 Hz)
Shock	IEC 60068-2-27 (15 g/11ms half-sine)
EMC	Directive 2004/108/EC (CE conform)
Emission	EN 61326-1, EN61000-6-4, EN61000-3-2/3 FCC Subpart B of Part 15 Class A
Immunity	EN 61326-1, EN61000-6-2, EN 61000-4-2/3/4/5/6/11
Safety	Directive 2006/95/EC (CE conform) EN 61010-1, EN 60950-1, UL 61010-1, CAN/CSA-C22.2 No 61010-1-04
Miscellaneous	
Weight	14.7 kg (32.4 lbs)
Dimensions (W x H x D, without handle)	450 x 145 x 390 mm (17.7 x 5.7 x 15.4 in)
Certifications	TUV-GS

¹ Guaranteed values valid over one year within 23 °C ± 5 °C (73 °F ± 10 °F), in the frequency range of 10 ... 100 Hz at nominal value. Specifications for three-phase systems under symmetrical conditions (0°, 120°, 240°).

² THD+N: Values at 50/60 Hz with 20 kHz bandwidth

³ All current and voltage outputs are fully overload and short-circuit proof and protected against external high-voltage transient signals and overtemperature

F

Siemens IEDs setting

Firstly, the correct settings need to be implemented in the IED through the DIGSI 5 software. In the following figure, the implementation of the earth-fault protection setting in the IED on the ZZ1 transformer is shown. The current thresholds are to be entered in their secondary values.

The screenshot displays two configuration panels for protection stages. The top panel, 'Definite-T 1', lists parameters for seven protection elements (addresses 21.211.751.1 to 21.211.751.6). The bottom panel, 'Definite-T 2', lists parameters for seven protection elements (addresses 21.211.752.1 to 21.211.752.6). Each element has a set of settings including Mode, Operate & fit.rec. blocked, Dynamic settings, Method of measurement, Threshold, Dropout ratio, Dropout delay, and Operate delay.

Address	Mode	Operate & fit.rec. blocked	Dynamic settings	Method of measurement	Threshold	Dropout ratio	Dropout delay	Operate delay
21.211.751.1	on							
21.211.751.2		no						
21.211.751.26			no					
21.211.751.8				RMS value				
21.211.751.3					0.25			
21.211.751.4						0.95		
21.211.751.101							0.00	s
21.211.751.6								5.00 s

Address	Mode	Operate & fit.rec. blocked	Dynamic settings	Method of measurement	Threshold	Dropout ratio	Dropout delay	Operate delay
21.211.752.1	on							
21.211.752.2		no						
21.211.752.26			no					
21.211.752.8				RMS value				
21.211.752.3					0.42			
21.211.752.4						0.95		
21.211.752.101							0.00	s
21.211.752.6								0.30 s

Similarly, as for the Sprecher IED, the second stage of the earth-fault protection ($I_{e>>}$) is not used to trip the CB on the ZZ feeder. This signal must be removed from the circuit breaker interaction table, as shown in the following figure.

Circuit breaker 1	
Trip logic	
Protection group	Trip
(All)	(All)
▶ 50/51 OC-3ph-A1	X
▼ 50N/51N OC-gnd-A1	*
▶ Definite-T 1	X
▶ Definite-T 2	
▶ 46 I2 1	X

The following thing to be done is to configure the GOOSE messages that need to be communicated.

This is done through the IEC 61850 System Configurator, which runs as a standalone module in coordination with DIGSI 5. An important thing for properly configuring the IEC 61850 communication is to ensure that all of the involved devices belong to the same sub-network. Afterward, all of the devices can be found in the GOOSE tab. This is where it is chosen which signals are transmitted as GOOSE messages from the sources and what their destination is. An example of this is shown in the following figure.

GOOSE messages					
Source	CDC	Description	Defau...	Destination	Description
IEC station 1				*	
GOOSE Application_8022				*	
GOOSE Application_0001				*	
GOOSE ZZ1				*	
S7SA86_A/Ln1_46121/LLN0/DataSet (2/200)				*	
S7SA86_A/Ln1_5051NOCgndA1/LLN0/DataSet (2/2...				*	
S7SA86_A/Ln1_5051NOCgndA1/ND_PTOC2/Op	ACT	Ln1_51N-A1/Definite-T 2/Operate		*	
3-pole	SPC			*	
S7SA86_A/Ln1_5051NOCgndA1/ND_PTOC2/Op/...	SPC	Ln1_51N-A1/Definite-T 2/Operate/3...		S7SA86_B/Mod3/LLN0/R...	E:ETH-BB-2FO/Mod3/LLN0/LLN0/RxOp
S7SA86_A/Ln1_5051NOCgndA1/LLN0/DataSet_1 (2...				*	
S7SA86_A/CB1/LLN0/DataSet (2/200)				*	
GOOSE BUS1				*	

The proper communication and network protocols for SV streaming must be chosen in the appropriate communication module. The IEC 61850-9-2 communication protocol has to be chosen, as well as the time-synchronization network protocol IEEE 1588, as shown in the following figures.

General	
IP interfaces	Communication
IP interface 1 settings	
MTU size settings	
IP routes	
Details	
Protocols	
Communication	
Redundancy	
Network	
Service	

IEC61850			
Select	Protocols	Mapping	Settings
<input checked="" type="checkbox"/>	IEC 61850-8-1		Not Applicable
<input type="checkbox"/>	9-2 Client		
<input checked="" type="checkbox"/>	9-2 Merg.unit		Not Applicable
<input type="checkbox"/>	9-2 MU 75S85CU		

General	
IP interfaces	Network
IP interface 1 settings	
MTU size settings	
IP routes	
Details	
Protocols	
Communication	
Redundancy	
Network	
Service	

Network			
Select	Protocols	Mapping	Settings
<input checked="" type="checkbox"/>	DCP		Not Applicable
<input type="checkbox"/>	SNTP		
<input checked="" type="checkbox"/>	IEEE 1588		Settings
<input type="checkbox"/>	SNMP		

Finally, in the Merging-unit routing tab, it can be chosen which measurements it is required to be streamed. Additionally, this tab contains the identification of the particular SV stream.

Stream name	Stream type	SMV ID	Consumed channels	Current-measuring points		Voltage-measuring points	
				Meas.point I-3ph 1	Meas.point V-3ph 1	Meas.point I-3ph 1	Meas.point V-3ph 1
F:ETH-BD-2FO							
Merging unit 11SMV Stream	IEC 61869-9	S7SA86AMod3MU103	4(32)		X		
Add New							



MATLAB centralized platform based on GOOSE messages

At the beginning stage of the algorithm, communication has to be established between MATLAB and RTDS through the TCP protocol, as shown in the figure below. After that, the tripping signals' initial conditions are set to zero. Three tripping signals are being sent from the MATLAB centralized algorithm:

- CB_trip(1) - trip signal to incoming feeder 1 and to the bus coupler CBs
- CB_trip(2) - trip signal to incoming feeder 2 and to the bus coupler CBs
- CB_trip(3) - trip signal only to the bus coupler CBs

The sums used to track the time during which a condition is true are also set to zero at the program's initial start. The sums, as well as the conditions for which they are used, are the following:

- sum_BUS1_1 - condition: Fault is in section 1, only ZZ transformer 1 is connected
- sum_BUS1_2 - condition: Fault is in section 1, only ZZ transformer 2 is connected
- sum_BUS2_1 - condition: Fault is in section 2, only ZZ transformer 1 is connected
- sum_BUS2_2 - condition: Fault is in section 2, only ZZ transformer 2 is connected
- sum_BC - condition: Fault is on the bus coupler, only one ZZ transformer
- sum_all - condition: Fault is on the busbar system, two ZZ transformers are connected
- breaker_reset - condition: a tripping signal has been issued

```

1 -   clc
2 -   clear
3 -   close all force
4 -   instreset
5 -   format long g
6
7 -   % The IP address of the GTNETx2 module that is used for the
8 -   % communication between the RTDS and MATLAB must be inserted here.
9 -   % The port number has to match the one that is entered in the GTNET-SKT
10 -  % component in the RSCAD.
11
12 -  ServerIP='131.180.164.24';
13 -  Port = 4700;
14
15 -  % Command to establish the TCP communication between MATLAB and RTDS
16
17 -  Skt_Dev = tcpclient(ServerIP, Port, 'Timeout', 10);
18
19 -  % The initial conditions for the trip signals are set to zero at the
20 -  % beginning of the simulation
21
22 -  CB_trip(1, 1:3) = 0;
23
24 -  % The initial conditions for the sums are set to zero at the
25 -  % beginning of the simulation. These sums are used as help variables to be
26 -  % able to keep track of the time during which a condition is true
27
28 -  sum_BUS1_1 = 0;
29 -  sum_BUS1_2 = 0;
30 -  sum_BUS2_1 = 0;
31 -  sum_BUS2_2 = 0;
32 -  sum_BC = 0;
33 -  sum_all = 0;
34 -  breaker_reset = 0;

```

After that, a while cycle is started, which runs until it manually receives a command to stop or until the data from the RTDS is no longer received. The data from the RTDS is received in the data type unsigned integer of 8 bits ('uint8'), after which is converted to a data type unsigned integer of 32 bits ('uint32') before it is further processed. After that, internal variable names are given to all the messages received from the RTDS. The translation table of how these variables coincide with the GOOSE signals from the IEDs can be seen in the following table:

MATLAB variables	GOOSE signals
ZZ_Ie_1	<i>Ie</i> _{>>} .Str (ZZ1 IED)
ZZ_Ineg_1	<i>Ineg</i> _{>} .Str (ZZ1 IED)
ZZ_Ie_2	<i>Ie</i> _{>>} .Str (ZZ2 IED)
BC1_Ie	<i>Ie</i> _{>} .Str (BC1 IED)
BC2_Ie	<i>Ie</i> _{>} .Str (BC2 IED)
V0_bus1	<i>V0</i> _{>} .Str (BUS1 IED)
V0_bus2	<i>V0</i> _{>} .Str (BUS2 IED)
out1_Ie	<i>Ie</i> _{>} .Str (Out IED)

The first condition that is checked is whether the outgoing feeder is detecting a zero-sequence current or whether the ZZ transformer is detecting a negative-sequence current. If any of these two conditions is true, the *Ie*_{>>}.Str signals from both of the ZZ transformers are set to zero. This is done with the help of new variables 'ZZ1_Ie' and 'ZZ2_Ie', which are used internally in MATLAB. These two signals later in the algorithm will represent the new *Ie*_{>>}.Str signals of the ZZ transformers. If none of the above-mentioned conditions are true, then the signals 'ZZ1_Ie' and 'ZZ2_Ie' coincide with the signals 'ZZ_Ie_1' and 'ZZ_Ie_2', respectively.

```
35
36 - while 1
37
38     % Reading the data from the RTDS and converting it to unsigned integer
39     % data type for further operation with them
40
41     TCPIP_buffer_data = read(Skt_Dev, 32, 'uint8');
42     goose = swapbytes(typecast(TCPIP_buffer_data, 'uint32'));
43     ZZ_Ie_1 = double(goose(1));
44     out1_Ie = double(goose(2));
45     BC1_Ie = double(goose(3));
46     BC2_Ie = double(goose(4));
47     V0_bus1 = double(goose(5));
48     V0_bus2 = double(goose(6));
49     ZZ_Ie_2 = double(goose(7));
50     ZZ_Ineg_1 = double(goose(8));
51
52
53     % The first conditions are used to check whether an outgoing feeder is
54     % detecting a zero-sequence current. Based on this information a
55     % blocking of the busbar TRIP is made
56
57     if out1_Ie == 1 || ZZ_Ineg_1 == 1
58         Block_Ie = 0;
59     else
60         Block_Ie = 1;
61     end
62     ZZ1_Ie = Block_Ie * ZZ_Ie_1;
63     ZZ2_Ie = Block_Ie * ZZ_Ie_2;
```

After this, the first condition that is checked is whether the fault is on the bus coupler. If this condition is true, 'sum_BC' is increased by one, and if not, it is restored to zero. In this way, the time during which this condition is true is effectively measured. The same protection scheme logic is also applied for the case when only ZZ transformer 1 is switched in or only the ZZ transformer 2 is switched in.

```

64 %%%%%%%%%%%%%%%%%%%%%%%%%%%%%%%%%%%%%%%%%%%%%%%%%%%%%%%%%%%%%%%%%%%%%%%%%%%
65
66 % The first logic implemented is the one to check whether the fault is
67 % between the bus section CBs. While the conditions are true, the sum
68 % gets increased by 1 at every data communication step, and when they
69 % are not true the sum gets restarted to its initial value of 0.
70
71 - if (BC1_Ie == 1 && BC2_Ie == 0) || (BC1_Ie == 0 && BC2_Ie == 1)
72 -     sum_BC = sum_BC + 1;
73 - else
74 -     sum_BC = 0;
75 - end
76 %%%%%%%%%%%%%%%%%%%%%%%%%%%%%%%%%%%%%%%%%%%%%%%%%%%%%%%%%%%%%%%%%%%%%%%%%%%
77
78 % The second set of logic operations is to check the location of the
79 % fault under the assumption that only the ZZ transformer on Section 1
80 % is switched in. While the conditions are true, the sum gets increased
81 % by 1 at every data communication step, and when they are not true the
82 % sum gets restarted to its initial value of 0.
83
84 - if ((ZZ1_Ie - ZZ2_Ie) == 1 && (BC1_Ie + BC2_Ie == 0)) && V0_bus1 == 1
85 -     sum_BUS1_1 = sum_BUS1_1 + 1;
86 - else
87 -     sum_BUS1_1 = 0;
88 - end
89
90 - if ((ZZ1_Ie - ZZ2_Ie) == 1 && (BC1_Ie * BC2_Ie == 1)) && V0_bus2 == 1
91 -     sum_BUS2_1 = sum_BUS2_1 + 1;
92 - else
93 -     sum_BUS2_1 = 0;
94 - end
95 %%%%%%%%%%%%%%%%%%%%%%%%%%%%%%%%%%%%%%%%%%%%%%%%%%%%%%%%%%%%%%%%%%%%%%%%%%%
96
97 % In this set of logic operations the location of the fault is checked
98 % under the assumption that only the ZZ transformer on Section 2 is
99 % switched in. While the conditions are true, the sum gets increased
100 % by 1 at every data communication step, and when they are not true the
101 % sum gets restarted to its initial value of 0.
102
103 - if ((ZZ2_Ie - ZZ1_Ie) == 1 && (BC1_Ie * BC2_Ie == 1)) && V0_bus1 == 1
104 -     sum_BUS1_2 = sum_BUS1_2 + 1;
105 - else
106 -     sum_BUS1_2 = 0;
107 - end
108
109 - if ((ZZ2_Ie - ZZ1_Ie) == 1 && (BC1_Ie + BC2_Ie == 0)) && V0_bus2 == 1
110 -     sum_BUS2_2 = sum_BUS2_2 + 1;
111 - else
112 -     sum_BUS2_2 = 0;
113 - end
114 %%%%%%%%%%%%%%%%%%%%%%%%%%%%%%%%%%%%%%%%%%%%%%%%%%%%%%%%%%%%%%%%%%%%%%%%%%%
115

```

Finally, the logic in the situation when both of the ZZ transformers are switched in, and a fault is detected on the busbar system is programmed. At the end of each iteration cycle, all sums are checked to see whether any of the conditions were true for longer than the allowed time. The sums are checked based on the fact that we know that the frequency with which the data is transmitted from RTDS to MATLAB is 400 Hz. This means that if 400 consecutive data points have the value of 1, in reality, this signal has the value of 1 for 1 second. By using this logic, we can calculate the thresholds for the sum comparison as :

$$threshold = time_setting * 400 \quad (G.1)$$

, where the *time_setting* is equal to the tripping time we want, expressed in seconds.

```

115
116 % The final set of logic operations serves to enable a complete
117 % disconnection of the busbar system when a fault occurs
118 % (and is not on a ZZ feeder or an outgoing feeder) and both of the
119 % ZZ transformers are switched in. While the conditions are true, the
120 % sum gets increased by 1 at every data communication step, and when
121 % they are not true the sum gets restarted to its initial value of 0.
122
123 - if ((ZZ1_Ie * ZZ2_Ie) ==1 && (BC1_Ie * BC2_Ie == 1))
124 -     sum_all = sum_all + 1;
125 - else
126 -     sum_all = 0;
127 - end
128 %%%%%%%%%%%%%%%%%%%%%%%%%%%%%%%%%%%%%%%%%%%%%%%%%%%%%%%%%%%%%%%%%%%%%%%%%
129
130 % If the sum reaches a certain number (meaning that for a consecutive
131 % time the condition was true, a TRIP signal is written and
132 % communicated to the RTDS. This number that the sum needs to be
133 % reached in order for a tripping signal to be sent is calculated based
134 % on the time settings according to which the protection should operate
135 % and based on the fact that the data from the RTDS is communicated to
136 % MATLAB with a frequency of 400Hz.
137
138 - if sum_BC >= 40
139 -     CB_trip(3) = 1;
140 -     write(Skt_Dev, typecast(swapbytes(uint32(CB_trip)), 'uint8'));
141 - end
142
143 - if (sum_BUS1_1 >= 240) || (sum_BUS1_2 >= 240)
144 -     CB_trip(1) = 1;
145 -     CB_trip(3) = 1;
146 -     write(Skt_Dev, typecast(swapbytes(uint32(CB_trip)), 'uint8'));
147 - end
148
149 - if (sum_BUS2_1 >= 240) || (sum_BUS2_2 >= 240)
150 -     CB_trip(2) = 1;
151 -     CB_trip(3) = 1;
152 -     write(Skt_Dev, typecast(swapbytes(uint32(CB_trip)), 'uint8'));
153 - end
154 - if sum_all >= 240
155 -     CB_trip(1:3) = 1;
156 -     write(Skt_Dev, typecast(swapbytes(uint32(CB_trip)), 'uint8'));
157 - end
158

```

Finally, it is checked whether any trip command has been sent. If a trip command is being sent, it is allowed after a specific time for the tripping commands to be reset, thus allowing for another simulation case to be tested. After the while cycle is stopped, and with that, the whole centralized algorithm, a command is issued to stop the communication between RTDS and MATLAB.

```

158
159 % If any of the CBs is tripped, a new sum is started. When this sum
160 % reaches a certain value, all of the TRIP signals are restarted to 0,
161 % meaning that the CBs can be re-closed with a command in the RTDS.
162 % This command serves to make the simulations in the RTDS easier.
163
164 - if sum(CB_trip) >= 1
165 -     breaker_reset = breaker_reset + 1;
166 - else
167 -     breaker_reset = 0;
168 - end
169
170 - if breaker_reset >= 400
171 -     CB_trip(1:3) = 0;
172 -     write(Skt_Dev, typecast(swapbytes(uint32(CB_trip)), 'uint8'));
173 - end
174
175 - end
176 - clear Skt_Dev
177
178

```



MATLAB centralized platform based on SV messages

At the beginning stage of the algorithm, communication has to be established between MATLAB and RTDS through the TCP protocol, as shown in the figure below. After that, the tripping signals' initial conditions are set to zero. Three tripping signals are being sent from the MATLAB centralized algorithm:

- CB_trip(1) - trip signal to incoming feeder 1 and to the bus coupler CBs
- CB_trip(2) - trip signal to incoming feeder 2 and to the bus coupler CBs
- CB_trip(3) - trip signal only to the bus coupler CBs

```
1 - clc
2 - clear
3 - close all force
4 - instrreset
5 - format long g
6
7 - % The IP address of the GNETx2 module that is used for the
8 - % communication between the RTDS and MATLAB must be inserted here.
9 - % The port number has to match the one that is entered in the GNET-SKT
10 - % component in the RSCAD.
11
12 - ServerIP='131.180.164.24';
13 - Port = 4700;
14
15 - % Command to establish the TCP communication between MATLAB and RTDS
16
17 - Skt_Dev = tcpclient(ServerIP, Port, 'Timeout', 10);
18
19 - % Setting of the threshold
20
21 - I_diff = 200;
22
23 - % The initial conditions for the trip signals are set to zero at the
24 - % beginning of the simulation
25
26 - CB_trip(1, 1:3) = 0;
27
28
```

The sums used to track the time during which a condition is true are also set to zero at the program's initial start. The sums, as well as the conditions for which they are used, are the following:

- sum_BUS1A - condition: Fault is in Section 1, in phase A
- sum_BUS1B - condition: Fault is in Section 1, in phase B
- sum_BUS1C - condition: Fault is in Section 1, in phase C
- sum_BUS2A - condition: Fault is in Section 2, in phase A
- sum_BUS2B - condition: Fault is in Section 2, in phase B
- sum_BUS2C - condition: Fault is in Section 2, in phase C

- sum_sectBC_A - condition: Fault is on the bus coupler, in phase A
- sum_sectBC_B - condition: Fault is on the bus coupler, in phase B
- sum_sectBC_C - condition: Fault is on the bus coupler, in phase C
- breaker_reset - condition: a tripping signal has been issued

```

29 % The initial conditions for the sums are set to zero at the
30 % beginning of the simulation. These sums are used as help variables to be
31 % able to keep track of the time during which a condition is true
32
33 - sum_bus1A = 0;
34 - sum_bus1B = 0;
35 - sum_bus1C = 0;
36
37 - sum_bus2A = 0;
38 - sum_bus2B = 0;
39 - sum_bus2C = 0;
40
41 - sum_sectBC_A = 0;
42 - sum_sectBC_B = 0;
43 - sum_sectBC_C = 0;
44
45 - breaker_reset = 0;
46

```

After that, a while cycle is started, which runs until it manually receives a command to stop or until the data from the RTDS is no longer received. The data from the RTDS is received in the data type unsigned integer of 8 bits ('uint8'), after which is converted to a data type 'single' before it is further processed. The translation of how these variables coincide with the network currents is the following :

- Bus1_A - current that is flowing in phase A of incoming feeder 1
- Bus2_A - current that is flowing in phase A of incoming feeder 2
- section1_A - current that is flowing in phase A of the bus coupler, entering from Section 1
- section2_A - current that is flowing in phase A of the bus coupler, entering from Section 2
- out_A - current that is flowing in phase A of the outgoing feeder
- zz_A - current that is flowing in phase A of ZZ transformer 1
- zz_2_A - current that is flowing in phase A of ZZ transformer 2

The same notation is also used for the currents in phases B and C. The difference in current is calculated in the primary values; thus, firstly, the received currents are multiplied by their respective CT ratio. By doing that, all of the currents are transferred to their primary value.

```

47 - while 1
48
49     % Reading the data from the RTDS and converting it to single
50     % data type for further operation with them
51
52     TCPIP_buffer_data = read(Skt_Dev, 84, 'uint8');
53     currents = swapbytes(typecast(TCPIP_buffer_data, 'single'));
54
55     % Current transformers with ratios 2500/1 for the incoming feeders 1
56     % and 2
57     Bus1_A = currents(1) * 2500;
58     Bus1_B = currents(2) * 2500;
59     Bus1_C = currents(3) * 2500;
60
61     Bus2_A = currents(4) * 2500;
62     Bus2_B = currents(5) * 2500;
63     Bus2_C = currents(6) * 2500;
64
65
66

```

```

67 | % Current transformers with ratios 600/1 for the outgoing feeder, the
68 | % ZZ transformer feeders and the bus coupler
69 |
70 - | section1_A = currents(7) * 600;
71 - | section1_B = currents(8) * 600;
72 - | section1_C = currents(9) * 600;
73 |
74 - | section2_A = currents(10) * 600;
75 - | section2_B = currents(11) * 600;
76 - | section2_C = currents(12) * 600;
77 |
78 - | out_A = currents(13) * 600;
79 - | out_B = currents(14) * 600;
80 - | out_C = currents(15) * 600;
81 |
82 - | zz_A = currents(16) * 600;
83 - | zz_B = currents(17) * 600;
84 - | zz_C = currents(18) * 600;
85 |
86 - | zz_2_A = currents(19) * 600;
87 - | zz_2_B = currents(20) * 600;
88 - | zz_2_C = currents(21) * 600;
89 |

```

Afterward, the differential current that exists in all of the three zones is computed. The signs of the currents are taken according to the polarity of the respective CTs in RTDS.

```

90 | %%%%%%%%%%%%%%%%%%%%%%%%%%%%%%%%%%%%%%%%%%%%%%%%%%%%%%%%%%%%%%%%%%%%%%%%%
91 |
92 | % Zone 1 - Protects section 1 from the busbar system. Takes into
93 | % account incoming feeder 1, the outgoing feeder, ZZ transformer 1 and
94 | % the bus coupler. Signs are taken accordingly to the RTDS CTs
95 | % orientation
96 |
97 - | Bus1_diff_A = Bus1_A - section1_A - out_A - zz_A;
98 - | Bus1_diff_B = Bus1_B - section1_B - out_B - zz_B;
99 - | Bus1_diff_C = Bus1_C - section1_C - out_C - zz_C;
100 |
101 |
102 | % Zone 2 - Protects section 2 from the busbar system. Takes into
103 | % account incoming feeder 2, ZZ transformer 2 and
104 | % the bus coupler. Signs are taken accordingly to the RTDS CTs
105 | % orientation
106 |
107 - | Bus2_diff_A = Bus2_A - section2_A - zz_2_A;
108 - | Bus2_diff_B = Bus2_B - section2_B - zz_2_B;
109 - | Bus2_diff_C = Bus2_C - section2_C - zz_2_C;
110 |
111 | % Zone 3 - Protects the bus coupler. Takes into whether the currents
112 | % entering and leaving the bus coupler are equal. Signs are taken
113 | % accordingly to the RTDS CTs orientation
114 |
115 - | sect_A = section1_A + section2_A;
116 - | sect_B = section1_B + section2_B;
117 - | sect_C = section1_C + section2_C;
118 |
119 | %%%%%%%%%%%%%%%%%%%%%%%%%%%%%%%%%%%%%%%%%%%%%%%%%%%%%%%%%%%%%%%%%%%%%%%%%

```

For each zone, it is checked whether the differential current exceeds the threshold. This check is performed for each phase separately. If the differential current exceeds the threshold, the respective sum is increased by 1. This sum is used to keep track of the time for which the condition is true.

```

120
121 % Calculation of the differential condition for Zone 1
122
123 - if abs(Bus1_diff_A) >= I_diff
124 -     sum_bus1A = sum_bus1A + 1;
125 - else
126 -     sum_bus1A = 0;
127 - end
128 - if Bus1_diff_B >= I_diff
129 -     sum_bus1B = sum_bus1B + 1;
130 - else
131 -     sum_bus1B = 0;
132 - end
133 - if Bus1_diff_C >= I_diff
134 -     sum_bus1C = sum_bus1C + 1;
135 - else
136 -     sum_bus1C = 0;
137 - end
138
139 % Calculation of the differential condition for Zone 2
140
141 - if abs(Bus2_diff_A) >= I_diff
142 -     sum_bus2A = sum_bus2A + 1;
143 - else
144 -     sum_bus2A = 0;
145 - end
146 - if Bus2_diff_B >= I_diff
147 -     sum_bus2B = sum_bus2B + 1;
148 - else
149 -     sum_bus2B = 0;
150 - end
151 - if Bus2_diff_C >= I_diff
152 -     sum_bus2C = sum_bus2C + 1;
153 - else
154 -     sum_bus2C = 0;
155 - end
156
157 % Calculation of the differential condition for Zone 3
158
159 - if abs(sect_A) >= I_diff
160 -     sum_sectBC_A = sum_sectBC_A + 1;
161 - else
162 -     sum_sectBC_A = 0;
163 - end
164 - if sect_B >= I_diff
165 -     sum_sectBC_B = sum_sectBC_B + 1;
166 - else
167 -     sum_sectBC = 0;
168 - end
169 - if sect_C >= I_diff
170 -     sum_sectBC_C = sum_sectBC_C + 1;
171 - else
172 -     sum_sectBC_C = 0;
173 - end
174

```

If any sum exceeds the specified threshold (for different zones, different times apply), tripping signals are sent to the respective CBs.

```

175 - %%%%%%%%%%%%%%%%%%%%%%%%%%%%%%%%%%%%%%%%%%%%%%%%%%%%%%%%%%%%%%%%%%%%%%%%%
176 -
177 - % If the sum reaches a certain number (meaning that for a consecutive
178 - % time the condition was true, a TRIP signal is written and
179 - % communicated to the RTDS. This number that the sum needs to be
180 - % reached in order for a tripping signal to be sent is calculated based
181 - % on the time settings according to which the protection should operate
182 - % and based on the fact that the data from the RTDS is communicated to
183 - % MATLAB with a frequency of 400Hz.
184 -
185 - if (sum_bus1A >= 240 || sum_bus1B >= 240) || sum_bus1C >= 240
186 -     CB_trip(1) = 1;
187 -     CB_trip(3) = 1;
188 -     write(Skt_Dev, typecast(swabbytes(uint32(CB_trip)), 'uint8'));
189 - end
190 -
191 -
192 - if (sum_bus2A >= 240 || sum_bus2B >= 240) || sum_bus2C >= 240
193 -     CB_trip(2) = 1;
194 -     CB_trip(3) = 1;
195 -     write(Skt_Dev, typecast(swabbytes(uint32(CB_trip)), 'uint8'));
196 - end
197 -
198 -
199 - if (sum_sectBC_A >= 40 || sum_sectBC_B >= 40) || sum_sectBC_C >= 40
200 -     CB_trip(3) = 1;
201 -     write(Skt_Dev, typecast(swabbytes(uint32(CB_trip)), 'uint8'));
202 - end
203 -

```

Finally, it is checked whether any trip command has been sent. If a trip command is being sent, it is allowed after a specific time for the tripping commands to be reset, thus allowing for another simulation case to be tested. After the while cycle is stopped, and with that, the whole centralized algorithm, a command is issued to stop the communication between RTDS and MATLAB.

```

204 - % If any of the CBs is tripped, a new sum is started. When this sum
205 - % reaches a certain value, all of the TRIP signals are restored to 0,
206 - % meaning that the CBs can be re-closed with a command in the RTDS.
207 - % This command serves to make the simulations in the RTDS easier.
208 -
209 - if sum(CB_trip) >= 1
210 -     breaker_reset = breaker_reset + 1;
211 - else
212 -     breaker_reset = 0;
213 - end
214 -
215 - if breaker_reset >= 30
216 -     CB_trip(1:3) = 0;
217 -     write(Skt_Dev, typecast(swabbytes(uint32(CB_trip)), 'uint8'));
218 - end
219 -
220 - end
221 -
222 - clear Skt_Dev;

```